UNIVERSITAT DE BARCELONA

Pathophysiology of osteoarthritis

Aina Farrán Díaz-Cano

Doctoral Thesis

Pathophysiology of osteoarthritis

Aina Farrán Díaz-Cano

May 2017

PATHOPHYSIOLOGY OF OSTEOARTHRITIS

Thesis by

Aina Farrán Díaz-Cano

To obtain the title of

PhD of the University of Barcelona

Directors: Dr. Jordi Monfort and Dr. Laura Tío.

Tutor: Dr. Lluïsa Vilageliu

Dr. Jordi Monfort Dr. Laura Tío

Dr. LLuïsa Vilageliu (tutor)

Por muy larga que sea la tormenta,

el Sol siempre vuelve a brillar entre las nubes.

Khalil Gibran

A mi madre, mi padre, mi hermano y en especial, a mi mayor admiradora,

Ana Alhambra Gigante.

AKNOWLEDGEMENTS

Arriba el moment de fer recompte; recompte de persones que han estat clau per mi durant aquest llarg camí.

Primer de tot vull agraïr als meus directors de tesi, el Dr. Jordi Monfort i la Dra. Laura Tío, per confiar en mi desde el primer dia i pel vostre suport a nivell professional i personal. Jordi, sense la teva ajuda no hagués acabat mai vivint i treballant al Canadà, i la meva vida no hagués fet el gir que ha fet. Gràcies per donar-me l'oportunitat de fer ciència i per apostar i confiar en mi quan ni tan sols jo ho feia. Laura, gràcies per treure-li ferro als moments més difícils, pels *skypes* BCN-MTL que no sempre han estat per parlar de ciència.

Je voudrai remercier le prof. Johanne Martel-Pelletier et le Dr. Pierre Pelletier pour me permettre travailler avec eu et pour m'apprendre à faire de la science. Johanne, comme nous avons parlé pendant notre dernier rendez-vous, travailler avec toi est pas toujours facile, mais j'ai appris beaucoup et je vous remercier pour ça. To the people in the lab, François Mineau, you are my hero! How lucky I was to find you in the lab!! Thanks for being always so kind and helpful, for your patience teaching me, for your good mood in the lab and your "colisse de tabarnak!" moments with the printer machine... It was a huge pleasure to work with you!! I wish you all the best for your new life outside the lab. David, my other hero!! I remember the first day I arrived to the lab and Johanne told you that you had to work with me... hahaha, your face! But at the end, it wasn't that bad, was it? Thanks for your friendship, for your patience and your help with all the molecular part of my project. I really missed you during the last year when you were gone! Un gros merci aussi à toi Fred, pour être toujours disponible, pour ton professionnalité et pour ton implication dans le projet OPTC, tu as travaillé très fort! To my lovely Changshan, always so kind and friendly. To François Ceril for your help in the culture room and your stories about Isle Mauritius. I will never forget you my friends!! Muchas gracias también a ti Gladys, por tu ayuda a nivel profesional y personal. Por enseñarme todo sobre los ratones, por tus consejos sobre cómo trabajar con la doctora, que han sido claves! Pero sobretodo por abrirte a mí como a una amiga! Y a ti Gemma, qué suerte encontrarte en el trabajo! Gracias por la complicidad, los

cafés, el cariño... eres muy buena y estoy segura de que os irá genial a ti y a Lola!

Many many thanks as well to the girls at the office; Santa, Lise and Virginia. You are great professionals and you were always so nice to me that you made me feel part of the "family". Thanks for all your support and for providing me with delicious chocolate during these years!!

Thanks to all my friends from the CRCHUM; Shunya, Marwa, Cayetana, Lia, Angus, Jenna, Lawrence, Manu, Henna, Gemma... I hope I don't forget anyone! With you in the CRCHUM my everyday life was much easier and fun! I love you guys!

Moltes gràcies també a la gent del IMIM: la Nats, el Guy, la Laureta, la Maria i el Sergi. Tot i que al principi no m'adaptés molt bé al vostre "humor", sabeu que en el fons us estimo molt! Nats, gràcies també per la teva ajuda tècnica al lab (amb els gels 2D, les digestions de les isoformes, i altres que ara no recordo...)! Muchas gracias también a ti, Susanita, el destino te pone a personas en el camino que son claves para tomar una u otra dirección, y tu eres una de ellas. Millones de gracias a mi madrileña favorita, Selene!! Fué genial trabajar juntas y ya sabes que tienes una amiga en Barcelona!

I also want to thank all the staff working at the IMIM and CRCHUM "kitchen", I really appreciate your work. Also thanks to the staff at the CRCHUM cafe for the best muffins ever!

Com no agraïr a tots els meus amics que han "patit" amb mi durant aquest llarg procés. Per on començar? Per les fades, es clar! Sarita, gràcies per visitar-me aquell estiu, va ser genial! Clara, gràcies per estar sempre "allà" i pel teu suport incondicional. Lídia, gràcies per donar-me la millor notícia en "directe". Ju, gràcies per ser la meva fan número 1. Ari, moltes gràcies per ajudar-me a trobar pis a BCN! Amanda, pel teu carinyo i suport; Irene, per donar-me força i energía; Lops per transmetre'm lo millor de la natura i de la Catalunya rural; Rous, perquè sé que em portaràs en barco aquest estiu! Leti, mil gràcies pel teu optimisme i energia, pels teus consells de tot cor. Ets com una germana per mi i has sigut clau en aquesta etapa per tots els skypes que tant m'han ajudat a passar

els mals moments i per acollir-me a casa teva durant les meves visites... gràcies a totes i cadascuna per fer-me sentir aprop tot i estar a 7000 km de distància, pels vostres consells, per escoltar-me, per les rebudes amb tanta il·lusió cada cop que he vingut de visita, per estimar-me tal i com sóc. Gràcies també a les "golfes" per la vostra amistat; Raquel gràcies per visitar-me aquell primer estiu! Cris, "sister", gràcias por ser como eres! Mong, tu també!! us estimo molt! Continuo per les tites del pis de Guilleries: Airin, Paula, Adri, Anna; sou les millors amigues i companyes de pis que es pot tenir! gràcies per fer-me la vida més fàcil durant els anys viscuts a Gràcia i per la vostra amistat que encara dura i que segur que serà per sempre! Mil gràcies també als meus biologuit@s preferits: Laura Bu, Elvis, Marona, Robert, Ainhoa, Da, Marc, Ivan, Alex, Fabi, Annes... i a tots els que falten! Gràcies també als amics del PRBB pels moments (tant divertits) compartits durants els meus primers anys de tesi: als "fisios" que em van adoptar com a una mésal grup; Anna, Cris, Biuss, Gerard, Amado, Eva... als "snails" Alex Frías (PRBBest friend!) Estel, Rosa Vinyas, als "neurofar" Samantha Mancino, Elk, Thomas, Laura Cutando, als informàtics Ricard i David, i a la meva panto, Laura Buxó, t'estimo!

Un gros merci a tous mes amis québécois, pour votre accueil chaleureux dans le magnifique "dudes ranch"! Pour me recevoir à l'aéroport le premier jour, pour me montrer comment survivre le froid et pour votre amitié. Je vous aime, tabarnak! Surtout a toi Angie, tu étais comme une sœur pour moi! I was so lucky that I had two sisters in Canada, one from the East and one from the West; April, thank you sooo much for all the moments we spent together! For the road trip to Tadoussac, the summer bike rides, yoga classes, beers, dinners, English lessons, laughs, parties...! You both know you have a sister in BCN. Moltes gràcies també a la família "catalana" de Montréal; Agnès, Laura i Arnau, Susanna, Mire, Océane i Marcel, Ciccio i Marian, Marta i Ernest, sou molt bona gent i hi hà hagut un abans i un després a la meva vida desde que us vaig conèixer. Gràcies per tots els moments compartits!

Gracias a mi sevillano preferido, Rafa! siempre me has escuchado y aconsejado en los peores momentos de la tesis y tenerte "cerca" durante mi estancia en Canadá ha sido genial! te quiero Rafita!

Milers i milers de gràcies a l'Aina Monfort, gran professional que va fer que la meva vida fes un gir de 180º. Si no fós per tu, no sé si hagués arribat fins aquí.

Però sobretot gràcies a la meva família, a la meva mare Carme i al meu germà Emili. Mama, todo lo que tengo y lo que soy te lo debo a ti. Gracias por ayudarme tanto en todos los aspectos, por tus consejos desde el corazón y la experiencia, por tu cariño incondicional, por tu tiempo y dedicación... no hay palabras suficientes para describir lo agradecida que estoy y lo mucho que te quiero. Tete, gracias por todo lo que me has enseñado, por ser mi referente en la vida, por tu cariño, tus consejos, tu apoyo. Os quiero muchísimo. Sarai, muchas gracias a ti por ser como eres y por traer al mundo a la cosita que más quiero, mi sobri! Muchas gracias también a Angel por cuidar de mi madre y de mi abuelita con tanto cariño, por traer a mi madre a Montréal a visitarme, y por todo lo que has ayudado para montar el piso.

And finally, thank you Shoma for your everyday love and support. You appeared in my life at the right moment and since then everything is much easier. I really love and admire you and I am very happy to be able to share my life with you in Barcelona. T'estimo moltíssim. Arigato!

INDEX

ABBREVIATIONS

ACR	American college of rheumatology
ADAMTS	A disintegrin and metalloproteinase with thrombospondin motifs
APMA	4-aminophenylmercuric acetate
BMI	Body mass index
BMP	Bone mineral protein
CCL2	CC-chemokine ligand 2
CS	Chondroitin sulfate
COL3	Collagenase-3
COL3-DEL	Collagenase-3 isoform with a deletion
COL3-9B	Collagenase-3 isoform with extra exon 9
CXCL13	CXC-chemokine ligand 13
DNA	Deoxyribonucleic acid
DNase	Deoxyribonuclease
ECM	Extracellular matrix
EGF	Endothelial grtowth factor
E.L.I.S.A	Enzyme-linked immunosorbent assay
EULAR	European league against rheumatism
FBS	Fetal bovine serum
FLS	Fibroblast-like synoviocytes
GAG	Glycosaminoglycan
GDF-5	Growth differentiation factor-5
GM-CSF	Granulocyte-macrophage colony- stimulating factor
GuHCl	Guanidine chloride
GWAS	Genome-wide association study
HA	Hyaluronic Acid
HIFs	Hypoxia-inducible factors
IL-1β	Interleukine-1β
IL-1Ra	IL-1 receptor antagonist

LIF	Leukemia inhibitory factor
LRR	Leucine rich region
LTB4	Leukotriene B4
MMP	Matrix metalloproteinase
mRNA	Messenger ribonucleic acid
NAMPT	Nicotinamide phosphoribosyl transferase
NGF	Nerve growth factor
NO	Nitric oxide
NSAIDs	Non-steroidal anti-inflammatory drugs
OA	Osteoarthritis
OARSI	Osteoarthritis research society international
PCR	Polymerase chain reaction
PGs	Proteoglycans
PGE2	Prostaglandin E2
PRELP	Proline-arginine-rich end leucine-rich repeat protein
P38 MAPK	P38 Mitogen-activated protein kinases
SDS	Sodium dodecyl sulfate
SLRPs	Small leucine rich proteoglycans
SNPs	Single nucleotide polymorphisms
TIMPs	Tissue inhibitor of metalloproteinases
TNF	Tumor necrosis factor
UTR	Untranslated region
VCAM-1	Vascular cell adhesion molecule 1
VEGF-A	Vascular endothelial growth factor-A
WHO	World Health Organisation

INTRODUCTION

1. Osteoarthritis

1.1. Definition

Osteoarthritis (OA) is a multifactorial disease characterized by a progressive degeneration and eventual failure of the synovial joint functionality. Although it has been traditionally considered as an exclusive disease of the articular cartilage, nowadays it is considered as a whole joint disease. Therefore, the progression of the disease involves articular cartilage degeneration, osteochondral bone sclerosis and synovial membrane hypertrophy. Any joint from spinal vertebrae to the feet can be affected by OA although it is more frequent in hand, hip and knee. Symptoms vary depending on the grade and the location of the disease; however, most common symptoms are pain, stiffness or loss of movement, swelling and heat around the affected joint[1]. The etiology of OA can be classified as "primary OA" (idiopathic or spontaneous), when the cause is not apparent or "secondary OA" when there is an obvious triggering cause[2].

In order to identify and grade OA, Kellgren and Lawrence (K&L) described radiological criteria for the classification of knee OA[3]; formation of osteophytes, narrowing of joint space, sclerosis of subchondral bone and cyst, as well as altered shape of the bone ends (see table 1).

Radiographic grade	0	I	II	III	IV
Classification	**Normal**	**Doubtful**	**Mild**	**Moderate**	**Severe**
Description	No features of OA	Possible osteophyte development; normal or doubtful joint-space narrowing	Definite osteophyte; possible joint-space narrowing	Moderate osteophyte; joint-space narrowing, sclerosis and possible bone deformity	Large osteophyte; Joint-space greatly reduced; severe subchondral sclerosis and joint deformity

Table 1: Update of Kellgren and Lawrence (K&L) standardized radiographic grading of knee OA modified from D. Schiphof *et al*.2008[4].

1.2. Risk factors

Risk factors can be divided into two major categories; systemic factors and local factors (see Table 2). Systemic factors create a systemic environment where the joint is susceptible to be damaged. On the other hand, local factors result in abnormal biomechanical loading that will likely end up triggering OA in a vulnerable joint[5].

Risk Factors for OA	
Systemic Risk Factors	**Local Risk Factors**
Ethnicity	Joint injury
Age	SES
Gender	Physical activity/sports
Genetics	Joint biomechanics
Bone density	
Nutrition	
Obesity	

Table 2. Classification of OA risk factors, modified from Garstang SV *et al*. 2006[5].

1.2.1. Systemic factors

1.2.1.1. Ethnicity

Epidemiologic studies[6,7] have shown that OA prevalence varies between ethnic groups. However, it is important to note that ethnic differences are not only related to genetic factors but also to other variables including lifestyle, nutrition and probably the healthcare disparities between populations. For example, Chinese women rarely have hip OA while Caucasian women are

genetically predisposed to have hip anatomic abnormalities[6]. On the other hand, Chinese women present more prevalent knee OA than the American women[8] , what might be due to physical activities culturally more common for Chinese women such as manual labor and squatting[9].

1.2.1.2. Age

Age is the strongest risk factor for OA[10]. The presence of radiographic OA rises with age at all joint sites. In a Dutch study, 10–20% of women around 40 years old had evidence of severe radiographic OA of their hands or feet, and by age 70, it increased to approximately 75%[11]. This could be explained by several causes. On one side, during aging, chondrocytes, the only cell type of the articular cartilage, do not respond to reparative growth factors[12] and fail to produce extracellular matrix components like aggrecan and collagen type II, while expresses more matrix metalloproteinase. Furthermore, there is an accumulation of reactive oxygen species (ROS) that leads to mitochondrial dysfunction and chondrocyte death[13].

1.2.1.3. Gender

Evidence supporting sex differences in OA prevalence, incidence and severity was reported in a meta-analysis. They described that women present a higher risk to develop OA but the risk is site specific: they exhibited higher prevalence in knee and hand, higher incidence in knee, hand and hip and higher OA severity in knee[14]. Importantly, this study also showed that age was a significant contributor to the effect of sex in the observed heterogeneity on OA. It reported that females over 55 years old have a higher prevalence of knee and hand OA than men of same age, fact that could be explained by the hormonal effect of menopause. Therefore, in order to be more accurate when studying the

risk of OA, the interaction of both factors should be taken into account. Prieto-Alhambra *et al*[15] studied this interaction and concluded that the incidence of knee and hip OA increases continuously with age for both genders, while hand OA risk peaks around menopause in women.

1.2.1.4. Genetics

As with other complex diseases, Genome Wide Association Studies (GWAS) have tested the association between thousands of single nucleotide polymorphisms (SNPs) in the whole genome and OA. Until now, 17 loci have been associated to hip, knee and hand OA and they seem to be joint-site specific and even gender specific[16] (see figure 1). Among them, the loci coding for growth/differentiation factor 5 (GDF5) a member of the bone morphogenic protein (BMP)[17] is the first and most consistently demonstrated OA genetic factor[18]. Even if the study of genetic factors implicated in OA susceptibility has shown a progress in the last years, the number of susceptibility genes is relatively low compared to other complex diseases. In order to find new susceptibility genetic factors, field researchers have proposed to increase the sample size of studies, standardize patients' phenotypes and extract more information from old GWAS with new study strategies[18].

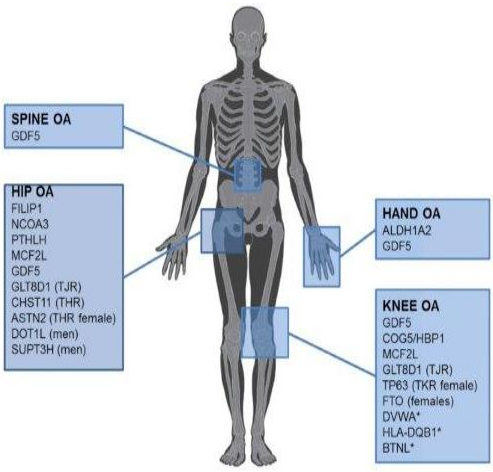

Figure 1. Identified genetic loci for each of the joint sites with genome-wide significant ($p < 5 \times 10^{-8}$) or genome-wide suggestive ($p < 10^{-7}$) evidence. The gene names that are annotated nearest to the DNA variant associated are shown. Some of the hip or knee associated loci, show only association in a certain subgroup: Total Joint Replacement (TJR); Total hip replacement (THR); Total knee replacement (TKR); *only significant in the Asian population. Figure from J.B.J van Meurs 2017[16].

1.2.1.5. Bone mineral density

In the recent years and with the help of new technologies, the association between bone mineral density (BMD) and OA has started to be clarified. Several studies concluded that, in women, an increased BMD is highly associated with the onset of knee OA[19-21] while it also prevents OA progression[22]. Furthermore, new 3-dimensional (3D) imaging methods such as computed tomography (CT), combined with custom image processing, has been used to measure BMD in relation to depth from the subchondral surface[23] as a marker of OA progression. This depth-specific method identified alterations in patellar subchondral bone density in OA patients with high levels of pain at rest[24] as well as association of depth-specific proximal tibial subchondral bone density and OA-related nocturnal pain[25], among others[26].

1.2.1.6. Nutrition

Some epidemiological studies have shown serum cholesterol to be a risk factor for OA development[27]. However, it has been shown that long-chain omega-3 polyunsaturated fatty acids (PUFAs) could decrease inflammatory eicosanoids, cytokines and reactive oxygen species[24]. Furthermore, diabetes has been described as an independent risk factor for OA, leading to the concept of a diabetes-induced OA phenotype [28]. This may be explained because hyperglycemia causes oxidative stress which induce chondrocyte dysfunction, matrix stiffness and subchondral bone destruction[29]. Finally, Vitamin D deficiency was found to be positively associated with the development and worsening of knee OA, including cartilage loss and increased joint space narrowing[30].

1.2.2. Local factors

1.2.2.1. Joint injury

There is a clear association between joint injury and OA. Examples of joint injury include striking a joint with a football helmet, or falling so that the joint hits directly on a hard surface. Disruption of the periarticular and articular soft tissues, including joint capsule, ligament, or meniscal injuries, does not directly damage articular cartilage, but the joint instability that occurs as a result of some capsular, ligamentous, and meniscal injuries causes repetitive increased loading of articular cartilage that results in joint degeneration[31]. Studies on both animal and human models convincingly demonstrated that a loss of anterior cruciate ligament integrity, damage to the meniscus, and meniscectomy lead to knee OA[32]. For example, Murell *et al*. showed that patients with cruciate rupture present cartilage and meniscal loss[33].

1.2.2.2. Obesity

A high number of studies have shown that obesity represents one of the most important risk factors and it is also a predictor for OA progression[34], especially in knee joint. Relationship between body mass index (BMI) and OA of the knee is mainly linear[35]. Consequently, weight loss in obese OA patients slows disease progression and improves symptoms and functional capacity[36]. Although there are studies about obesity and hand OA that are contradictory, some studies have shown an association, suggesting that obesity may predispose to hand OA, perhaps via an inflammatory or metabolic intermediary that has not yet been identified[37]. This means that obesity plays a role not only as a local factor but as a systemic as well.

1.2.2.3. Socioeconomic status

The effect of socioeconomic status (SES) on the rates of knee and hip replacement due to OA was assessed recently in a cohort study in Sweden[38]. Less educated groups of OA patients may be more likely to have physically demanding occupations, which has been considered to be a risk factor for knee OA and its progression. However, in the Swedish study they found that lower SES is associated with a lower likelihood of joint replacement[38]. This may indicate inequity regarding access to joint replacement, possibly due to differences in health-seeking behavior.

1.2.2.4. Sports and physical activity

The effect of sports on the risk of OA is highly associated with the subject´s joint health and the participation on high-impact sports; sports that cause minimal joint impact and torsional loading by people with a normal joint anatomy and neuromuscular function has minimal effect on the risk of OA[39].

Furthermore, sports with a high joint impact such as running is not associated with OA risk in runners that have been training since young ages and have a low BMI[40]. However, people with abnormal joint anatomy or alignment, previous joint injury or surgery, joint instability, articular surface incongruity or dysplasia, disturbances of joint or muscle innervations, or inadequate muscle strength have increased risk of OA during participation in any type of physical activity that include impact and torsion loading. On the other hand, soccer players and weight lifters have shown an increased prevalence of OA, possibly due to previous knee injury on the soccer players and usual high BMI of the weight lifters[40].

1.2.2.5. Joint biomechanics

Mechanical factors play important roles in promoting both the health of a joint and its degeneration. Appropriate loading is required to maintain healthy joint tissues, while aberrant loading contributes to the development and progression of OA. Abnormal joint anatomy or function, such as hip dysplasia or femoroacetabular impingement are long established risk-factors for OA[41,42]. Similarly, tibial and femoral bone morphology can predict the development of knee OA[43]

1.3. Epidemiology

Epidemiological data on OA incidence and prevalence are limited due to different definitions of the disease, different affected joints sites, and difficulties to determine its onset. However, the epidemiologic studies carried out showed that OA is the most common form of degenerative joint disease and in 2005, it was estimated that over 26 million people in the US had some form of OA[10,44]. Incidence of OA in the hand, hip and knee is raising with increasing average of age and BMI of general population, although it is more common in women especially after the age of 50 years old[45]. In the general adult population of Spain, the estimated prevalence OA is 10.2%[46]. According to World Health Organization, by 2050, 130 million people will suffer from OA worldwide, of whom 40 million will be severely disabled by the disease [47].

1.4. Burden of the disease

Hand OA is the most prevalent form of OA but knee and hip present the highest burden. Large weight-bearing joints present higher pain and stiffness that often lead to significant problems with mobility and disability requiring expensive surgical treatments[48]. Costs associated with OA include costs for

adaptive aids and devices, medicines, surgery, and time off at work[49]. Several studies have shown that the burden of OA is not only physical but also psychological as the loss of mobility is associated with loss of autonomy that ultimately affects the mental health of the patient. This effect is higher in OA disease compared with other chronic diseases. Penninx *et al.* described that psychological distress is more frequent in patients with OA compared to patients with other chronic diseases such as diabetes[50]. In addition, as shown by Hopman et al. OA patients on a waiting list for arthroplasty scored lower on physical components of quality of life scores than both healthy controls and heart failure patients[51].

1.5. Diagnose

Diagnose of OA is predominantly based on the symptomatology and the use of X-ray radiography to detect structural changes such as osteophyte formation, narrowing of the joint space width, subchondral sclerosis and cysts. These structural changes and symptoms are usually referred when the disease is advanced and, therefore, probably irreversible. Magnetic resonance imaging (MRI)[52] is used to assess morphologic changes in cartilage preferably than radiography. However, morphologic changes are not always present in early-stage OA. In order to obtain a better diagnose and to allow following the progression of the disease during new therapeutic approaches, new quantitative imaging techniques to assess biochemical changes are evolving. For instance, the T2 mapping can be used to measure collagen content or orientation, and T1rho mapping to quantify GAGs[53].

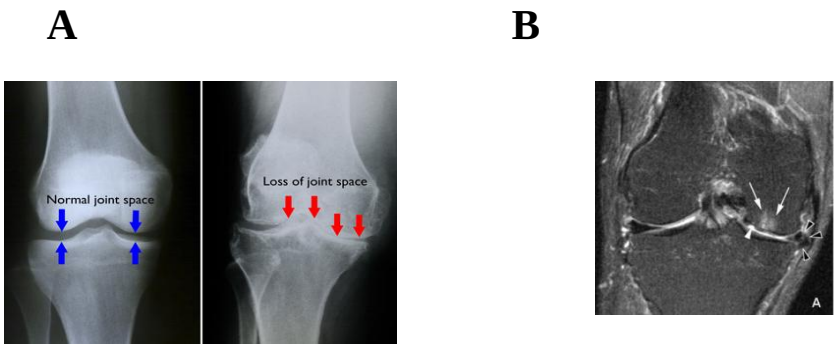

Figure 2. A) Left image represents the X-ray of a normal knee; the space between the bones indicates healthy cartilage (blue arrows). On the right image, an arthritic knee shows severe loss of joint space (red arrows). Image from orthoinfo.aaos.org. **B)** MRI image shows several features of early OA not detectable by X-ray. White arrowhead shows cartilage defect at central weight bearing part of medial femur. Arrows show subchondral bone marrow lesion. Black arrowheads show meniscal extrusion at medial joint line causing bulging of neighboring medial collateral ligament (no arrow). Image from Guermazi A *et al.* 2012[54].

Some molecules and protein fragments are candidate OA biomarkers since they are released and can be detected into the synovial fluid, blood system or urine[55-59]. Several biomarkers have been proposed and investigated, but none of them are yet well validated for use in clinical practice. Cartilage oligomeric matrix protein (COMP) and crosslinked C-telopeptides of type II collagen (CTX-II) are the most widely studied and the best examples of a good biomarker as they are degradation products of the cartilage extracellular matrix, and their urinary and serum concentrations can potentially predict the destruction of articular cartilage in OA, respectively[60,61].

1.6. Treatment

Unfortunately, up to date no therapy has shown consistency to delay the progression of OA. The first non-surgical approach is to alleviate the symptoms with non-steroidal anti-inflammatory drugs (NSAIDs) such as ibuprofen or

naproxen. However treatment guidelines actually recommend starting with acetaminophen since it has lower side effects[62]. These drugs are highly prescribed for OA treatment, although they act on the symptoms without improving the inflammatory and catabolic processes. For this reason, other pharmaceutical agents are being investigated as disease modifying OA drugs (DMOADs) although their efficacy is still controversial. Another strategy is to target degradative enzymes such as matrix metalloproteinases, but it seems that adverse events outweigh benefits. Together with the use of pharmacological agents, a change in lifestyle is recommended; weight loss improves symptoms of obese knee OA patients[63] as well as exercise to increase muscle strength[64].

Surgery is the last approach for OA treatment. Arriving at the end-stage of the disease, and due to the absence of disease-modifying treatments, joint replacement is the only effective treatment. Even so, in certain cases there are some surgical interventions that could prevent OA progression, for example, surgery has been shown to successfully delay the progression of the disease in cases of hip dysplasia by reorientation of the acetabulum[65] and arthroscopic joint surgery to treat and prevent femoroacetabular impingement has shown symptomatic benefit and it modifies the long-term risk of OA[66].

1.6.1. Symptomatic slow acting drugs for the treatment of OA

Due to the lack of effective therapies against OA, the continued use of NSAIDS in aged patient's results in problematic secondary effects such as gastro-intestinal tract erosions, ulcers and deleterious renal functions[67]. Furthermore, these drugs do not improve the structural damages of the joint. However, a group of natural compounds named Symptomatic Slow-Acting Drugs for the treatment of OA (SYSADOA) are under investigation for their effects on both symptoms and joint structural degradation[68]. The group includes glucosamine sulphate (GS), chondroitin sulphate (CS), diacerhein, avocado soybean unsaponifiable (ASU), and HA. Contrary to NSAIDS, SYSADOA do not present severe side effects but their effects on pain and mobility start after few weeks of therapy. Importantly, they have a remnant effect that can last for a couple of months after the interruption of the treatment. Hyaluronic acid (HA) is a glycosaminoglycan (GAG) found not only in joint cartilage, but also in synovial fluid, where it acts as a lubricant and its concentration is diminished in OA. Intra-articular administration of HA has been widely used as viscosupplementation. Although efficacy and safety are controversial[69] a recent systematic review and network meta-analysis concluded that intraarticular administration of HA is more effective than NSAIDs for pain[70]. Glucosamine sulphate and chondroitin sulphate, for example, showed anti-inflammatory properties *in vitro*[71] but they show conflicting results in clinical trials[62,72,73] probably due to the variability formulations caused by different animal source and purification procedure[74]. Of note, SYSADOAs are regulated and prescribed as drugs in Europe but not in USA, where they are sold as nutraceuticals. Therefore, European SYSADOA have to fulfill sever criteria of quality and safety while nutraceuticals in EEUU are not strictly regulated, consequently, the

composition and the efficacy of the compound can vary depending on the company.

CS is recommended as a SYSADOA by the EUropean League Against Rheumatism (EULAR)[75] in patients with OA. It is a GAG found in the ECM of connective tissues (e.g. bone, cartilage, skin, ligaments and tendons). The commercial CS is extracted and purified from cartilage of different species and tissues. However, the effect of the drug depends on the molecular composition, which varies depending on the source and the chemical and structural modifications during extraction. For this reason, a strictly standardized extraction protocol should be used by all the manufactures, in which quality of the drug is optimized and contaminants are minimized[76]. The mechanism of action of CS remains unclear. However, the fact that CS forms large molecules indicates that it does not penetrate into the cells but reacts with its membrane receptors, resulting in the inhibition of the inflammatory reaction caused by Damage-Associated Molecular Patterns (DAMPs) and the reduction of nuclear translocation of pro-inflammatory transcription factors[68].

2. Articular cartilage

Articular cartilage is a connective tissue composed of water (>70%) and a dense extracellular matrix (ECM) that encompasses the unique cellular type of the cartilage, the chondrocytes. The major component of the ECM is the collagen network consisting mainly of type II collagen fibers and type IX and XI collagen macromolecules attached to the surface of the fiber. Non-collagenous components such as GAGs, aggregated proteoglycans (mainly aggrecan) and small leucine rich proteoglycans (SLRP's) are also binding the collagen fiber. Cartilage is a no innervated and also an avascular tissue, thus gets its nutrients by diffusion from the synovial fluid. Due to this condition, chondrocytes live in a hypoxic environment, and intracellular survival factors, such as hypoxia-inducible factor 1α, are required for maintenance of homeostasis and adaptation to the mechanical environment[77]. Under physiological conditions, the collagen network and proteoglycan content is maintained by the chondrocytes. However, the previously mentioned local and systemic risk factors could lead chondrocytes to fail to maintain the ECM and thus the cartilage tissue is progressively degraded.

Chondrocytes are surrounded by a pericellular matrix (PCM) consisting of type VI collagen and other matrix proteins, forming a structure called the chondron[78] (Figure 3, C). The PCM plays a role in a number of important processes throughout the development, maintenance, and degeneration of articular cartilage, including organizing the growth plate, modulating enzyme and growth factor activity, transducing biophysical signals, and undergoing changes that contribute to the progression of OA[79]. Next to the PCM lies another type of ECM called territorial matrix (TM), and even further from the cell, there

is the interterritorial matrix (ITM) (Figure 3, C). Each zone of the ECM is formed by different collagen types and collagen-binding molecules.

Articular cartilage morphology is not homogenous all along its depth, and four zones could be distinguished, from top to bottom; superficial zone, transitional zone, deep zone, calcified cartilage zone:

2.1. Superficial zone

It is the thinnest of all layers, approximately 10% to 20% of articular cartilage, although the parallel arrangement of the collagen fibers makes it the most resistant to tensile and shears strength. It is covered by a thin film of synovial fluid, called 'lamina splendens' composed of proteins such as 'lubricin'[80]. This protein is responsible for providing an ultimate gliding surface to the articular cartilage[81]. Ellipsoid chondrocytes are lying parallel to the joint surface (Figure 3, B). Disruption of this zone alters the mechanical properties of the articular cartilage and thus contributes to the development of OA. This layer also acts as a filter for the large macromolecules, thereby protecting the cartilage from synovial tissue immune system.

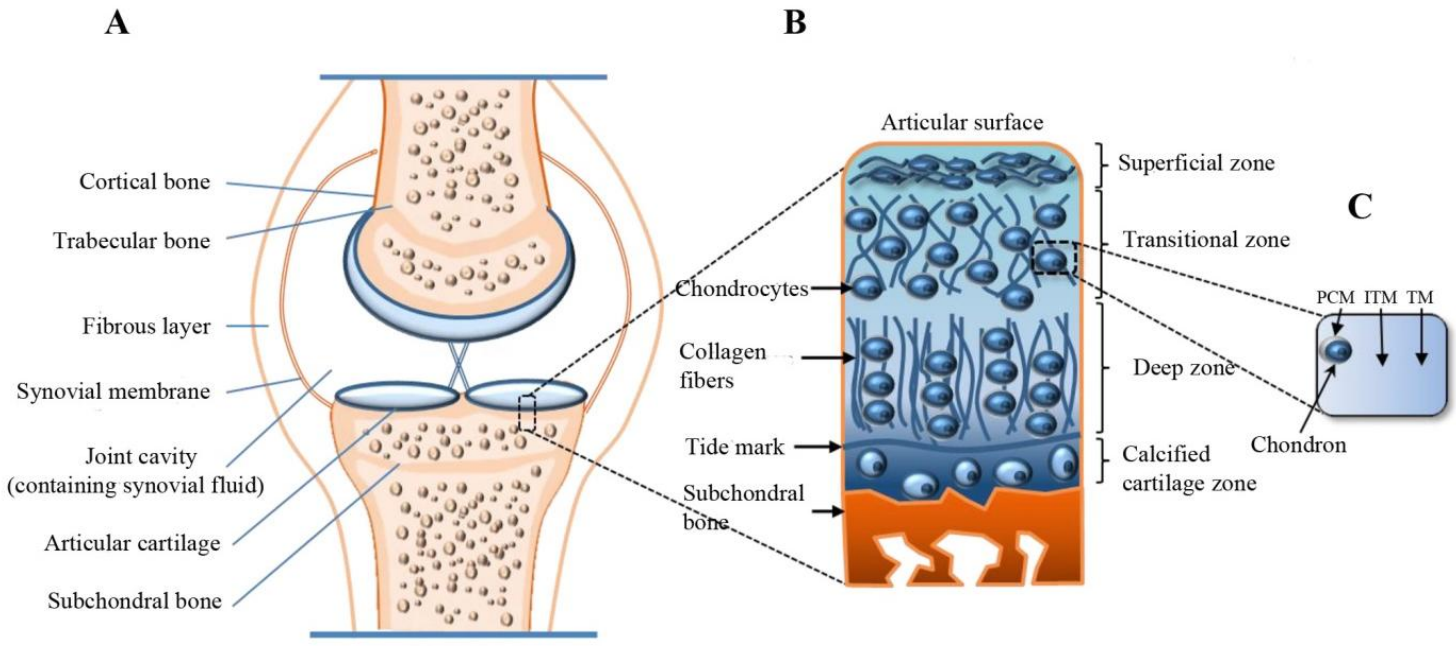

Figure 3. Properties of a normal joint. (A) In a diarthrodial joint, the edges of two or more adjacent bones are covered by a layer of articular cartilage that avoids the mechanical friction. The joint is encased in a capsule of connective tissue. **(B)** Cross-section of the articular surface of the joint illustrating the main structural elements, including superficial, transitional, deep, calcified cartilage zones and subchondral bone. Chondrocytes are arranged parallel to the surface in the superficial zone, obliquely perpendicular in the transitional zone and organized in columns parallel to the articular surface in the deep zone. In the calcified zone chondrocytes are hypertrophic and secrete type X collagen. **(C)** Chondrocytes of all zones are enclosed in a capsule made by collagen type VI called the chondron. The ECM can be classified as pericellular matrix (PCM), interterritorial matrix (ITM) and territorial matrix (TM) according to the distance from the cell and the molecular composition**.** Image modified from *Martel-Pelletier J et al. Nat Rev Dis Primers. 2016.*

2.2. Transitional zone

The transitional zone occupies 40% to 60% of the articular cartilage volume. The fibers of this zone are thicker than in the superficial zone and are aligned obliquely to the surface. The proteoglycan aggrecan concentration is higher in this zone. Due to these characteristics, this zone has a higher compressive strength than the superficial zone. The cell density is lower and chondrocytes are arranged perpendicular to the surface and present a more rounded shape than in the superficial layer (Figure 3, B).

2.3. Deep zone

The last 30% of the cartilage is called deep zone, where collagen fibrils are large in diameter and perpendicular to the surface. This layer contains the highest proteoglycan and lowest water concentration, and has the highest compressive modulus. The chondrocytes are typically arranged in columns parallel to the collagen fibers and perpendicular to the joint surface. The tidemark separates the deep zone from the calcified cartilage zone, which rests directly on the subchondral bone.

2.4. Calcified cartilage zone

This mineralized zone contains a small number of cells embedded in a calcified matrix and thus showing a very low metabolic activity. The chondrocytes in this zone present a hypertrophic phenotype. One of their characteristic is the Type X collagen synthesis, responsible for providing important structural integrity and also a shock absorber along with the subchondral bone. This zone offers an important transition to the less resilient subchondral bone[82].

3. Collagens

Collagens are the most abundant proteins in mammals (30% of total protein mass)[83]. The collagen superfamily comprises 28 members numbered with Roman numerals in vertebrates (I–XXVIII) but 80–90 percent of the collagen in the body consists of types I, II, and III. Collagens differ in their ability to form fibers and to organize the fibers into networks. The collagen network is the structural backbone of the cartilage ECM. It forms an oriented meshwork that provides the cartilage with tensile strength and is composed mainly of collagen type II and IX, that is located on the surface of the type II collagen fibril.

The common structural feature of fibrillar collagens is the presence of a triple helix consisting of three polypeptide chains, called α-chains. Collagen α-chains vary in size from 662 up to 3152 amino acids for the human α-1(X) and α-3(VI) chains respectively[83,84]. The three α-chains that conform the fibrils can be either identical to form homotrimers (e.g., collagen II) or different to form heterotrimers (e.g., collagen IX). The triple helix is stabilized by the presence of glycine at every third residue, a high content of proline and hydroxyproline, interchain hydrogen bonds, and electrostatic interactions[85], involving lysine and aspartate[86].

Type	Morphological location	Function
II	Principal component of the fiber (90–95%)	Tensile strength
VI	Pericellular matrix	Chondrocytes attachment to the matrix
IX	Cross-linked to surface of fiber	Tensile properties and inter-fibrillar connections
X	Exclusive of hypertrophied chondrocytes	Structural support and cartilage mineralization
XI	Within or on macrofibrils	Nucleates fibril formation

Table 3: Main collagen types on articular cartilage.

Type I collagen was the first collagen to be characterized and it has been studied in detail because it is abundant in tendon and easy to isolate. However, type II is the major collagen in cartilage. Its fibrils are smaller in diameter than type I and are oriented randomly in the viscous proteoglycan matrix. Type II fibers are rigid macromolecules that allow cartilage to resist large deformations in shape and to absorb shocks.

Collagen fibrillogenesis during normal cartilage development is finely regulated and involves multiple steps. During the first steps of fibrillogenesis, collagen molecules are assembled into quarter staggered arrays forming short small-diameter fibril intermediates (Figure 4). After the molecular assembly phase, fibrils associate and become both longer and larger in diameter. These fibrils are stabilized by interactions with fibril-associated molecules such as proteoglycans[87].

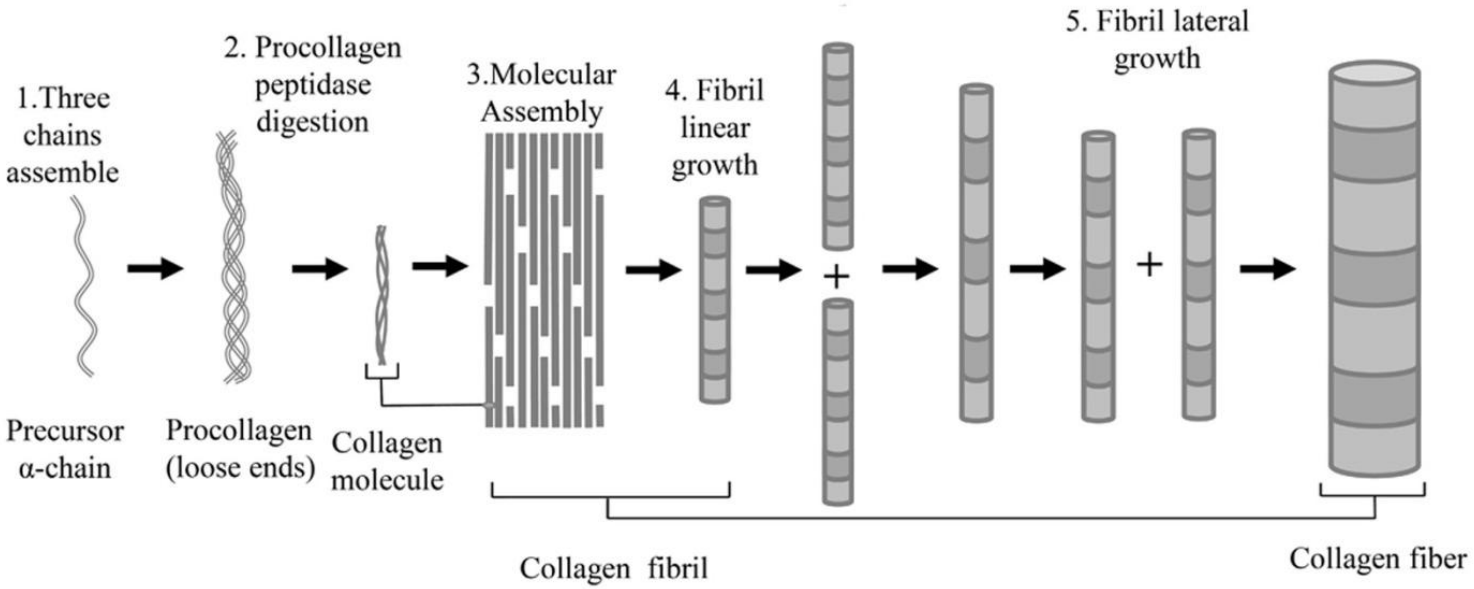

Figure 4: Representation of the collagen fibrillogenesis process. During development stages, three precursor α-chain peptides assemble to form a procollagen molecule with loosened ends. The action of procollagen peptidase enzymes is essential for maturation of the collagen molecule. Several collagen molecules will covalently bond to each other in a scattered arrangement to form a collagen fibril. Fibril length grows by end-to-end fusion of several fibrils. At the end of the process, fibers grow in width by lateral fusion.

4. Non-collagenous proteins

The ECM of the articular cartilage contains several non-collagenous proteins such as proteoglycans, glycoproteins or non-glycosylated proteins. Proteoglycans are negatively charged proteins composed of a core protein with one or more GAG chains covalently attached. There are five classes of GAGs such as chondroitin sulphate (CS), keratan sulphate (KS), dermatan sulphate (DS), HA and heparan sulphate (HS). Due to their negative charges they are able to entrap large amounts of water and create a swelling pressure that helps the cartilage to resist deformation and compression forces. They have several other functions, among them, enforce the collagen meshwork and interact with the collagen fibril to regulate collagen fibrillogenesis, induce signaling pathways by binding to cell surface receptors, cytokines, growth factors and other ECM members. They can be classified as aggregated or non-aggregated proteoglycans.

4.1. Aggregated proteoglycans

The most abundant aggregated proteoglycan in cartilage is aggrecan. It is a large proteoglycan of about 2,500kDa that forms aggregates by non-covalently bounds to HA that are stabilized by a glycoprotein named link protein. The protein core consists of three globular structural domains, G1 (N-term), G2, and G3 (C-term) that are involved in aggregation, hyaluronan binding, cell adhesion, and chondrocyte apoptosis. Between G2 and G3 there is a large inter-globular domain highly substituted with mainly CS but also KS and other O and N-linked oligosaccharides chains, forming a structure similar to a bottlebrush. The core protein of aggrecan is only 250kDa, so almost 90% of its mass is comprised of these GAG chains. Aggrecan forms a stiff and resistant to deformation network with collagen and is essential for the proper functioning of the cartilage because

it provides a hydrated gel structure swelling and expansion of the ECM. Other aggregated proteoglycans are versican[88], neurocan[89], brevican and CD44[90].

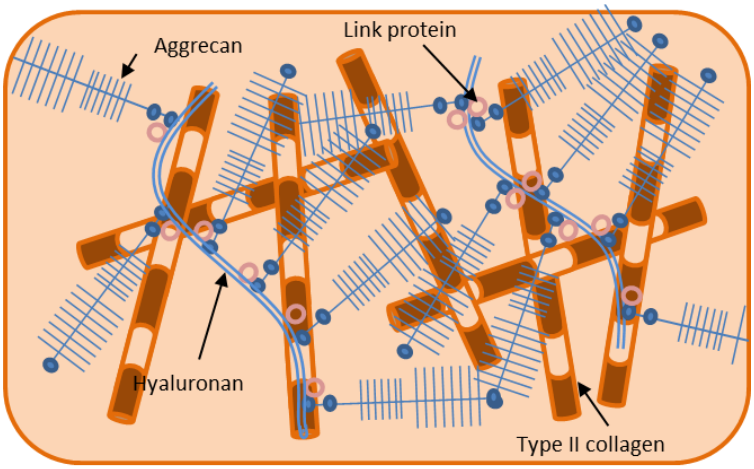

Figure 5: Representation of the aggregated complexes formed by aggrecan. Aggrecan is the most abundant chondroitin and keratan sulphated proteoglycan of the articular cartilage and is essential for its structure and function. It interacts with hyaluronan and link protein forming a large aggregated complex that, together with the collagen network**,** forms a scaffold for chondrocytes**.**

4.2. Small leucine rich proteoglycans (SLRPs)

The SLRPs are a family of secreted proteoglycans that have a small protein core (36-42 kDa) and that are present in many connective tissues. They are encoded in 18 different genes clustered on seven chromosomes, suggesting duplication to generate functional redundancy during evolution[91] . SLRPs are characterized by having a conserved domain of tandem leucine-rich repeats (LRRs) flanked by a cysteine-rich cluster and containing N-linked oligosaccharides and/or chondroitin/dermatan sulfate or keratan sulfate chains. The LRR regions consist of an α-helix and a β-strand, with a hallmark motif, LXXLxLXXNxL, where L indicates leucine, and x indicates any amino acid[92]. They have a horse-shoe structure specially designed for protein-protein interactions with a concave

surface formed by the LRR's β-sheets and a convex surface flanked by the LRR's α-helices and the SLRP's diverse carbohydrate moieties[93].

It is well known that SLRPs can participate in many biological functions not only as regulators of signaling pathways, but also as structural proteins. Studies with SLRP-deficient mice have demonstrated their capacity to bind to collagen and modulate fibril formation. These mice presented different pathologies related to the connective tissue, including OA, due to abnormal collagen fibril formation[94,95]. Furthermore, it has been proposed that SLRPs form a "surface coat" on the collagen fibrils surface, masking the collagenase cleavage sites and thus protecting the fibers from digestion of collagenases[96]. Being mostly extracellular, SLRPs bind to cell surface receptors, growth factors, cytokines and other ECM components and regulate ligand induced signaling pathways. Many recent studies have shown that some SLRP members have the ability to activate the complement system[97] and therefore, have a role in chronic inflammatory processes and OA pathogenesis.

Studies have highlighted the internal regulation of the ECM architecture by describing the rescue and/or compensation mechanisms by other members of the SLRP family when a single member is lacking or modified[98-100]. As an example, in fibromodulin-deficient mice, lumican, a SLRP belonging to the same class (Class II) and sharing 46% homology, is overexpressed compensating the lack of fibromodulin[100]. Even if most of the SLRPs members share functionality[94], they are subdivided in five different classes based on evolutionary conservation and homology, chromosomal organization and N-term Cys cluster sequence structure[101].

4.2.1. **Class I:** includes asporin (ASPN), biglycan (BGN) and decorin (DCN) (table 4). They all have eight conserved exons that encode for 10 LRRs and a unique N-term Cys sequence (CX_3CXCX_6C) that forms two disulfide bonds. ASPN is not a proteoglycan since it does not include any GAG chain, while BGN and DCN are substituted with one and two CS/DS side chains, respectively[91]. However, ASPN contains a stretch of Asp residues, an acidic domain also found in class II (osteoadherin), class III (epiphycan), and class V (podocan) members, located in either the N- or C-terminal region. BGN and DCN have similar structure; in fact they are thought to be the result of gene duplication[102]. BGN is located in the cell or in the PCM where it plays a role in assembly of collagen fibrils and muscle regeneration[103]. DCN has been found mainly in the ECM of the articular cartilage bound to collagen fibers by its core protein, not by the GAG chain[104,105]. This binding delays collagen fibrillogenesis and may play a role in interfibril interactions. DCN also interacts with TGF-β isoforms[106], fibronectin and thrombospondin.

4.2.2. **Class II:** includes fibromodulin (FMOD), lumican (LUM), osteoadherin (OSAD) and PRELP. Their genes present an organization in three exons. The proteins present a cluster of Tyr sulfate residues at their N terminal domain. They are mainly substituted with KS chains but also with polylactosamine, an unsulfated form of keratin sulfate. FMOD and LUM are very similar in their post-translational modifications and have a 47% sequence identity. FMOD and LUM are close homologues and, as DCN, play a role in the regulation of the assembly of collagen monomers into

fibrils, influencing collagen fibrillogenesis and fibril thickness[107,108]. Some studies reported that LUM influences at the initial formation of fibrils, while FMOD is responsible of their maturation[107]. Furthermore, FMOD has the ability to activate the classical pathway of the complement by binding to C1q factor[109]. LUM is proposed to modulate TGF-β signaling sequestering the growth factor in the extracellular matrix[110]. PRELP is synthesized in high amounts in cartilage and differs from the other proteins of this family by its N-term. This domain is rich in Pro and Arg residues, responsible of its basic properties[111] and has the ability to bind heparin, heparan sulfate and tyrosine sulfate-rich domains of other extracellular matrix proteins, such as FMOD and OSAD[84,112]. Furthermore, this region has been shown to present antimicrobial activity against Escherichia coli, Staphylococchus aureus, and Bacillus subtilis similar to several other heparin-binding peptides[113]. PRELP can also bind to collagen via its LRR domain.

4.2.3. **Class III:** this class contains three members, epiphycan (EPYC), osteoglycin (OGN) and opticin (OPTC). They are characterized by a relatively low number of LRRs (seven LRRs) and a genomic organization comprising seven exons. Several studies have shown that EPYC plays an important role in maintaining joint integrity. For instance, EPYC knockout mice developed OA with age but the severity of the disease was higher on EPYC/BGN double-deficient mice, indicating genetic interaction between members of different classes[114]. OGN was firstly isolated from bovine bone as an inducer of matrix mineralization[115] and was originally called osteoinductive factor. Nowadays, it is known that OGN is expressed in other

tissues such as cartilage (in hypertrophic chondrocytes)[116] and arteries (adventitia)[117]. OPTC, as ASPN, is a glycoprotein as it is not substituted with GAG chains, instead it has Serine and Threonine residues that are heavily substituted with sialylated O-linked oligosaccharides. It was firstly described in the vitreous humor of the eye[118] where it inhibits pathogenic angiogenesis[119] but in later studies, it was shown to be expressed also in brain, ligament, liver, testis, muscle, skin, cartilage and synovial membrane[120,121]. OPTC was found to be of interest in human OA process since normal cartilage showed higher OPTC staining in superficial layer of the ECM than OA cartilage[121]. Moreover, OPTC is degraded by several proteases involved in OA development[122] and specially by MMP-13, which cleaved OPTC after only 2h of incubation[121].

4.2.4. **Class IV:** the members of this non-canonical class, chondroadherin (CHAD), tsukushi[123] and nyctalopin[124], have 11 homologous LRRs flanked by a N-terminal Cys-rich region. CHAD is known to interact with collagen type II[125], and mediate cell-matrix interactions through binding to integrin $\alpha 2\beta 1$[126] and heparan sulphate[126]. Tsukushi is expressed in early development stages where it functions extracellularly as a key coordinator of multiple signaling networks. However, its implication in OA has not been elucidated yet. Nyctalopin is expressed in the retina, anchored to the cell membrane[127] and it is required for normal vision[124].

4.2.5. **Class V:** a new non-canonical class that contains two members, podocan (PODN)[128] and a highly homologous podocan-like protein 1(PODNL1)[129]. Although these proteins have a different C-terminal Cys-rich cluster, they have 20 LRRs with homology to class I and II

SLRPs. PODN mRNA expression was found in cardiomyocytes and Vascular smooth muscle cells (VSMC) and the protein showed functional properties shared by other SLRP members like binding to collagen I[128] PODNL1 gene is expressed in mineralized tissues and osteoblast and its protein is secreted into the ECM[129].

SLRP	GAG	Expression in main tissue and articular joint tissues
CLASS I		
Asporin (ASPN)	-	Cartilage, periosteum
Biglycan (BGN, PGS1)	CS/DS	Cartilage, bone, tendon, cornea
Decorin (DNC, PGS2)	CS/DS	Cornea, cartilage, tendon, muscle, bone.
CLASS II		
Fibromodulin (FMOD)	KS	Cartilage, tendon, ligament
Lumican (LUM)	KS	Cartilage, bone, skin, cornea
Osteoadherin (OSAD)	KS	Bone
Proline And Arginine Rich End Leucine Rich Repeat Protein (PRELP)	KS	Cartilage, lung, sclera, tendon, skin, heart
CLASS III		
Epiphycan (EPYC, PG-Lb, DSPG-3)	CS/DS	Cartilage
Osteoglycin (OGN), mimecan (MIME), osteoinductive factor (OIF)	KS	Cartilage, bone, cornea, skin
Opticin (OPTC)	-	Eye, cartilage, synovium, brain
CLASS IV		
Chondroadherin (CHAD)	KS	Cartilage, bone, eye, tendon
Tsukushi (TSKU)	-	Chick embryo
Nyctalopin (NYX)	-	Retina

CLASS V		
Podocan (PODN)	-	Kidney, cardiovascular tissues
Podocan-like 1 (PODL-1)	-	Bone

Table 4: Small leucine rich proteoglycans super-family members, GAGs attached to the protein core and tissue expression.

5. Synovium

The synovium is composed of the synovial membrane and the synovial fluid. The synovial membrane is a specialized semi-permeable connective tissue that seals the joint cavity and regulates the transfer of molecules in and out of the joint. In a healthy synovium, the majority of cells of the synovial membrane are fibroblast-like synoviocytes (FLS) and few macrophages. The membrane is responsible for the maintenance of synovial fluid volume and composition, mainly by producing lubricant factors, such as lubricin and hyaluronic acid (HA). Furthermore, the synovial fluid is also the responsible for the nutrient supply of the chondrocytes.

A common feature of OA is the inflammation of the synovium (synovitis) which is characterized by hyperplasia of the synovial membrane, increased vascularity andinfiltration of T and B lymphocytes and macrophages. Products of cartilage breakdown released into the synovial fluid are phagocytosed by synovial cells, amplifying synovial inflammation. In turn, activated synovial cells in the inflamed synovium produce catabolic and pro-inflammatory mediators that lead to excess production of the proteolytic enzymes responsible for cartilage breakdown, creating a positive feedback loop.

Biomarkers of synovitis can be detected in the circulation of OA patients. Increased concentrations of C-reactive protein are associated with an increasing degree of inflammatory cell infiltration of the synovial tissue, increasing levels of IL-6 (a cytokine released mainly by synovial tissue) in synovial fluid and is also predictive of rapid disease progression in early knee OA. In OA, the concentration of IL-6 in synovial fluid is positively correlated with the total leukocyte count. Fragments of type II collagen or aggrecan are potential biochemical markers of the synthesis and degradation of these proteins. Finally, the synovial cells of patients with rapidly destructive hip OA, a typical form of inflammatory OA, contain increased concentrations of matrix metalloproteases (MMPs; MMP-3 and MMP-9). and concentrations of these enzymes are also elevated in the synovial fluid, plasma and sera of these patients[130].

Synovitis is directly responsible for several clinical symptoms and reflects the structural progression of the disease; it is a key factor in OA pathophysiology because of the action of several soluble mediators (Figure 6). Hence, treatments that specifically target this previously neglected component of OA could be beneficial for both the symptoms and structural changes that occur in OA.

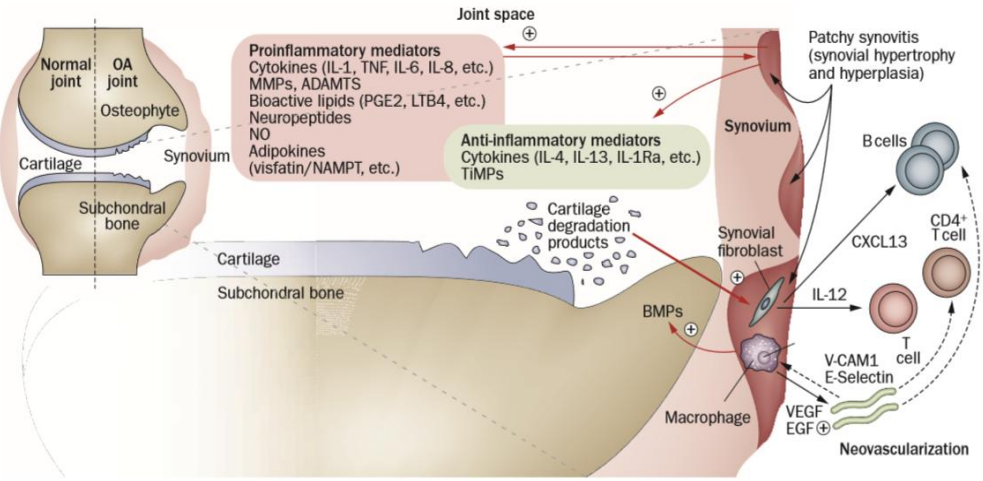

Figure 6: Involvement of the synovium in OA pathophysiology. Cartilage degradation products are released and phagocytosed by synoviocytes, resulting in amplified synovial inflammation. At the same time, activated synoviocytes produce catabolic and pro-inflammatory factors that lead to the overexpression of proteolytic enzymes responsible for cartilage degradation, creating a positive feedback. The inflammatory response is amplified by activated synovial T cells, B cells and infiltrating macrophages. To counteract this inflammatory response, the synovium and cartilage may produce anti-inflammatory cytokines. In addition to these effects on cartilage inflammation and breakdown, the inflamed synovium contributes to the formation of osteophytes via BMPs. Image from Sellam, J. & Berenbaum, F. Nat. Rev. Rheumatol. 2010.

6. Bone

Bone structure and composition is adapted via cell-mediated processes involving osteoblasts, and osteoclasts that synthesize or absorb bone, respectively, in response to biomechanical factors. The bone beneath the articular layer is organized into a plate-like layer called subchondral bone, that is made of cortical (compact) bone, and the subchondral trabecular bone which is a contiguous region of cancellous bone[131] (Figure 7). Distinctions between the subchondral plate and subchondral trabecular bone might not seem clear, but these two tissues are differently organized, adapt to mechanical loads in different ways, and have quite different mechanical properties.

There is *in vivo* and *in vitro* evidence of chemical crosstalk between chondrocytes and bone cells[132], For example, Sanchez *et al*. have described a co-culture system[133,134], in which osteoblasts derived, respectively, from 'sclerotic' (more severely osteoarthritic) or 'non-sclerotic' regions of the subchondral bone in human patients with knee OA were separated by a membrane from chondrocytes that were derived from the articular knee cartilage and grown in alginate beads. Compared with chondrocytes cultured alone chondrocytes in the presence of 'sclerotic' osteoblasts, but not 'non-sclerotic' osteoblasts, showed reduced production of the cartilage matrix protein aggrecan and increased expression of the cartilage degrading enzyme, matrix metalloproteinase MMP-3 and MMP-13. In response to the altered mechanical and biochemical environment during OA, bone cells (osteoclast, osteoblast and osteocytes) show a different profile of gene expression. These modifications mediate changes in this tissue, mainly reflected in an increased thickness in the cortical plate, alterations in the subchondral trabecular bone architecture and bone mass, formation of bone cysts (fluid-filled

holes), and appearance of bone marrow lesions and osteophytes (bony outgrowths at the joint margins)[135].

7. Pathophysiology of OA

OA has been commonly described as a non-inflammatory disease in order to distinguish it from 'inflammatory arthritis', such as rheumatoid arthritis (RA). Despite this, inflammation is increasingly recognized as contributing to the symptoms and progression of OA[136]. Inflammatory cytokines (such as IL-1 and TNF-α), chemokines, and other inflammatory mediators are produced by cells from the principal tissues implicated in OA: synovium, subchondral bone and cartilage. In fact, synovial membrane inflammation is one of the principal processes that take place in the development of the disease, along with degradation of the articular cartilage and subchondral bone affectation, mainly by neovascularization, sclerosis and new bone formation (osteophytes). Therefore, three main processes are implicated in the OA pathophysiology: angiogenesis, inflammation and degradation. These three processes are also deeply related with the main OA symptomatology: swelling and pain[137].

7.1. Angiogenesis and inflammation

In normal joints, oxygen pressure in synovial fluid ranges from 50 mmHg to 60 mmHg[138]. However, during the development of OA the inflammation of the synovial membrane increases the oxygen demand of this tissue that cannot be compensated by the vascular expansion of the hyperplastic synovium[139]. Under hypoxic situations, the hypoxia-inducible factor 1 (HIF-1) is the major activated transcription factor and is the mainly responsible for the "angiogenic switch"[140]. It activates the expression of target genes involved in essential pathways regulating cellular survival under conditions of hypoxia, such as angiogenesis

and glycolysis. Under normal oxygen tension, the HIF-1a subunit is marked for ubiquitination and rapid proteosome-mediated degradation by the von Hippel-Lindau tumor suppressor (pVHL). During hypoxia, ubiquitination and degradation are inhibited, increasing the steady-state level of HIF-1a protein in the cytoplasm. HIF-1a subsequently translocates to the nucleus, where it dimerizes with HIF-1b, the constitutively expressed HIF-1 subunit, forming the transcription complex HIF-1[141]. In addition to hypoxia, HIF-1a expression can be induced by numerous other factors, including inflammatory cytokines, reactive oxygen species (ROS)[142], nitric oxide, and hormone-like growth factors, such as Insulin-like growth factor (IGF)[143] and TGF-b (Transforming Growth-factor b)[144].

Physiological angiogenesis is controlled by a balance between endogenous pro- and anti-angiogenic factors. The most potent pro-angiogenic molecule is the vascular endothelial growth factor (VEGF). In mammals, five VEGF ligands, which occur in several different splice variants and processed forms, have been identified so far. These ligands bind in an overlapping pattern to three receptor tyrosine kinases (RTKs), known as VEGF receptor-1, -2 and -3 (VEGFR1–3). It was recently demonstrated that compared to normal, human inflammatory synoviocytes from OA patients produced more VEGF and less anti-angiogenic factors[145]. On the other hand, the inhibitory effect of Tumor necrosis factor superfamily 15 (TNFSF15) (also known as VEGI or TL1A) and Thrombospondin 1 (TSP1) on angiogenesis has been largely described[146,147]. VEGI, a cytokine produced predominantly by EC in established blood vessels, is a specific inhibitor of EC proliferation[148]. TSP1 inhibits angiogenesis directly by blocking endothelial cell proliferation, migration, and apoptosis, and indirectly by reducing the availability of angiogenic factors[149]. TSP1 synthesis is paralleled by a strong decrease in TSP1 protein expression in severe osteoarthritis[150].

In the pathophysiology of OA, inflammation can occur locally, within the synovium, and systemically, with inflammatory agents circulating in the blood. In early OA, as an attempt to repair, the chondrocyte exhibits a transient proliferative response, increasing the synthesis of cartilage matrix, cytokines and matrix-degrading enzymes. Elevated levels of inflammatory cytokines have been measured in OA synovial fluid[151,152] and have been shown to play important roles in the destruction of cartilage, synovitis, and pain. One of the most influent pro-inflammatory cytokine on the pathophysiology of OA is IL-1β. In short, IL-1β suppresses the synthesis of type II collagen[153] and aggrecan[154], induces the production of MMPs[136] and other inflammatory cytokines such as IL-6 and IL-8[155], and plays an important role in pain sensitivity[156]. Breakdown products from damaged cartilage act as damage-associated molecular patterns (DAMPs) and are released into the synovial cavity where they initiate synovial inflammation. Hence, immune cells are attracted into the synovium, angiogenesis is increased and chondrocytes behavior shifts towards a hypertrophic phenotype, characterized by type X collagen synthesis. This process results in a positive feedback, as chondrocytes produce additional inflammatory cytokines and proteolytic enzymes that eventually increase cartilage degradation and induce further synovial inflammation.

7.2. Degradation of the articular cartilage

Tissue breakdown is a sequential process that begins at the articular surface with the digestion of non-collagenous proteins[96,157,158] and continues by degrading the type II collagen fibrillar network[159,160]. The degraded components of the ECM are dragged through the matrix and out the surface, further softening the matrix. Even though the chondrocytes produce increased amounts of the proteoglycan components in response to matrix damage, there is limited proteoglycan aggregation and immobilization within the matrix due to the loss of the collagen structural integrity. Several proteases are implicated in the ECM cartilage degradation mainly grouped as serine proteases, cysteine proteases and metalloproteinases that in turn comprise matrix metalloproteases (MMPs), a disintegrin and metalloprotease (ADAMs) and a disintegrin and metalloproteinase with thrombospondin motifs (ADAMTs).

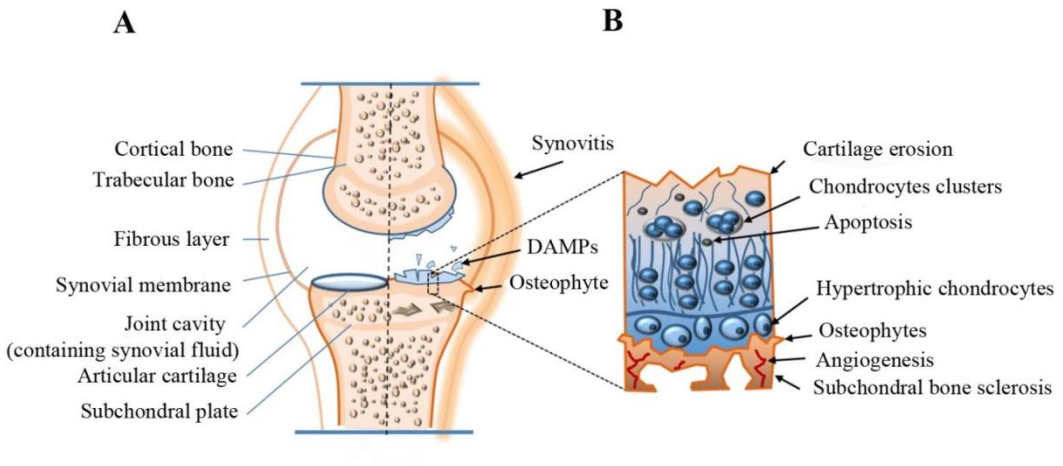

Figure 7. Properties of an OA joint. Hallmarks of OA such as synovial membrane inflammation, cartilage degeneration with the release of danger-associate molecular patterns (DAMPs), osteochondral bone formation (osteophytes) **b)** magnification of a cross-section of the tissue with evidence of subchondral bone sclerosis, hypertrophic chondrocytes, apoptotic chondrocytes, and chondrocyte clusters. Image modified from Martel-Pelletier J *et al.* Nat Rev Dis Primers. 2016.

7.2.1. ADAMTs

In OA, the larger proteoglycan aggrecan is digested by members of the proteinase family ADAMTS (A disintegrin-like and metalloproteinase domain with thrombospondin type 1 motif), specially ADAMTS-4 and ADAMTS-5. They have the characteristic conserved ADAM-like protease domain: an N-terminal signal sequence that is followed by a pro-domain, a metalloprotease domain, a disintegrin domain and a cysteine-rich region usually containing an EGF repeat. Most members of the ADAMs family also have a transmembrane domain followed by a cytoplasmic tail at the C-terminus. Although the metalloprotease domains are relatively well conserved, only 15 of those identified contain the catalytic site consensus of the zinc-binding peptidase (HEXXH), and are thus, predicted to be catalytically active. The rest are probably lacking in metalloprotease activity. However, ADAMTs differ from conventional ADAMs with a distinct feature: a thrombospondin type 1 (TSP1)-repeat found between the disintegrin-like and the cysteine-rich domain. This is also followed by a varying number of TSP1-like repeats at the C-terminus. Importantly, unlike the ADAMs, these proteins lack transmembrane domains and are, therefore, secreted into the ECM. ADAMTS-4 and -5 are also named aggrecanase-1 and -2, respectively, due to their capacity to cleave aggrecan in an exclusive site between Glu373 and Ala374[161].

Cleavage of aggrecan liberates the major part of the molecule from the cartilage which affects the compressive resistant and shock absorbing capability of the tissue under loading. Nevertheless, in early OA there is a compensatory increase of aggrecan synthesis that replaces the lost molecules[162]. In vivo studies suggest that dual inhibition of ADAMTS-4 and ADAMTS-5 may be a reasonable strategy for inhibiting aggrecanase activity in human OA since the

double knock out mice presented a protection against OA without affecting normal physiology[163].

7.2.2. MMPs

Matrix metalloproteinases (MMPs)[164] are a family of zinc dependent endopeptidases able to degrade most of the components of the ECM.. There are four subfamilies of MMPs mainly classified by its preferred substrate; collagenases, stromelysins, gelatinases and membrane-type matrix metalloproteinases. Canonical MMP structure consists of an N-terminal signal sequence for secretion, a pro-domain for latency, a catalytic domain with a zinc motif linked to a C-terminal hemopexin (Hpx) domain[165] by a hinge region. The Hpx domain is designed as a four–bladed propeller with the first and fourth blades connected by a disulphide bridge. Several functions have been conferred to this domain, mainly related to substrate recognition and inhibition, as it has been described to contribute to the binding of tissue inhibitor of metalloproteinases (TIMPs). MMPs are secreted as latent pro-enzymes and are activated by proteases, such as MMP-14 and MMP-2[166], or intracellularly by other mechanisms[167,168].

7.2.3. Collagenases

Collagenases (collagenase-1 [MMP-1][169], collagenase-2 [MMP-8][170] and collagenase-3 [COL3, MMP-13][171] have the ability to degrade non-collagenous and non-fibrillar collagen ECM components, as well as to destabilize the fibrillar collagen triple-helix and digest its fibers. Collagenases have the capacity to unwind the triple helix and cleave the native helix of types I, II, and III fibrillar collagens at a single peptide bond, generating fragments approximately 3/4 and 1/4 the size of the original molecule[172]. MMP-8 is the predominant collagenase

in healing wounds and its overexpression is involved in the pathogenesis of non-healing ulcers[173]. In OA, MMP-1 is the most abundant protease while MMP-13, presents the higher collagenolytic activity[174]. Of note, it cleaves type II collagen between six and seven times more efficiently than type I or III collagen[166,174]. COL3 was firstly described in breast tumours[164], and for a long time it was thought to be only expressed in foetal development and overexpressed in healing and pathological processes, such as arthritis. However, recently it has been shown that COL3 is constitutively produced by healthy human chondrocytes but rapidly endocytosed by the receptor LRP1 and finally degraded[175]. Many factors are implicated in the complex regulation of COL3 production by chondrocytes. Interleukin-1α (IL-1α), a major cytokine implicated in arthritic inflammation and cartilage/bone destruction[176], is one of the most studied factors. Due to its elevated presence in OA process and its degrading efficiency, COL3 has become a target for the inhibition of the arthritic progression. Early broad spectrum MMP inhibitors have been ineffective because of their toxicity; therefore the current research is focused in the development of specific COL3 inhibitors with reduced side effects[177].

Studies have demonstrated that COL3, in contrast to other MMPs, is transcribed in different mRNA transcripts[178]. It has been described that chondrocytes produce five different COL3 RNA transcripts that are derived from alternative polyadenylation sites, internal deletion, alternative splicing and different transcription initiation sites. Moreover, it was also demonstrated the potential of each of these transcripts to be translated into a cellular environment[178]. Among these transcripts, two of them, derived from alternative splicing, the COL3-DEL and COL3-9B isoforms, demonstrated a modified Hpx domain, suggesting catabolic and regulatory activities different from the canonical COL3. COL3-DEL is translated with an internal deletion and an

addition of 4 amino acids, and COL3-9B is translated with an additional exon (exon 9 added) resulting from a non-spliced intron. They have an amino acid sequence identical to canonical COL3, except for the Hpx domain. The deletion in the COL3-DEL isoform leaves intact the first two blades but the last ones are removed. For COL3-9B, three blades are complete, but the sequence of the last one, although of similar size, is altered because of the non-spliced intron, preventing the establishment of the disulphide bridge.

8. Animal models of OA

Animal models play a key role in order to study the pathophysiology of OA and to test new potential drugs. Different animals can be used depending on the type and length of the experiments. Small animals such as mouse and rat are easy to handle, and the induction of OA is simple, fast and reliable. Moreover, the use of genetic engineering technics in order to generate transgenic mice has been well stablished[179]. However, the efficacy of the drugs studied may not be directly translatable to human due to the differences in anatomy and histology and molecular components between rodents and humans. In these cases, the use of large animal models is a better choice due to a more similar anatomy to humans. For instance, the cartilage thickness of dogs is less than half the size of humans, while the cartilage of mice is at least 70 times smaller than in humans[179].

As mentioned before, OA can be classified into primary and secondary based on the etiology of the disease. According to this classification, there are animal models for primary OA such as naturally-occurring or spontaneous OA models, and for secondary OA such as surgically-induced models. OA develops spontaneously on certain mice strains after a long period of time, what makes them less appropriate for short studies. Commonly used surgically-induced

models include anterior cruciate ligament transection (ACLT), and destabilization of the medial menisci (DMM). DMM model is preferred over the ACLT model, as it induces a slowly-progressive and moderate OA allowing for the evaluation of disease modifying drugs. Instead, ACLT model produce a severe OA, and surgery is much more difficult to perform and therefore, it requires a greater exposure of the tissues to the environment, increasing the risk of infection[180].

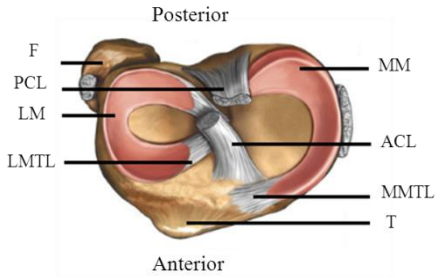

Figure 8. Diagram of the superior (top) view of the right knee joint. T = tibia; F = fibula; MM = medial meniscus; LM = lateral meniscus; ACL = anterior cruciate ligament; PCL = posterior cruciate ligament; MMTL = medial meniscotibial ligament; LMTL = lateral meniscotibial ligament. The MMTL is transected to generate destabilization of the medial meniscus (DMM). *Image modified from http://www.nucleusinc.com*

OBJECTIVES

The objectives of this thesis are grouped into three chapters. A brief summary of the initial hypothesis precedes each chapter.

CHAPTER 1:

COL3-DEL, a newly discovered MMP-13 isoform with a deletion in the hemopexin domain, is expressed in osteoarthritic cartilage and exhibits differential proteolytic activity

Hypothesis: Five different transcripts from COL3 cDNA were found in a cDNA library. Our hypothesis was that:

1. At least two, COL3-DEL corresponding to a deleted form and COL3-9B corresponding to a form with an extra exon, are expressed and translated into proteins and can be detected in samples from OA patients.

2. In order to produce COL3 isoforms, our hypothesis is that the baculovirus system is adequated for the expression of functional recombinant proteins in insect cells.

3. The modifications on the Hpx domain of collagenases alter their enzymatic activity, and therefore, our hypothesis is that COL3 isoforms present different proteolytic activities compared to canonical COL3.

Objectives:

1) Characterize the presence of the COL3 isoforms in human OA cartilage using polyclonal specific antibodies.
2) Produce the recombinant COL3 isoforms in sf9 insect cells and purify them from the culture media.
3) Analyze COL3 isoforms proteolytic activity against SLRPs from different classes.

CHAPTER 2:

***In vivo* effect of OPTC deficiency during development and OA.**

Hypothesis: OPTC is a class III SLRPs firstly described in eye, but also present in other tissues, such as cartilage and synovial membrane. Some studies suggest that OPTC binds non-covalently to collagen fibrils and studies in SLRPS-KO mouse models suggest that SLRPs regulate fibril morphology, spacing, and organization. Therefore, our hypothesis was that:

1. DMM surgery is a good OA induction model for the study of OPTC role in the development of the disease.

2. OPTC has a protective role in OA articular joints and therefore, after DMM surgery, *Optc*$^{-/-}$ mice present more articular joint defects than *Optc*$^{+/+}$, evidenced by higher cartilage degradation, elevated synovial hypertrophy and higher expression of pro-inflammatory and catabolic mediators.'

Objectives:

1) Confirm OPTC expression in mice knee articular cartilage.
2) Induce OA by DMM method on 10-weeks-old *Optc*$^{-/-}$ and *Optc* $^{+/+}$ mice
3) Analyze the effect of OPTC deficiency on OA development, evaluating the cartilage degradation and synovial membrane hypertrophy 10-weeks after the DMM surgery.
4) Compare the expression of pro-inflammatory, catabolic and anabolic markers between *Optc*$^{-/-}$ and *Optc*$^{+/+}$ mice.
5) Analyze the production in cartilage of different SLRP members in *Optc*$^{-/-}$ mice.
6) Analyze collagen fiber ultrastructure and organization.

CHAPTER 3:

Chondroitin sulfate effect on OA synovial fibroblasts under inflammatory and hypoxic environment.

Hypothesis: Inflammation is a remarkable feature of OA. As response to this process there is a gene expression activation cascade that encompasses the establishment of a hypoxic cell environment. Our hypothesis are:

1. The hypoxic environment established in OA joints is in part responsible of the neovascularization process developed in OA synovial membrane.

2. CS, a drug for knee and hip treatment, and suspected to have anti-inflammatory effect, is also able to modulate the angiogenic process associated with OA progress

Objective:

1) Mimic hypoxic and inflammatory conditions *in vitro* on human OA synoviocytes.
2) Study the expression and production of angiogenic mediators by OA synoviocytes, under hypoxic and/or inflammatory conditions.
3) Study the effect of CS pre-treatment in human OA synoviocytes culture regarding the modulation angiogenic mediators.
4) Study the interaction between OA synoviocytes secretome and endothelial cells behaviour under hypoxic and/or inflammatory conditions, with or without CS pretreatment.

MATERIALS AND METHODS

Human biological samples collection

- **Cartilage specimens**

Knee cartilage was obtained from patients previously diagnosed with OA according to the American College of Rheumatology clinical criteria who underwent total knee arthroplasty., and that had not received intra-articular steroid injections or any medication that would interfere with bone and cartilage metabolism within the three months preceding surgery.

- **Synovial membrane**

Synovial membranes were obtained from OA patients with grade III or IV in the KL scale, undergoing total knee joint replacement. All OA patients were evaluated by a certified rheumatologist and diagnosed based on the criteria developed by the ACR Diagnostic Subcommittee for OA [20]. At the time of surgery, they were treated with analgesics and/or nonsteroidal anti-inflammatory drugs (NSAIDS). None had intra-articular steroid injections within 3 months prior to surgery.

Cell Culture

- **Synoviocytes cell culture**

Each synovial membrane was aseptically dissected from underlying fibrous and fatty tissues and rinsed in cold PBS. For cell releasing, sequential enzymatic digestion was performed with 1 mg/ml trypsin (SigmaAldrich Oakville, ON, Canada) for 1 h, followed by 6 h with 2 mg/ml collagenase (type IA, SigmaAldrich) at 37°C in DMEM (see annex). Synovial fibroblasts were then seeded in high density (10^5 cells/cm^2) in tissue culture flasks (Falcon (3824, Lincoln Park, NJ, U.S.A.), and cultured until confluence in DMEM at 37°C in a

humidified atmosphere of 5% CO2. At the end of the incubation period, the cells were trypsinazed and counted in a Neubauer chamber. Cells were then seeded in different conditions depending on the experiment (see table 5). In order to synchronize the cell cycle, FBS was reduced to 0,5% 24h before starting the treatments. To study the effect of CS on hypoxic and inflammatory response, cells were pre-treated with or without 200µg/ml of CS (CS*b*Bio-Active®, Bioibérica, Spain) for 24h and then, stimulated with or without IL-1β (casa comercial) (100 pg/ml), to mimic inflammation[181], and with or without $CoCl_2$ (150µM) for 4h, to mimic hypoxia[182]. Cell viability was confirmed by light microscopy before starting experiments analysis to assure cell integrity after the treatments.

Experiment	Well plate	Cells/well	Culture medium (ml)
E.L.I.S.A	24 w-p	150.000	1
mRNA extraction.	12 w-p	300.000	2
Nuclear extraction.	6 w-p	600.000	4

Table 5: Synoviocytes cells density and culture medium volume used for different cell culture plates depending on the final experiment.

- **Human umbilical vein endothelial cells (HUVECs)**

HUVEC cells were kindly provided by Dr. Royal from the University of Montreal and were cultured at high confluence (5000 cel/cm^2?). on 0,2% gelatin-coated tissue culture dishes with M200 medium (see annex). For the experiments only cell from passage 1 to 4 were employed.

RNA expression study

- **RNA Extraction with TRIzol® REAGENT (Thermo Fisher)**

The mRNA collection was done following RNase free conditions and the procedure was different depending on the source:

- **mRNA extraction from cell culture:** Culture medium from synoviocytes cell cultures were removed and cells were lysed in 1ml TRIzol® Reagent and collected to RNase free tubes. Samples were incubated for 5 min at RT to ensure a complete cell membrane lysis.
- **Mice cartilage tissue:** Femoral and humoral heads were carefully dissected, washed in PBS and immediately deposited in 500 µl TRIzol® Reagent. Tissue was homogenized with a Polytron homogenizer (Kinematica, Bohemia, USA).

In order to separate RNA, DNA and proteins in different density phases, 0.2ml of chloroform was added per 1 ml TRIzol® Reagent. Samples were shacked vigorously (by hand) for 15 sec. and incubated for 2-3 min. at RT. To easily identify the three phases, samples were centrifuged at 12000g for 15 min at 4ºC. RNA is found in the top aqueous phase; therefore it has to be transferred carefully into a new tube, without touching the interphase to avoid DNA contamination. RNA was then precipitated by adding 0.5 ml of isopropanol and 1µl of glycerol per 1 ml TRIzol® Reagent and incubated for 10 min. at RT or overnight at -20ºC for better precipitation. After centrifuging at 12000g for 10 min at 4ºC, supernatant was carefully discarded. RNA pellet was washed with 1ml of 75% ethanol per 1 ml TRIzol® Reagent, mixed and vortex. Samples were centrifuged at 12000g for 5 min at 4ºC. Supernatant was discarded and the RNA pellet was dried completely. RNA was re-suspended in 25µl RNase-free water.

- **DNase treatment**

RNA samples were subjected to RapidOut DNA Removal Kit (Thermo Fisher) treatment to ensure complete removal of chromosomal DNA. rDNase-I, is an endonuclease that non-specifically cleaves DNA to release di-, tri- and oligonucleotide products with 5´-phosphorylated and 3´-hydroxylated ends[183]. For 25µl of re-suspended RNA, 3µl of 10X DNase buffer, 0,5µl of rDNase I and 1,5µl of dH_2O were added. Samples were incubated for 30minat 37ºC. Reaction was stopped by adding 3µl/sample of DNase inactivating agent. Samples were incubated for 2min and centrifuged at 10000rpm for 5min at RT. Supernatant were transferred into a clean tube and RNA quantified in NanoDrop spectrophotometer (Thermo Fisher).

- **Revers-transcriptase (RT) and real-time PCR reaction**

The RT reactions were primed with random hexamers and real-time quantitation performed in the GeneAmp 5700 Sequence Detection System (Applied Biosystems, Foster City, CA, USA) with QuantiTect SYBR Green PCR Master Mix (Qiagen, Valencia, CA, USA), used according to the manufacturer's specifications. Data of representative SLRP members from each class (table 6) were collected and processed with Rotor-Gene Q6 software version 6.1 (Corbett Research, Mortlake, CIC, Australia) and given as a threshold cycle (C_T).

Gene	Sense	Anti-sense
Asporin	5'-GGTCAGGGGCAAATACCAAGGACTCT-3'	5'-CTCTACATGGTTGTCAGGAATGTG-3'
Biglycan	5'-CTGAGGGAACTTCACTTGGA-3'	5'-CAGATAGACAACCTGGAGGAG-3'
Chondroadherin	5'-CAGTCTGGTCTTTCTTGCCA-3'	5'-ATGTCGTTGTGGGACAGGTA-3'
Decorin	5'-TTGTCATAGAACTGGGCGGC-3'	5'-CAGACCTTGAGGGATCGCAG-3'
Epiphycan	5'-GGTCAGGGGCAAATACCAAGGACTTCT-3'	5'-CTCTACATGGTTGTCAGGAATGTG-3'
Fibromodulin	5'-TCAACCCAAGAGACAAAAATGCAG-3'	5'-CTCAGAGGGCTCATAGGGGT-3'
Lumican	5'-GAGTAAGGTCACAGAGGACTTGC-3'	5'-ATTCTGGTGCACAGTTGGGT-3'
Nyctalopyn	5'-GCCGGGTTTTAAAGCATACA-3'	5'-GCCTGACACCCAAAGTTGTT-3'
Osteoglycin	5'-CTACTGTGAAGAAGTTGACATTGATGCTG-3'	5'-GGTAAATTAGGAGGCACAGATTCCAGG-3'
Podocan	5'-GCAGGAGGATGAGCATTAGC-3'	5'-TCTGGTCATTTGGGCTTTTC-3'
PRELP	5'-CTGCAGTCCGTGGTCATCTA-3'	5'-TTTAGACCGGAGCAGGTTA-3'
Tsukushi	5'-GAACCCTCTGGCTACCATCA-3'	5'-GCCTGAAAACACCTCAGCTC-3'

Table 6: Sequences of the mouse gene-specific primers used for qPCR.

DNA sequencing

- **Genotyping *Optc* mice**

Routine genotyping was carried out on DNA from ear punch biopsy samples using specific primers. Genomic DNA was isolated with Direct PCR lysis reagent containing proteinase K (Qiagen Biotech) according to the manufacturer's instructions. The polymerase chain reaction (PCR) was performed on the DNA isolated using primers that could differentiate between *Optc*$^{-/-}$ and *Optc*$^{+/+}$ mice (see table 7). Schematic representation of the *Optc*$^{-/-}$ construct and primer design is illustrated in Figure 9. The presence of the 400bp band indicates amplification of the fragment corresponding to the knocked out *Optc* gene, while the 350bp corresponds to the wild type gene and the presence of the two bands indicates heterozygosis.

Gene	Sense	Anti-sense
***Optc*$^{-/-}$**	5'-CAAGCTCCATCCATCCAAGAA-3'	5'-TGTGGCTGATGTGGTTGAA-3'
***Optc*$^{+/+}$**	5'-CAAGCTCCATCCATCCAAGAA-3'	5'-CTTCTGGTGGAGATGATGACTG-3'

Table 7: Primers used for *Optc* mRNA expression in mice ear samples for genotyping.

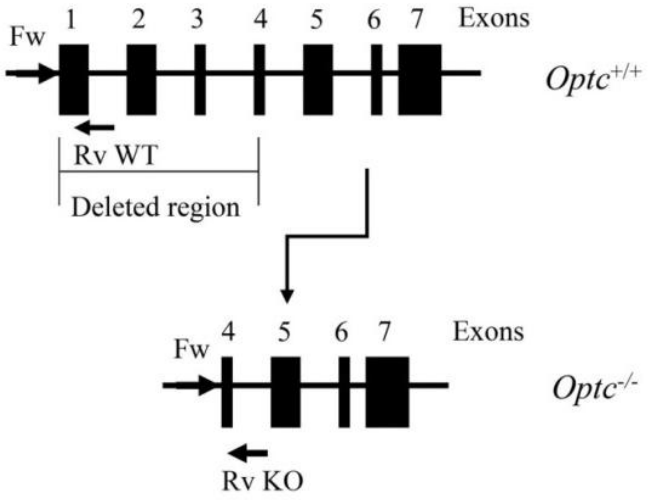

Figure 9. Representative diagram of mouse *Optc* gene indicating the deleted region in *Optc*$^{-/-}$ mice and the position of genotyping primers forward (Fw), reverse wild-type (Rv WT) and reverse knockout (Rv KO).

Protein extraction and purification

- **Cartilage protein extraction and purification**

Human: cartilage tissue was cut into slices of about 2 mm^3 and washed in PBS 1x. Sections were incubated with four-fold excess (weight/volume) of 4M GuHCl (Thermo Fisher Scientific, Burlington, ON) in 0.1 M sodium acetate (pH 6.0) containing a cocktail of protease inhibitors (cOmpleteTM EDTA-free, Roche, Laval, QC) at 4ºC with continuous stirring for 48 h. The extract was then filtered through glass wool, and dialyzed (see Figure 10) for 48 h against dialysis buffer (see annex).

In the case of chapter 1, immunoprecipation of COL3 isoform from the protein extract were performed following the next protocol. To avoid unspecific protein binding, samples were first pre-cleared with non-related goat antibody and agarose beads for 3 h at 4ºC, with continuous stirring. After centrifugation, pre-cleared supernatants were incubated with COL3 mouse monoclonal antibody (R&D Systems, Minneapolis, MN), overnight at 4ºC, in order to allow antigen-antibody binding. Agarose beads conjugated with goat anti-mouse IgG (whole molecule) (SigmaAldrich) were added to the samples and incubated for 48 h at 4ºC. Immunoprecipitation of the antigen-antibody conjugate was performed by centrifugation at 12000 rpm for 10 min.

In the case of samples for 2D gel electrophoresis, the protocol for proteins extraction were as follows. Cartilage tissue was crushed at -80C with a pestle and proteins were extracted with 500 mM NaCl 50mM HEPES pH=7.2 and protease inhibitors for 1h at RT under continuous agitation. Posterior to centrifugation at 6000g for 5min, GAGs were quantitated and precipitated from the supernatant with 1% cetylpyridinium chloride (CPC)[184] for 1h at RT under continuous

agitation. Posterior to centrifugation at 12000g for 5min at 4C, supernatant proteins were quantitated and purified with the “clean up kit” from Amersham

Mice: cartilage tissue was obtained from femoral and humorous heads of newborn (P03) and adult (10-weeks-old) mice and was processed as mentioned above. Compared to human, mice cartilage tissue is very small, so the protocol had to be adjusted: after extraction for 48 h at 4 ºC the samples were centrifuged at 15000g for 15 min and supernatants were subjected to buffer exchange. Due to the low volume of the supernatant recovered (approx. 100µl) a specific method was followed to perform the dialysis with the proper buffer (see annex). Samples were placed in a 1,5ml tube with a modified cap where a hole has been sliced. A dialysis membrane was placed in between the tube cap and the tube, in a way that the buffers could be exchanged through the hole (see figure 10). Dialysis buffer was changed 5 times during 48 hours. The extracts were cleared by centrifugation, and the supernatant was subjected to precipitation with 9 volumes of 95% ethanol. The protein precipitates were re-precipitated twice with 9 volumes of 95% ethanol after resuspension in 0, 05 M NaOAc, pH 5.8. Finally, the precipitates were dissolved in SDS-polyacrylamide gel electrophoresis sample buffer for further analysis by Western Blot.

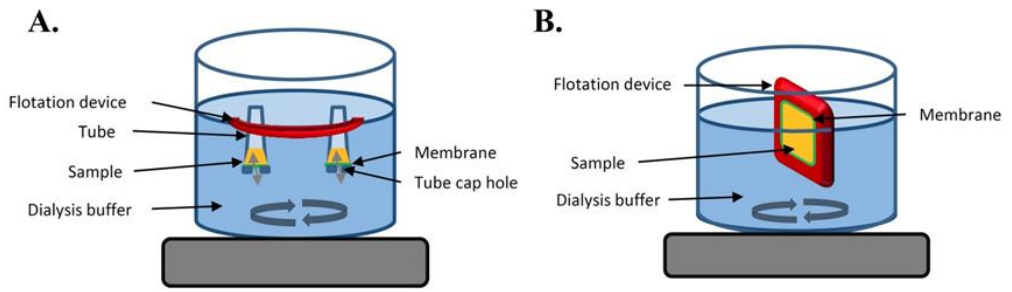

Figure 10: representation of the procedure of small volumes (A) and big volumes (B) dialysis.

- **Sf9 insect cells protein production and purification**

The recombinant human COL3 isoforms (COL3-DEL and COL3-9B) were expressed in a baculovirus/Sf9-cell expression system according to the manufacturer's protocol (Bac-to-Bac® Baculovirus Expression System, Thermo Fisher).

Briefly, COL3 cDNA fragments previously obtained from the cDNA library and cloned into the vector pRC-CMV2[178] were subcloned into the vector pFastBacTM1 (Thermo Fisher). DH10 bacteria transformation was carried out with the vector donors containing the cDNA sequence of each COL3 isoform (COL3, COL3-DEL and COL3-9B). Recombinant bacmids containing COL3 isoforms were produced by transposition. The verification of the cloned and transferred sequences was performed by DNA sequencing. Once confirmed, the recombinant bacmid constructs were extracted and transfected to Sf9 cells using a Cellfectin (Thermo Fisher) transfection reagent according to the manufacturer's instructions. Briefly, Sf9 cells in the log phase and adapted to serum-free medium were seeded in 6-well tissue culture plates at 9x105 cells/well. For each transfection sample, bacmid DNA (1 µg)-Cellfectin® Reagent complexes were prepared and added to each well containing cells. They

were cultured in 2 ml unsupplemented Grace's insect medium without antibiotics/antimycotics (Thermo Fisher), at 27°C without CO_2 in a humidified incubator until signs of viral infections were observed. The supernatant of these Sf9 cells was collected and used to amplify baculoviral stock until a suitable titer was reached (10^8 pfu/mL).

For protein expression, Sf9 cells in the mid-logarithmic phase of growth were seeded in 24-well tissue culture plates at a density of 106 cells/well. Baculoviral stock was added to each well at a multiplicity of infection (MOI) of 5 and incubated for 72 h, at which time the medium containing the COL3 isoforms was harvested. Uninfected Sf9 cells and pFastBac™-Gus were used as negative and positive control, respectively.

Proteins expressed from Sf9 cells were concentrated using methylcellulose powder to extract the excess liquid and posteriorly dialyzed against buffer containing 20 mM Tris-HCl, 5 mM CaCl2 and 0.05% NaN3, for 4 h at 4oC. After dialysis, the medium was filtrated through a Sephacryl S300 (Pharmacia Fine Chemicals, Piscataway, NJ). The presence of the eluted enzymes was confirmed by optical density at 280 nm. The selected fractions were subjected to liquid chromatography and the presence of COL3 isoforms was determined by Coomassie Blue staining and by Azocoll activity (Calbiochem, San Diego, CA). This method[185] was also used to perform a relative quantification of each purified isoform. Briefly, 0.5 mM 4-aminophenylmercuric acetate (APMA) in TCNB buffer (50 mM Tris–HCl (pH 7.5), 150 mM NaCl, 10 mM CaCl2 and 0.05% Brij 35 (SigmaAldrich) and a cocktail of protease inhibitors that do not inhibit metallo- and aspartic proteases (CompleteTM EDTA-free, Roche) was added to the fractions selected to activate the latent form of the enzymes, and then incubated with the Azocoll substrate. The zinc chelator EDTA was added to the

fractions (25 mM) to use as blank for the quantification. Enzyme activity was calculated in units of which 1 unit corresponded to the amount of COL3 needed to hydrolyze 1 pg of substrate (Azocoll) in 1h at 37°C. The purified isoforms were named irCOL3, irCOL3-DEL and irCOL3-9B, corresponding to the canonical, the deleted, and the alternative spliced out form, respectively.

- **Nuclear extraction protocol on synoviocytes**

For the nuclear proteins extraction, cells were seeded and cultured as mentioned for mRNA extraction from cell culture section. After a maximum of 5 hours after induction of hypoxic condition in **s**ynoviocytes cell culture (peak of HIF1α nuclear translocation), cells of every conditioned well were washed with cold PBS 1X and a volume of 400µl of Buffer A was added per well. Cells were kept on ice for 10min., scraped vigorously with a cell-scraper and transfer to 1,5ml clean tubes. The collected cells were vortex for 5sec. to ensure cell membrane lysis and centrifuged at maximum speed for 30sec. Supernatants containing cytoplasmic fraction were collected into new tubes and stored at -80°C for further studies. A second centrifugation was carried out in order to remove completely the Buffer A remnants. A volume of 30µl of Buffer C was added to the pellets and they were incubated for 20min. on ice while vortexing 3-4 times to ensure nuclear membrane lysis. After incubation, lysed pellets were centrifuged at maximum speed (14000 rpm) for 2min. at 4°C in order to separate the soluble proteins from nuclear debris. Supernatants containing nuclear fractions were collected into new tubes and proteins quantified by BCA method.

Detection, quantification and activity of proteins in the samples studied

- **BCA protein assay**

Samples were centrifuged to discard debris before starting the total protein quantification. A calibration curve was made with protein standards of 1µg to 30µg of BSA diluted in the same buffer as samples. Samples and protein standards were diluted 1:10 in 50µl of H2O, and added to a 96-well-plate. BCA reagent was prepared according to manufacture indications (Pierce Chemical). A volume of 250µl of BCA reagent mix was added per well and samples were incubated for 30min at RT. Optical density was read at 562nm on a microplate reader, and concentration determined in reference with the calibration curve constructed.

- **PolyAcrylamide Gel Electrophoresis (PAGE) and staining methods**
  - **1D SDS-PAGE**

    Protein samples were boiled for 5 min in 4X sample buffer and were separated by electrophoresis in a polyacrylamide gel with sodium dodecyl sulfate (SDS-PAGE). Gels were prepared in reducing conditions with a concentration of acrylamide:bisacrylamide (37,5:1) from 7.5-12%, according to the expected molecular weight of the protein of interest in each study.

  - **Coomassie blue gel staining**

    The gel was washed with ddH_2O to discard acrylamide leftover pieces. Afterwards, the gel was fixed with fixative solution for 10 min at RT, previous to the Coomassie staining with the working solution (see

annex) for 1h in agitation at RT. To fade the background destaining solution was added and incubated from 1h to O/N.

- **2 dimensional gel electrophoresis**

200 μg of protein extracts prepared for 2D gel electrophoresis were applied to 18cm strips with a pH gradient of 4-7 by passive overnight rehydration (see annex for rehydration buffer composition). The first dimension separation, isoelectric focusing (IEF), was performed at 20°C in an IPGphor instrument (GE Healthcare) for a total of 64,000 Vhr. The second dimension separation was run on an Ettan DALT six system (GE Healthcare) after equilibration of the strips (see equilibration buffer composition in annex 1). Electrophoresis was performed in a 12, 5% polyacrylamide gel at 80mA for 4h with 1X Tris-glycine electrophoresis buffer as the lower buffer (anode) and 2X Tris-glycine as the upper buffer (cathode).

- **Silver staining**

Gels were fixed overnight at 4ºC with fixative buffer (see annex), washed extensively with pure H2O and sensitized with 0.02% thiosulfate. After washing out the thiosulfate, gels were stained with 0,1% AgNO3 at 4ºC. Gels were developed with 3% Na2CO3 and 0,05% Formaldehid. Developing reaction was stopped with 5% acetic acid.

- **Western blot**

Proteins subjected to PAGE, were transferred to nitrocellulose membranes (Hybond-C Extra, Amersham Pharmacia Biotech Piscataway, NJ) in transfer buffer, at 200 mA for 90 min at 4ºCC (1D SDS-PAGE gels) or by semi-dry

transfer method for 75’ at 45V and 400mA (2D SDS-PAGE gels). Membranes were stained with Red Ponceau in order to confirm a correct migration and transference of the proteins. After washing off the rest of colorant, membranes were blocked with TBS-Tween 0, 05% containing 5% of low-fat dry milk for 1h at RT and with continuous agitation. After blocking, membranes were incubated with the appropriate primary antibody (see table 8), prepared at the desired concetration in TBS-Tween 0,05% containing 5% of low-fat dry milk, at 4C O/N with continuous stirring. After primary antibody incubation, membranes were washed with TBS-Tween 0, 05% (3 times for 10 min) and incubated for 1h at RT with a horseradish peroxidase secondary antibody that recognize the IgG of the animal where the primary antibody was generated. Signal was revealed by adding the substrate (Super Signal® West Dura Extended Duration substrate (Pierce Biotechnology), which gives a chemo fluorescence light that can be detected with auto radiographic films or with the ChemiDoc imaging system (Bio Rad). Depending on the conditions GAPDH levels or Coomassie blue staining were used as protein loading control. For multiple protein detection, membranes were stripped with 50mM Tris pH 6, 8 100mM β-mercaptoethanol and 2% SDS, before blocking again the membrane and reincubated it with the new desired antibody.

Antibodies for specific COL3 isoform detection in chapter 2 were not commercially available so different peptides were synthesized in vitro (Peptide Synthesis Facility, University Pompeu Fabra, Barcelona, Spain) for the generation of specific antibodies against each isoform. The epitope selected for the generation of the canonical COL3 antibody corresponds to an exclusive aa sequence of the isoform (table 8). For the COL3-DEL antibody, the peptide synthesized contained four aa specific for the isoform, but also 10 aa in common

with the canonical isoform. For the COL3-9B antibody, the specific peptide selected for its immunogenic properties was also isoform-exclusive (table 8). All peptides were conjugated with keyhole limpet hemocyanin (KLH) as carrier protein.

The rabbit polyclonal antibodies against each COL3 isoform were produced by the Antibody Production Unit of the Autonomous University of Barcelona. Briefly, for each antibody production, two rabbits were first immunized with 1 ml of specific isoform peptide conjugated with KLH (500 μg/ml) emulsified in full Freund adjuvant. The reminder doses were administered every 21 days with incomplete Freund adjuvant up to the 5th immunization. Ten days after the last immunization, the rabbits were exsanguinated and serum collected. Antibody purifications were performed in an affinity column with the specific peptide immobilized. In the case of COL3-DEL, two columns were needed to purify antibodies recognizing only this isoform. The first one contained the peptide previously described that could retain antibodies recognizing both COL3 and COL3-DEL. For the second column the peptide used (CSELGLPKEV) did not include the 4 aa specific for COL3-DEL, retaining the antibodies that could identify the canonical COL3 isoform.

ANTIBODY	ANTIGEN	TYPE	DILUTION	SOURCE
CHAPTER 1:				
Canonical COL3	*SNRIVRVMPANSILWC*	Rabbit polyclonal anti-human	1/1000	
COL3-DEL	*CSELGLPKEVNKL*	Rabbit polyclonal anti-human	1/150	Antibody Production Unit of the Autonomous University of Barcelona
COL3-9B	*SSLQPPPPGFKRFSC*	Rabbit polyclonal anti-human	1/1000	
Fibromodulin	Carboxyl-terminus of the SLRP core proteins[186]	Rabbit polyclonal anti-human	1/1.000	McGill University, Montreal, Canada.
Biglycan		Rabbit polyclonal anti-human	1/1.000	R&D Systems
Lumican		Rabbit polyclonal anti-human	1/5.000	R&D Systems
MMP-13	Leu20-Cys471	Goat polyclonal anti-human	1/1.000	R&D Systems
MMP-13	Leu20-Cys471	Mouse monoclonal anti-human	-	
CHAPTER 2:				
Fibromodulin	337-364 aa from C-t	Rabbit polyclonal anti-mouse	1:1.000	Thermo Fisher
Lumican	64-91 aa from N-t	Rabbit polyclonal anti-mouse	1:5.000	Thermo Fisher

ANTIBODY	ANTIGEN	TYPE	DILUTION	SOURCE
CHAPTER 3:				
VEGFA	Ala207- Arg371			
GAPDH	synthetic peptide near the C-t of hGAPDH			
pP38	Thr180-Tyr182			
HIF-1α	synthetic peptide around Ser653			

Table 8: Antibodies used for protein evaluation by Western blot.

- For COL3 isoforms identification after IP from OA human cartilage extracts, the primary antibody dilutions were 1/150 for the COL3-DEL antibody and 1/1000 for COL3 (isoform specific) and COL3-9B antibodies. In order to avoid cross-reaction between the secondary antibody and the antibody used for the immunoprecipitation, and present in denatured state in the membrane, 1/5000 dilution of protein A conjugated with horseradish peroxidase (Amersham) was used for the second incubation.

- **E.L.I.S.A**

VEGFA, TSP-1 and VEGI levels were quantified by E.L.I.S.A (R&D Systems/Cedarlane Minneapolis, MN, USA, Preprotech, Rocky Hill, NJ, USA), supernatants from synoviocytes cell culture were collected in tubes and kept on ice for E.L.I.S.A analysis. In order to normalize the results from supernatants with the total amount of proteins, cells were washed with PBS and total cell lysate was collected in RIPA buffer with protease inhibitors and 0,5% of SDS and proteins were quantified with BCA method.

- **irCOL3 isoform activity assay**

To assess the activity of each isoform against non-collagenous ECM components, the rate of degradation of three SLRPs (fibromodulin [class II], biglycan [class I], and lumican [class II]) was assessed by Western blot, using proteoglycan extracts from moderated fibrillated OA cartilage. The extracts were incubated for 0-8 h with the three irCOL3 isoforms previously activated with APMA. Briefly, 0.5 mM 4-aminophenylmercuric acetate (APMA) in TCNB buffer (50 mM Tris–HCl (pH 7.5), 150 mM NaCl, 10 mM $CaCl_2$ and 0.05% Brij

35 (Sigma Aldrich, Monsheim, France) and a cocktail of protease inhibitors that do not inhibit metallo- and aspartic proteases (Complete^{TM} EDTA-free, Roche) was added to the fractions selected to activate the latent form of the enzymes. The digestion was performed at a protease/proteoglycan ratio of 1 unit/5 µg. The reaction was stopped by addition of EDTA at a final concentration of 15 mM.

Optc$^{-/-}$ mice experimentation

- ***Optc*$^{-/-}$ mice breeding**

Frozen embryos of *Optc* heterozygous (*Optc*$^{+/-}$) mice were generously provided by Dr. Bishop, University of Manchester, UK[187]. This transgenic mouse model presents a *Optc* gene deletion produced using a targeting vector that encompasses exon 1 to exon 4. Frozen embryos were thaw, washed and transferred to recipients "pseudo-pregnant" albino CD-I (Charles River) females. Females were isolated until the pups were born. The six recovered *Optc*$^{+/-}$ mice became the foundation stock. The only *Optc*$^{+/-}$ female obtained was breed with an *Optc*$^{+/-}$ male. Offspring at three week old were screened for the transgene and a mix of homozygous (*Optc*$^{-/-}$ and *Optc*$^{+/+}$) and heterozygous mice were obtained. We continued to expand the colony until we obtained a significant number of *Optc*$^{-/-}$ and *Optc*$^{+/+}$ for the purpose of these studies. All mice were maintained under a 12-hour light/dark cycle. Food and water were available ad libitum[188]. All procedures involving animals were performed according to regulations of the Canadian Council on Animal Care and were approved by the Animal Care Committee of the University of Montreal Hospital Centre.

- **Procedure for destabilization of the medial meniscus (DMM) in mice**

As shown in Figure 11, OA was surgically induced in 10-week-old male mice (*Optc*$^{+/+}$ and *Optc*$^{-/-}$) for a time of 10 weeks by destabilization of the medial meniscus (DMM) of the right knee as previously described[180,188]. In brief, the mice were anesthetized with isoflurane, and right knee joint was destabilized by transection of the anterior ligament of the medial meniscus to the tibial plateau by a certified surgeon. A SHAM surgery, which involves a similar incision to the knee without compromising the joint capsule, was also performed on the right knee of 10-week-old *Optc*$^{+/+}$ and *Optc*$^{-/-}$ mice as a control. To ensure OA development, mice had free access to the exercise-wheel from the same day of the surgery, and were observed daily in order to verify healing and to ensure comparable use of both limbs.

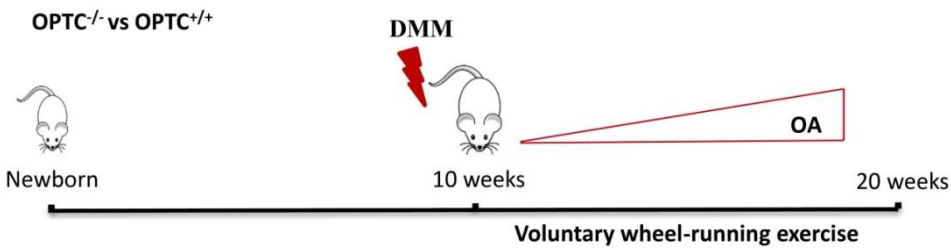

Figure 11: Chronological diagram of OA induction in Optc mice by destabilization of the medial meniscus.

- **Analysis of the effect of DMM in *Optc*$^{-/-}$ mice**

  - **Evaluation of knee joint swelling**

    Knee joint swelling was measured[189] in the mediolateral plane using a digital caliper (model 2071M; Mitutoyo) on DMM (right) knee in *Optc*$^{+/+}$ and *Optc*$^{-/-}$ mice (n=6). Mice were examined at baseline (day 0) and every 3 days following surgery until day 15 post-surgery.

- **Mice length and weight measurements**

  Mice length was measured from the tip of the nose to the base of the tail with a digital caliper of *Optc*$^{+/+}$ and *Optc*$^{-/-}$ mice. Mice were also weighed on a digital scale.

Histology

- **Sample collection and processing**

DMM and SHAM mice were euthanized at 10 weeks after surgery. Non-operated control mice at an equivalent age (20 weeks) were also euthanized. The right knee joints of the specimens were dissected free of tissue, fixed in 4 % paraformaldehyde pH 7,4 for 16 h at 4°C (SigmaAldrich). In order to prepare good-quality paraffin sections, samples were decalcified in 10% EDTA pH 7,3 for 12 days (Wisent, St-Bruno, QC, Canada). Posteriorly, samples were dehydrated in progressively increased concentrated ethanol solutions, followed by xylene incubations. Finally, samples were embedded in paraffin blocks (Paraffin TissuePrep, ThermoFisher). Sections of 5µm were cut in a microtome (Leica RM2145) and mounted on a glass microscope slide Globe Scientific Inc. (Paramus, NJ, USA) the preparations were dried at 40ºC O/N. Previously to staining protocol, samples were deparaffinised in xylene followed by a graded series of alcohol washes.

- **Study of cartilage degradation**

Paraffin sections were stained with Safranin O–fast green (SigmaAldrich). Briefly, after deparaffination, slides were re-hydrated with distilled water and incubated for 5min with Weigert's Iron Hematoxylin. After washing the excess of dye slides were differentiated in 1% Acid Alcohol for 2sec and rinsed in distilled water. Slides were then incubated with 0.02% Fast Green for 1min and

posteriorly in 1% Acetic acid for 30sec. Afterwards, slides were incubated with 1% of Safranin O for 10min and rinsed in 95% EtOH. Slides were then dehydrate and rinsed with xylene before mounting on a coverslip. The severity of the OA cartilage lesions was determined using the OA Research Society International (OARSI) scoring method (table 9)[190].

CARTILAGE STRUCTURE	S-O STAINING	CELLULARITY	SCORE
Normal	Normal/Slight Loss	Normal	0-0,5
Small fibrillations	Slight Loss	Clusters	1
Fibrillations below the superficial layer and some loss of lamina	Moderate Loss	Hipocellularity	2
Erosion extending to the calcified cartilage up to 25% of the cartilage width	Severe Loss	Hipocellularity	3
Erosion extending to the calcified cartilage up to 50% of the cartilage width	Severe Loss	Hipocellularity	4
Erosion extending to the calcified cartilage up to 75% of the cartilage width	Severe Loss	Hipocellularity	5
Erosion extending beyond 80% of the cartilage width including ulceration	Severe Loss	Hipocellularity	6

Table 9. Modified OARSI histologic grading score for murine OA[190].

- **Study of collagen organization.**

Sirius red staining is specific for collagen fibers and it is used to evaluate collagen organization under polarized light. Tightly packed and organized fibers are highly birefringent under polarized light while disorganized and loose fibers show less birefringence[191].

Slides were stained in 0.1% Sirius red stain (F3B/direct red 80 (SigmaAldrich) prepared in saturated picric acid for 1hour. After washing 2x in 0, 5% acetic acid samples were dehydrated in two successive baths of 3' each in 80%, 95%, absolute ethanol and xylene. Finally, samples were mounted and analysed with polarized light microscopy (Leitz Diaplan). Collagen disorganization evaluation was done using a modified scale of 0 – 2, where 2 = normal cartilage (high birefringence); 1 = partial disorganization (less birefringence); and 0 = total disorganization (no birefringence). Three areas were evaluated, and the scores summed (maximum score 6).

- **Synovial membrane hypertrophy**

Histomorphometric quantitative analysis of the anterior synovial membrane thickness was performed on Safranin-O sections. Images were captured at 63X with a Leitz Diaplan microscope (Leica Microsystems,Wetzlar, Germany) coupled to a personal computer, and histomorphometric data determined with Bioquant OSTEO II Image Analysis Software (Nashville, TN, USA); data are expressed as µm. The synovial membrane lining hyperplasia was graded on a scale of 0-2, where 0=absence; 1=hyperplasia of lining <50% of the surface; and 2=hyperplasia of lining >50% of the surface. The synovial membrane fibrosis was graded on a scale of 0-3, where 0=normal, 1=mild, 2=moderate and 3=severe changes.

For each procedure, two independent observers who were blinded with regard to group allocation evaluated the preparations. Three sections were prepared from each block, each slide was examined, and the final score was a consensus between the 2 observers.

Immunohistochemistry

Immunohistochemistry was performed on 5 µm paraffin sections of *Optc*$^{+/+}$ and *Optc*$^{-/-}$ right knees at 10 weeks post-DMM surgery. Antigen retrieval was performed by pretreating with 0.25 units/ml of protease-free chondroitinase ABC (SigmaAldrich) in PBS 1X and 1% hyaluronidase in 0.1M Tris acetate for 60 minutes at 37°C. The specimens were then incubated for 18 hours at 4°C with the following primary antibodies diluted in PBS-Tween 0,1%:

After incubation with primary antibodies, each slide was washed 3 times in PBS (pH 7.4) and incubated with a biotinilated secondary antibody using a Vectastain ABC kit (Vector) and following the manufacturer's instructions. The color was developed with 3,3-diaminobenzidine containing hydrogen peroxide, and slides were counterstained with methyl green.

Following the same experimental protocol the following control procedures were performed: 1) omission of the primary antibody, 2) substitution of the primary antibody with a nonspecific IgG from the same host as the primary antibody (Santa Cruz Biotechnology), and 3) a third control for type-X collagen was performed by adsorption with the peptide YNRQQHYDPRSGIFTCKIPGIYYFSYGGC (provided by Dr. E. Lee, Shriners Hospital for Children, McGill University Hospital Centre, Montreal, Quebec, Canada) at a 10-fold concentration.

ANTIBODY	TYPE	DILUTION	COMPANY
lumican	rabbit polyclonal anti-mouse	1:50	Thermo Fisher
fibromodulin		1:100	Thermo Fisher
epiphycan	rabbit polyclonal anti-human	1:50	SigmaAldrich
biglycan	rabbit polyclonal anti-human	1:100	Proteintech
V-DIPEN*	rabbit polyclonal anti-mouse	1:800	Dr. J. S. Mort, McGill University Hospital, Montreal, Quebec, Canada
type X collagen	rabbit polyclonal anti–rat	1:2000	Abcam, Toronto, ON, Canada

Table 10: Antibodies for immunohistochemistry of mouse cartilage. *anti-C terminal peptide of aggrecan G1 domain fragment generated by MMP cleavage of (does not recognize intact aggrecan). **type II collagen primary cleavage site

For each specimen, positive cells were quantified in 1 assigned microscopic field (250X), and were separated in three groups: cells in the upper zone of the cartilage (first half), cells in the bottom zone of the cartilage (second half) and cells in total area (upper and bottom zones). For each section, using the medial meniscus as a point of reference, the percentage of chondrocytes staining positive was quantified following the determination of the total number of cells with the maximum score being 100%. Each slide was examined by two independent observers and scored blindly.

V-DIPEN staining was graded on a scale of 0–3, with the following punctuation: 0= no staining; 1= minor staining; 2= marked staining; and 3= maximal staining. Each slide was examined and scored by 2 independent observers who were blinded to group allocation.

Transmission electron microscopy (TEM)

Right knees from 10-week-old *Optc*$^{+/+}$ and *Optc*$^{-/-}$ mice were dissected and immediately fixed in 2,5% glutaraldehyde in 0,1 M cacodylate buffer for 24h, washed 3 times with PBS and post-fixed with 1% aqueous osmium tetroxide (OsO_4) and 1,5% aqueous potassium ferrocyanide for 2h at 4ºC, washed 5 times with ddH_2O. Samples were dehydrated through a series of increasing concentrations of acetone: 30%, 50%, 70%, 80%, 3X100%, each for 8 min, and infiltrated with Epon epoxy resin (Cedarlane, Burlington, ON, Canada)/acetone at increasing ratios (1:1, 2:1 and 3:1) during 48h in a rotator. Finally, samples were embedded in a glass mold containing Epon epoxy resin and polymerized at 60 ºC during 48h. Ultra-thin sections (100nm) from the zone of interest were obtained using a microtome (Leica Microsystems UCT ultramicrotome) and coated with 1-2nm platinum. From each specimen, images at 1200X (overview) and 30000X were taken from the deep zone of the cartilage,

Statistical analysis

Statistical significance was assessed by the Mann-Whitney test and one-sample t test where p values ≤ 0.05 were considered significant.

RESULTS

The results of this thesis are grouped into 3 chapters. The three chapters are preceded by a brief summary of the main findings and conclusions.

.

RESULTS CHAPTER 1:

Summary chapter 1: **COL3-DEL, a newly discovered MMP-13 isoform with a deletion in the hemopexin domain, is expressed in osteoarthritic cartilage and exhibits differential proteolytic activity**

Objective: Collagenase-3 (COL3) also known as MMP13, is a matrix metalloproteinase abnormally over-expressed in pathological processes. Several COL3 transcripts are expressed in human chondrocytes although their role in OA is still unknown. This study aimed to characterize the presence of two non-canonical COL3 isoforms, named COL3-DEL (deleted form) and COL3-9B (exon 9 added form) in human OA cartilage, and to analyse their proteolytic activity.

Design: COL3 isoforms were produced and purified from insect cells (insect-recombinant or irCOL3) and protein synthetizes was confirmed by Western-blot assays using polyclonal antibodies obtained from serum of rabbits immunized with specific peptides for each isoform. The same antibodies were used to detect the isoforms in osteoarthritic human cartilage. Catalytic assays were performed against proteins extracted from human OA cartilage and activity study over three proteoglycans was performed: lumican, fibromodulin and biglycan.

Results: COL3-DEL isoform, but not COL3-9B, could be detected in human OA cartilage samples. The catalytic activity of irCOL3-DEL and irCOL3-9B isoforms differed from that of the canonical irCOL3. irCOL3-DEL presented higher activity against lumican and fibromodulin compared to the irCOL3, while irCOL3 was more efficient in the digestion of biglycan. irCOL3-9B isoform showed poor activity against the substrates tested.

Conclusions: Our data confirmed that COL3-DEL isoform is expressed in OA cartilage, and it displays a different catalytic activity than canonical COL3.

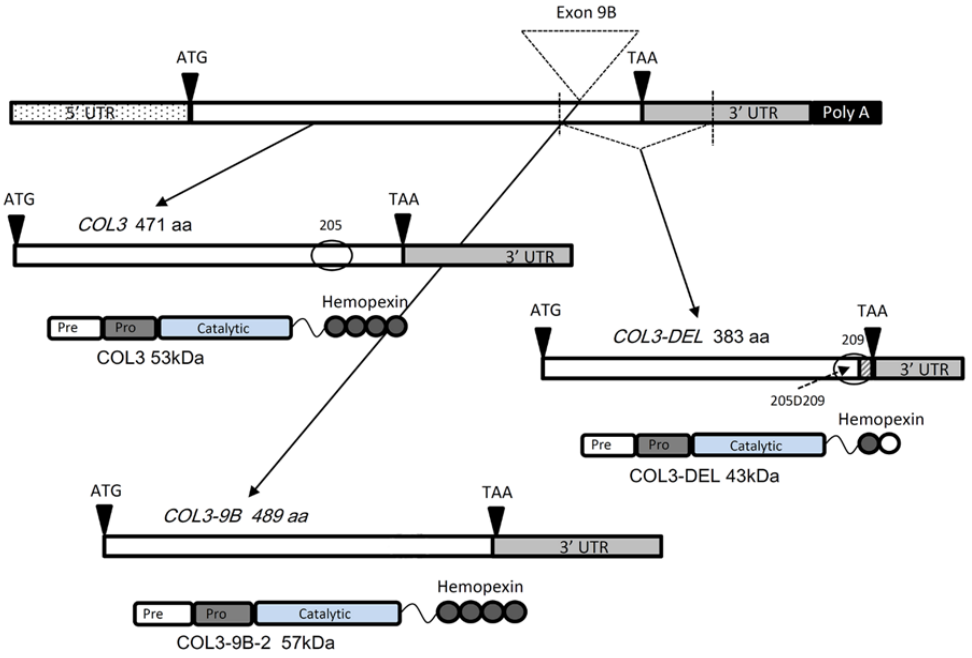

Figure 12: Schematic representation of COL3 transcripts and COL3-DEL and COL3-9B cDNA transcripts downstream of the promoter sequence. The resulting deletion (387 bp) on the COL3-DEL isoform is indicated by a bent line on the original COL3 gene sequence. Under each transcript, there is a representation of the primary structure of each isoform. Pre-, pro- and catalytic domains are represented by rounded rectangles and hemopexin domains are represented by dark circles. The COL3 isoform presents the same structure as the original enzyme and has a molecular weight of 53 kDa. In COL3-DEL, the open circle in the hemopexin domain represents the change due to deletion and insertion of 4 new amino acids (aa). The COL3-9B isoform has an extra exon (exon 9B) coming from intron 9 that usually splices out and consequently the isoform has an expected higher molecular weight (MW) of 57 kDa. The numbers to the right of transcript names represent the number of aa deduced from the DNA sequence and the numbers to the right of isoform names represent the expected MW. The locations of the peptides used to produce the specific antibodies are indicated by circles, and the number above indicates the name of the peptide. Peptide 205D209 corresponds to the nonspecific sequence of COL3-DEL isoform Reproduced in part with permission from Tardif G. et al. OA and Cartilage 2003, 11(7):524-537.

Results

Results 1.1: Study of the COL3 protein isoform presence in human OA samples

In order to confirm that the different COL3 mRNA isoforms described by Tardif *et al.* were translated to protein, the presence of the hypothesized isoforms were studied on protein extracts from OA articular cartilage from patients (n = 16) previously diagnosed with OA that were selected according to the American College of Rheumatology clinical criteria, and underwent total knee arthroplasty. The mean age of the patients was 71±9 (SD) years, and none had received intra-articular steroid injections or any medication that would interfere with bone and cartilage metabolism within the three months preceding surgery. All procedures followed the guidelines of the Institutional Review Board (IRB) of New York University School of Medicine for use of surgically discarded human tissues. The use of human articular tissues was approved by the CRCHUM Ethics Review Board for Research on Human Subjects.

- COL3 isoform antibody (Ab) production:

The specific antibodies produced for COL9B and COL3-DEL were not able to detect the recombinant COL3 protein (Figure 13, A, lane rhMMP-13). In contrast, COL3 Ab generated a signal of the expected size (53kDa) for the canonical COL3 isoform (Figure 13, B).

- COL3 protein isoforms detection in human OA protein extract:

Once the antibodies were purified and their specificity against each isoform was tested, we aimed to detect the COL3 isoforms in protein extracts. The immunoblotting approach was to increase the COL3 isoforms concentration through immunoprecipitation, as they were initially not expected to be

expressed in larger amounts in the tissues. The COL3-DEL Ab was able to detect the isoform as a signal of approximately 50 kDa. Unexpectedly, the identification could be performed not only in immunoprecipitated samples, but also directly in the human protein extracts (Figure 13, A, lane PG's cartilage OA) although, as predicted, with lower signal intensity (Figure 13, A, lane IP mouse monoclonal (m.m) anti-COL3). With regard to COL3-9B, no signal was obtained with the human cartilage protein extract even after IP (data not shown).

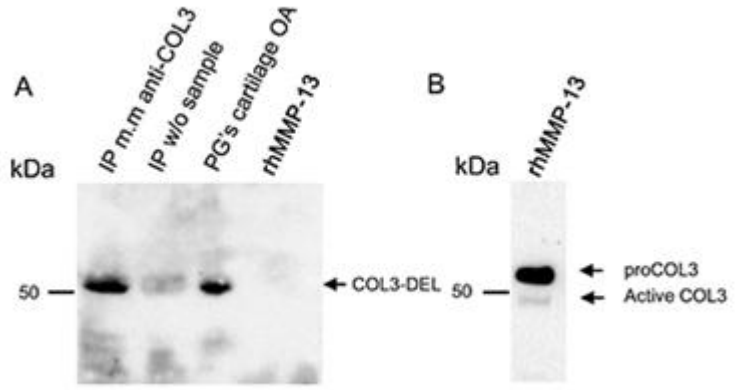

Figure 13. Detection of COL3-DEL isoform in human osteoarthritic cartilage. (A) COL3-DEL detection performed with the COL3-DEL Ab. The following samples were tested: immunoprecipitation of total COL3 isoforms from human OA cartilage protein extract, with a commercial mouse monoclonal antibody (lane IP m.m anti-COL3); immunoprecipitation without sample, only with extraction buffer (negative control, lane IP w/o sample); non-immunoprecipitated cartilage protein extracts (lane PG's cartilage OA); and recombinant human COL3 (lane rhMMP-13) (100 ng). **(B)** Commercial recombinant human COL3 (rhMMP-13) detected with the specific antibody against canonical COL3 generated in the present study. kDa: kilodaltons.

- Confirmation of COL3-DEL protein isoform detection by 2-dimensional electrophoresis.

COL3-DEL specific antibody that was able to detect the isoform as dotted area of approximately 50 kDa and pI 5.

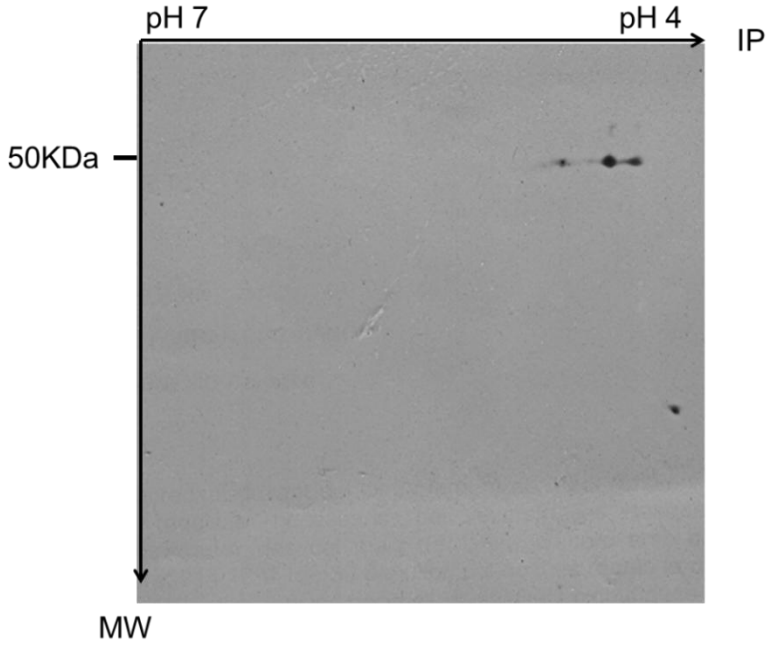

Figure 14: Detection of COL3-DEL isoform in human osteoarthritic cartilage. Human cartilage protein extracts were separated according to their molecular weight and their pI with 2D electrophoresis gel. Separated proteins were transferred in to a nitrocellulose membrane, where COL3-DEL isoform was detected by incubation with the specific antibody.

Result 1.2: COL3 isoforms proteolytic activity

Once the presence of the COL3 protein isoforms in human OA samples were confirmed, we aim to study their proteolytic activity. To achieve this purpose, it was necessary to produce recombinant protein in a system that could produce a high yield at the same that that could mimic the posttranslational modification introduce in these proteases in the mammal cells. Hence, the three different COL3 isoforms were produced in sf9 insect cells by the BAC to BAC system. These productions would allow us not only to analyze their collagenolytic activity but also to retest specificity of the polyclonal antibodies generated.

- COL3 protein isoforms production

The culture medium containing the recombinant proteins were submitted to a filtration column and the fractions eluted showing a single symmetrical peak were electrophoresed. Coomassie Blue staining of the SDS-PAGE gel displayed a band at the expected molecular weight for each isoform (Figure 15, A) according to their amino acid (aa) sequence. To confirm the COL3 isoforms' identification, immunoblotting with the antibodies produced for each specific isoform was performed. The antibodies against canonical COL3, COL3-DEL and COL3-9B were able to detect each isoform, without any cross-reaction with the other isoforms (Figure 15, B-D). Insect recombinant COL3 (irCOL3) migrated at an observed molecular weight of about 53 kDa and irCOL3-DEL of about 43 kDa (Figure 15, B and C). The COL3-9B antibody detected three major signals, one at the expected size for irCOL3-9B (60 kDa), and two of lower weight, about 25 and 15 kDa (Figure 15, D).

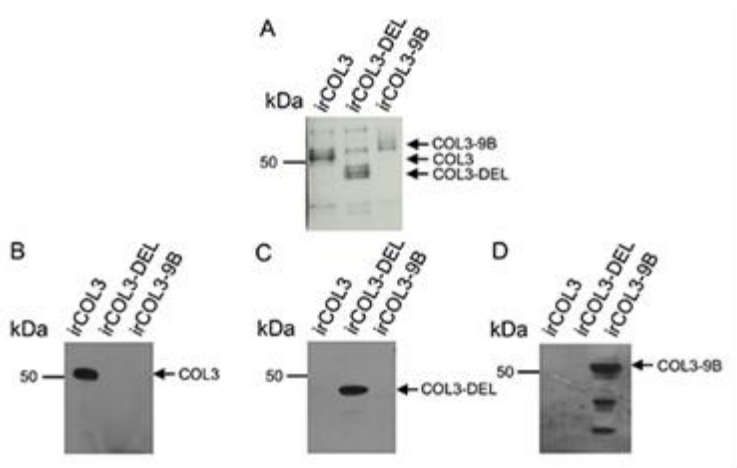

Figure 15. Immunoblotting of COL3 isoforms. (A) Purified isoforms irCOL3, irCOL3-DEL, and irCOL3-9B were subjected to electrophoresis on an SDS-polyacrylamide gel and visualized by staining with Coomassie Blue. **(B-D)** Purified irCOL3, irCOL3-DEL, and irCOL3-9B were blotted with the antibodies produced in the present study. **(B)** Rabbit polyclonal antibody specific for canonical COL3, **(C)** rabbit polyclonal antibody specific for the COL3-DEL isoform, and **(D)** rabbit polyclonal antibody specific for the COL3-9B isoform. kDa: kilodaltons

- <u>COL3 protein isoform catalytic activity</u>

Since COL3 isoforms had different Hpx domain their proteolytic activity was expected to be modified. Therefore, COL3 isoforms activity was tested against three SLRPs; lumican, fibromodulin and biglycan. COL3 production effectiveness differed between isoforms, with the highest yield for canonical COL3 followed by COL3-DEL (~15% lower) and COL3-9B (~30% lower) as calculated from the densitometry of Coomassie staining (Figure 15, A). The isoforms were present in the selected fractions as a mixture of proteins (Figure 15). This precluded precise quantification by the Bradford method of

the irCOL3 isoforms, which would allow performing stochiometric comparison between the isoforms' activities. In order to establish a common unit for the subsequent proteolytic activity studies, the Azocoll assay was used to assess the activity of each protein's production 23. These assays demonstrated that the irCOL3 samples present the highest activity (0.22 unit/µl), followed by irCOL3-DEL samples (0.072 units/µl) and irCOL3-9B samples (0.062 units/µl). These activity rates are in agreement with the isoform semi-quantification performed in SDS–PAGE by image analysis (Figure 15, A).

Further SRLP digestion was performed at a ratio of 1 unit of each isoform in 5 µg of cartilage protein extract and assessed by Western blot (Figure 16, A-C). Data showed that after 4 h of digestion with irCOL3, only biglycan showed degradation (Figure 16, C), while lumican and fibromodulin maintained their integrity (Figure 16, A and B). However, the two latter SLRPs started to degrade with irCOL3-DEL at 2 h of incubation (Figure 16, B and C) and biglycan at 30 min (Figure 16, C). However, the most evident activities were observed from 4 h of digestion. The irCOL3-9B isoform presented weak activity against the substrates tested, and some proteolytic activity could be observed only after 8 h of incubation (Figure 16, A-C).

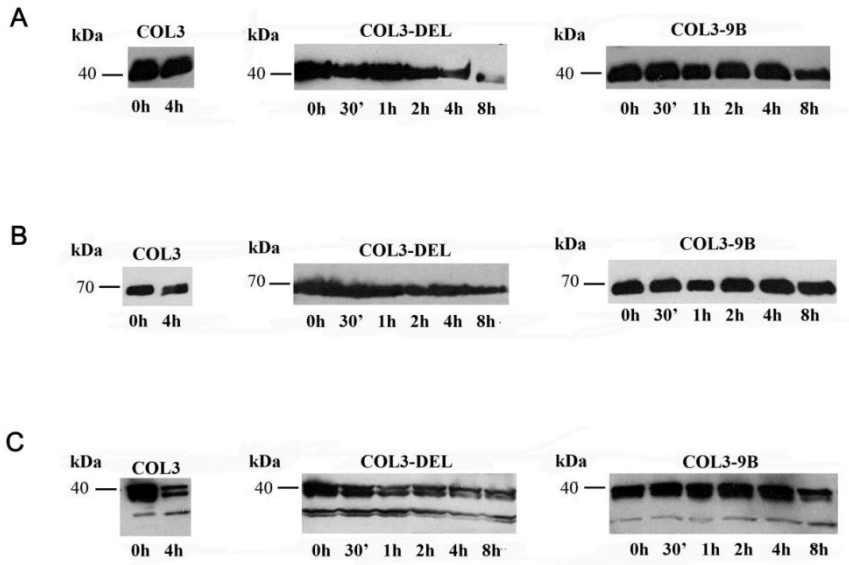

Figure 16. Time course of irCOL3, irCOL3-DEL and irCOL3-9B proteolytic activity on OA human cartilage protein extracts for **(A)** lumican, **(B)** fibromodulin, and **(C)** biglycan. Digestion products by COL3 isoform (4 hours), and by COL3-DEL and COL3-9B isoforms (time course of 0 to 8 hours) detected by Western blot. kDa: kilodaltons.

RESULTS CHAPTER 2:

***Summary chapter 2: In vivo* effect of opticin deficiency during development and OA**

Objective: Opticin (OPTC), a SLRP known to play a role in the assembly of the fibrillar collagens and the structural stability of the extracellular matrix, was previously demonstrated to be produced and degraded in osteoarthritic (OA) human cartilage. Here, we further investigated the OPTC role in OA cartilage by the study of the *in vivo* effect of OPTC deficiency in mouse model.

Methods: OA was induced in 10-week-old *Optc*$^{-/-}$ and *Optc*$^{+/+}$ mice by destabilization of the medial meniscus (DMM). Ten weeks post-surgery, cartilage was processed for histology and immunohistochemistry studies. Expression of several SLRPs was determined in mouse cartilage at day 3 (P03) and 10 weeks old. Cartilage collagen ultrastructure was analysed by transmission electron microscopy (TEM) and picrosirius red.

Results: OA *Optc*$^{-/-}$ mice demonstrated significant protection against cartilage degradation. Data revealed that in *Optc*$^{-/-}$ mouse cartilage, the SLRPs lumican and epiphycan were significantly up-regulated at P03 ($p \leq 0.010$) and 10 weeks old ($p \leq 0.007$), and fibromodulin down-regulated ($p \leq 0.001$). Immunohistochemistry showed a similar pattern. In OA *Optc*$^{-/-}$ mouse cartilage, markers of cartilage degradation and complement factors C5b-9 and CCL2 were all down-regulated ($p \leq 0.050$), and collagen fibers thinner and better organized ($p = 0.038$) than in OA *Optc*$^{+/+}$ mouse cartialge.

Conclusions: This work demonstrates a protective effect of OPTC deficiency during OA, resulting from an overexpression of lumican and epiphycan, known to bind and protect collagen fibers, and a decrease in fibromodulin, contributing to a reduction in the complement activation/inflammatory process.

Result 2.1: Characterization of the mouse colony

The rate of mating, lethality, and number of offspring per litter were comparable between *Optc*$^{+/+}$ and *Optc*$^{-/-}$ animals, as described[112]. Growth including weight and length at 5-days-postnatal 9(P05) and 1-days-postnatal (P16) was also monitored in males and females *Optc*$^{+/+}$ and *Optc*$^{-/-}$ mice and no differences were observed (data not shown).

- Genotyping of *Optc* mice.

In order to compare *Optc*$^{-/-}$ mice against *Optc*$^{+/+}$ littermates the offspring of the breeding *Optc*$^{+/-}$ mice were genotyped using PCR analysis. As illustrated in figure 17(A), samples showing PCR product of 450bp, 350bp and both bands correspond to Optc$^{-/-}$, Optc$^{+/+}$ and Optc$^{+/-}$ respectively.

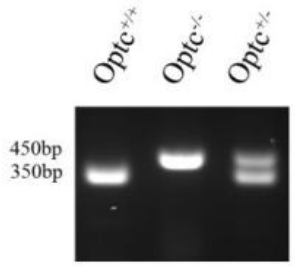

Figure 17. *Optc* mice genotyping. Electrophoresis separation of genotyping PCR products differentiating *Optc* wild-type (*Optc*$^{+/+}$), knockout (*Optc*$^{-/-}$) and heterozygous (*Optc*$^{+/-}$) with their respective sizes in base pairs (bp).

- Confirmation of the lack of Optc production in mice articular cartilage.

Confirmation of the lack of Optc production in the Optc$^{-/-}$ mice cartilage was performed by immunohistochemistry using the cartilage of 20-weeks-old DMM mice. Data demonstrated that OPTC was, as expected, not present in the Optc$^{-/-}$ mice cartilage (Figure 18). Additional Western blot analysis (figure 18, B) confirmed the lack of OPTC presence in the total protein extract of the eyes of Optc$^{-/-}$ (n=3) compared to Optc$^{+/+}$ mice (n=3).

A. **B.**

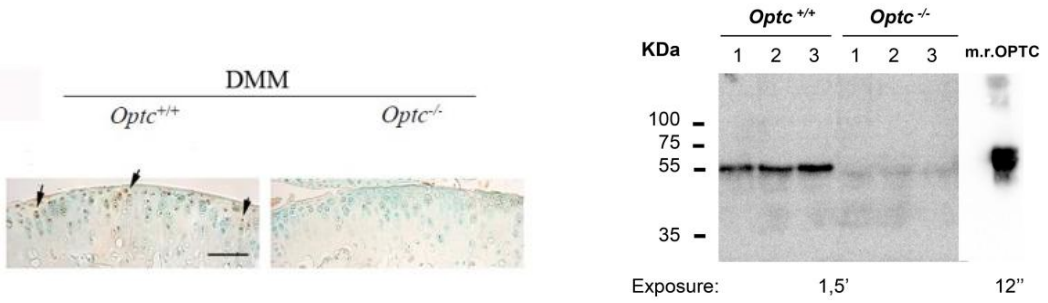

Figure 18. Confirmation of the lack of OPTC production in *Optc*$^{-/-}$ mouse. **(A)** Immunohistochemistry of OPTC on articular cartilage of *Optc*$^{+/+}$ and *Optc*$^{-/-}$ mice at 10 weeks after DMM surgery. Bar in **(A)** = 100 µm; original magnification X250. (**B)** Western blot analysis of OPTC production in *Optc*$^{+/+}$ and *Optc*$^{-/-}$ eyes protein extract. Mouse recombinant OPTC protein (m.r, OPTC) was used as a control.

Result 2.2: Effect of DMM surgery in *Optc*$^{+/+}$ and *Optc*$^{-/-}$ mice

Once mice were classified by their genotypes, the effect of DMM and Sham surgery was analyzed by means of inflammation, synovial hypertrophy and cartilage degeneration studies.

- Monitoring knee swelling on *Optc*$^{+/+}$ and *Optc*$^{-/-}$ mice after DMM surgery.

In order to detect any possible difference in inflammatory response between *Optc*$^{+/+}$ and *Optc*$^{-/-}$ mice, the diameter of the operated knee was monitored. As represented in Figure 19, the initial swelling (day 3 post-surgery) receded similarly in both Optc$^{+/+}$ and Optc$^{-/-}$ mice at 15 days post-surgery.

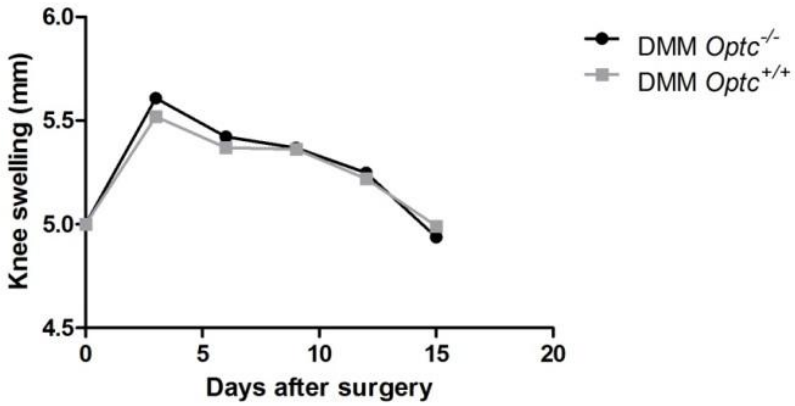

Figure 19. Knee joint swelling. Knee joint swelling was determined by the diameter (mm) of the DMM (right) knee in *Optc*$^{+/+}$ and *Optc*$^{-/-}$ mice (n=6). Mice were examined at baseline (day 0) and every 3 days following DMM surgery until day 15 post-surgery.

- Evaluation of synovial hypertrophy on *Optc*$^{+/+}$ and *Optc*$^{-/-}$ mice 10 weeks post-DMM surgery.

The effect of OPTC deficiency on synovial membrane inflammation was assessed by histomorphometric studies. Data from DMM mice samples, showed an increased in synovial membrane thickness in DMM *Optc*$^{+/+}$ (Figure 3, C) and DMM *Optc*$^{-/-}$ (Figure 21, D) compared with non-operated (data not shown) and SHAM controls (Figure 21, A, B). However, the synovial membrane thickness of the DMM-operated *Optc*$^{-/-}$ was significantly reduced compared to the DMM *Optc*$^{+/+}$ (Figure 21, E).

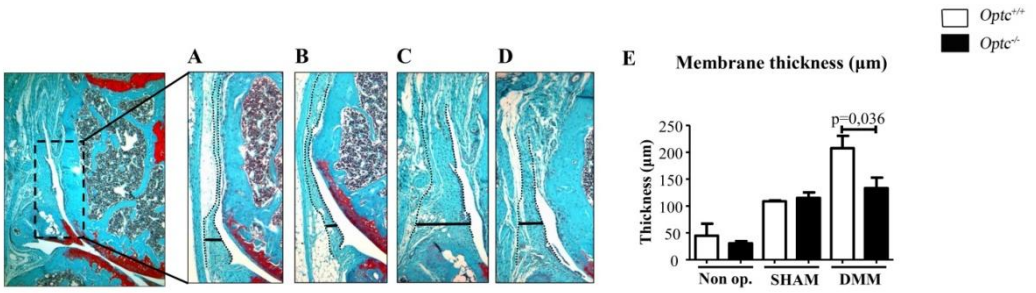

Figure 21. Synovial membrane inflammation. (A-D) Photomicrographs of representative histological sections of the synovial membrane obtained from *Optc*$^{+/+}$ **(A, C)** and *Optc*$^{-/-}$ **(B, D)** mice SHAM (Control) **(A, B)** and DMM **(C, D)** surgery. Dotted lines indicate synovial membrane area. Bars in **A-D** indicate synovial membrane thickness. Original magnification X250. **(E)** Histogram of the synovial membrane thickness in µm. Values are the mean±SEM of Non operated (n=6), SHAM (n=6) and DMM (n=9) mice. p values were determined by Mann-Whitney test, only significant p values are showed except for those between Non op. and SHAM with DMM groups for *Optc*$^{+/+}$ or *Optc*$^{-/-}$ which have a p< 0,01, excluding between SHAM *Optc*$^{-/-}$ and DMM *Optc*$^{-/-}$.

- Analysis of the cartilage degradation on Optc$^{+/+}$ and Optc$^{-/-}$ mice after DMM surgery

With the objective of studying the effect of OPTC deficiency in the progression of OA disease, the cartilage integrity in the medial tibial plateau in non-operated, sham (control) and DMM (OA) mice was assessed histologically (Figure 20). First, we compared the histology scores for the medial tibial plateau from the SHAM mice to the 20-week-old non-operated mice from both groups (n = 4 and n = 8, respectively). Data revealed no significant differences among these control groups (Figure 20, C-F). Comparison between DMM-Optc$^{+/+}$ and -Optc$^{-/-}$ mice (Figure 20, A and B) revealed a decreased loss of cartilage integrity in the Optc$^{-/-}$ mice, including Safranin O–fast green staining, cellularity, thinning of the cartilage, and fibrillation. These observations were corroborated by the OARSI scores (Figure 20, G), which showed significantly lower histologic scores in the DMM-Optc$^{-/-}$ mice ($p = 0.021$).

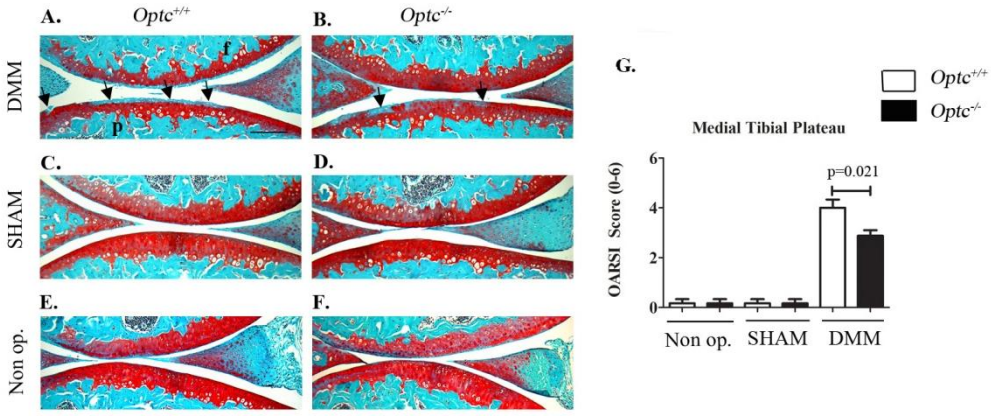

Figure 20. Articular cartilage degradation. (A-F) Photomicrographs of representative histological sections of the medial tibial plateaus **(A, p)** and femoral condyles **(A, f)** obtained from opticin *Optc*$^{+/+}$ **(A, C, E)** and *Optc*$^{-/-}$ **(B, D, F)** mice at 10 weeks after DMM **(A, B)**, SHAM (Control) **(C, D)** surgery and non-operated **(E, F).** Black arrows in **A** and **B** indicate areas of fibrillation, with loss of cartilage ultrastructure. Bar in **A** = 100 µm; original magnification X250. **(G)** Representative histogram of the OA Research Society International (OARSI) scores in the medial tibial plateau. White bars represent *Optc*$^{+/+}$ and black bars *Optc*$^{-/-}$ .Values are the mean$\pm$SEM of SHAM (n=6) and DMM (n=9). p values were determined by Mann-Whitney test, only significant p values are showed except for those between Non op./SHAM and DMM groups in medial tibial plateau which are < 0,01.

- Quantification of cartilage degradation markers and MMPs levels in $Optc^{+/+}$ and $Optc^{-/-}$ mice after DMM surgery

To corroborate the finding that $Optc^{-/-}$ mice exhibited a protective effect on cartilage degradation, the protein levels of three different degradative markers and two MMPs overexpressed during OA and involved in cartilage degradation were assessed by IHC. As expected, $Optc^{-/-}$ DMM mice, compared to $Optc^{+/+}$ DMM mice, demonstrated significantly reduced levels in all the markers studies:aggrecan degradation products (V-DIPEN) (p=0,021); type X collagen (p=0,004) and, MMP-13 (p=0,004) and MMP-3 (p=0,038) (Figure 22,A to D, respectively) .

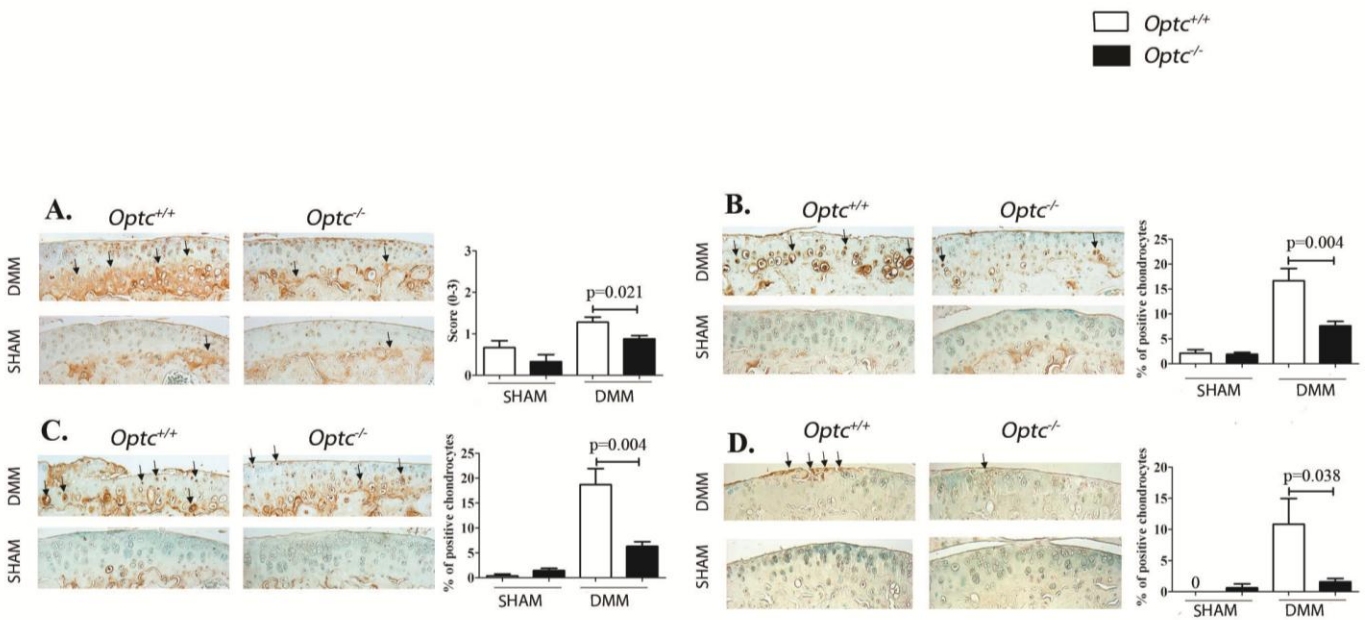

Figure 22. Immunohistochemistry of articular cartilage 10 weeks after surgery. (A-E) Representative immunohistochemistry images and histograms of the percentage of positive chondrocytes of cartilage degradation markers in medial tibial plateaus, such as V-DIPEN (A), Type X collagen (B), MMP-13 (C) and MMP-3 (D) from *Optc*$^{+/+}$ and *Optc*$^{-/-}$ mice at 10 weeks after SHAM (Control) and DMM surgery, counterstained with methyl green. Black arrows indicate positive-stained cells. Bar in **(A)** = 100 μm; original magnification X250. Values are the mean±SEM of SHAM (Control) (n=6) and DMM (n=12). pvalues were determined by Mann-Whitney test, only significant p values are showed except for those between SHAM and DMM groups that were always < 0,05.

Results 2.3: Comparison of the cartilage composition and chondrocytes expression between Optc$^{+/+}$ and Optc$^{-/-}$ mice after DMM surgery

To identify if the protective effect of Optc-/- mice against cartilage degeneration suggested by the previous results, was due to an overexpression of other SLRP members in order to compensate the lack of OPTC, SRLP expression and cartilage composition analysis were performed

- Study of the SLRPs expression in articular cartilage from *Optc*$^{+/+}$ and *Optc*$^{-/-}$ mice.

Expression of SLRP members from each class were analyzed. Data showed that articular cartilage mRNA levels of biglycan (class I), osteomodulin (class II), osteoglycin (class III), tsukushi and nyctalopyn (class IV), and podocan (class V) did not show any significant difference between Optc+/+ and Optc-/- mice at either day 3 (P03) and 10 week-old (data not shown). Interestingly, as represented at Figure 3, epiphycan, a member of the same class as OPTC (class III) and lumican (class II) were significantly overexpressed at both P03 ($p \leq 0{,}039$) and 10-week-old ($p \leq 0{,}010$) in Optc$^{-/-}$ mice compared to Optc$^{+/+}$ (Figure 3, A and B). Moreover, expression of fibromodulin and PRELP (class II) had similar values at P03 in mice from both genotypes, but were significantly downregulated at 10-week-old ($p=0.001$ and $p<0{,}001$ respectively) (Figure 3, C and D) in Optc$^{-/-}$ mice. compared to Optc$^{+/+}$. The overexpression of lumican and downregulation of fibromodulin was confirmed by Western blot (Figure 24).

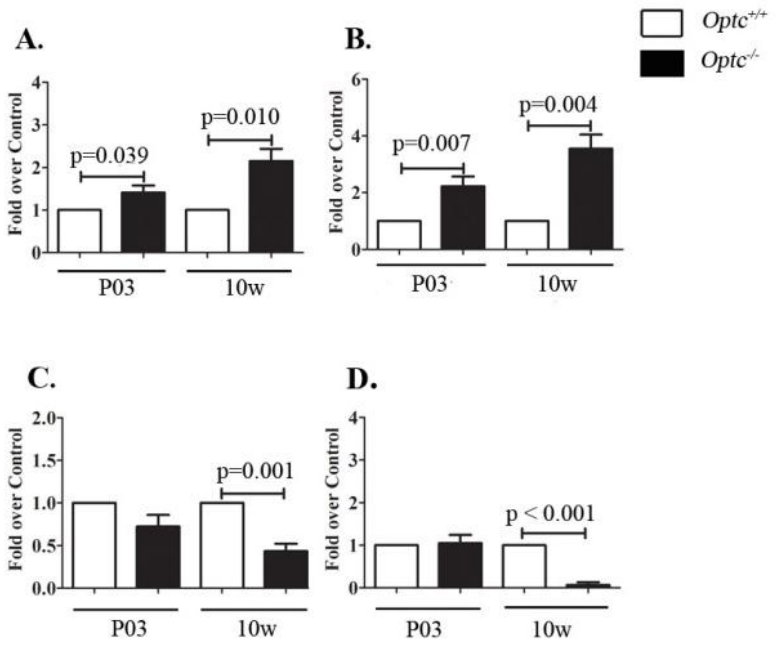

Figure 23. Articular cartilage small leucine-rich proteoglycans (SLRP's) expression (mRNA) Relative gene expression (mRNA) of lumican **(A)** epiphycan **(B)** and fibromodulin **(C)** and PRELP **(D)** in articular cartilage at day 3 (P03) and 10 week-old (10w) *Optc*$^{+/+}$ and *Optc*$^{-/-}$ mice. Values are the mean±SEM of (n= 6) mice per group. p values were determined by one sample t-test with control value = 1.

- Evaluation of the cartilage protein composition in DMM *Optc*$^{-/-}$ and *Optc*$^{+/+}$ mice

In order to corroborate the mRNA expression variance observed in *Optc*$^{-/-}$ cartilage mice is reflected in different protein levels, protein semi-quantification of the SLRP previously described was performed by IHC. Data showed that articular cartilage of DMM mice had a significant increase of the percentage of chondrocytes staining positive in *Optc*$^{-/-}$ than *Optc*$^{+/+}$ for epiphycan (total cartilage, p=0,015) (Figure 25, B) and lumican (upper zone, p=0,027) (Figure 25, A), but a significant decreased for fibromodulin (total cartilage, p=0,015) (Figure 25, C), concurring with the expression findings (Figure 3). However, PRELP levels did not show differences between DMM-operated *Optc*$^{-/-}$ with *Optc*$^{+/+}$ mice (data not shown). Furthermore, fibromodulin and lumican concentration in ECM cartilage was also studied by western blot in 3 days and 10 weeks old not operated mice (Figure 26). Data confirmed that the difference in protein production was previous to the surgical OA induction. As fibromodulin contributes to the complement activation and therefore to the inflammatory process, we further investigated the levels of two representative factors of the complement activation, C5b-9 and CCL-2. Data revealed that for both factors, *Optc*$^{-/-}$ DMM mice have a significant decrease on the levels (p=0,004 for both cases) than *Optc*$^{+/+}$ DMM mice (Figure 25, D and C)

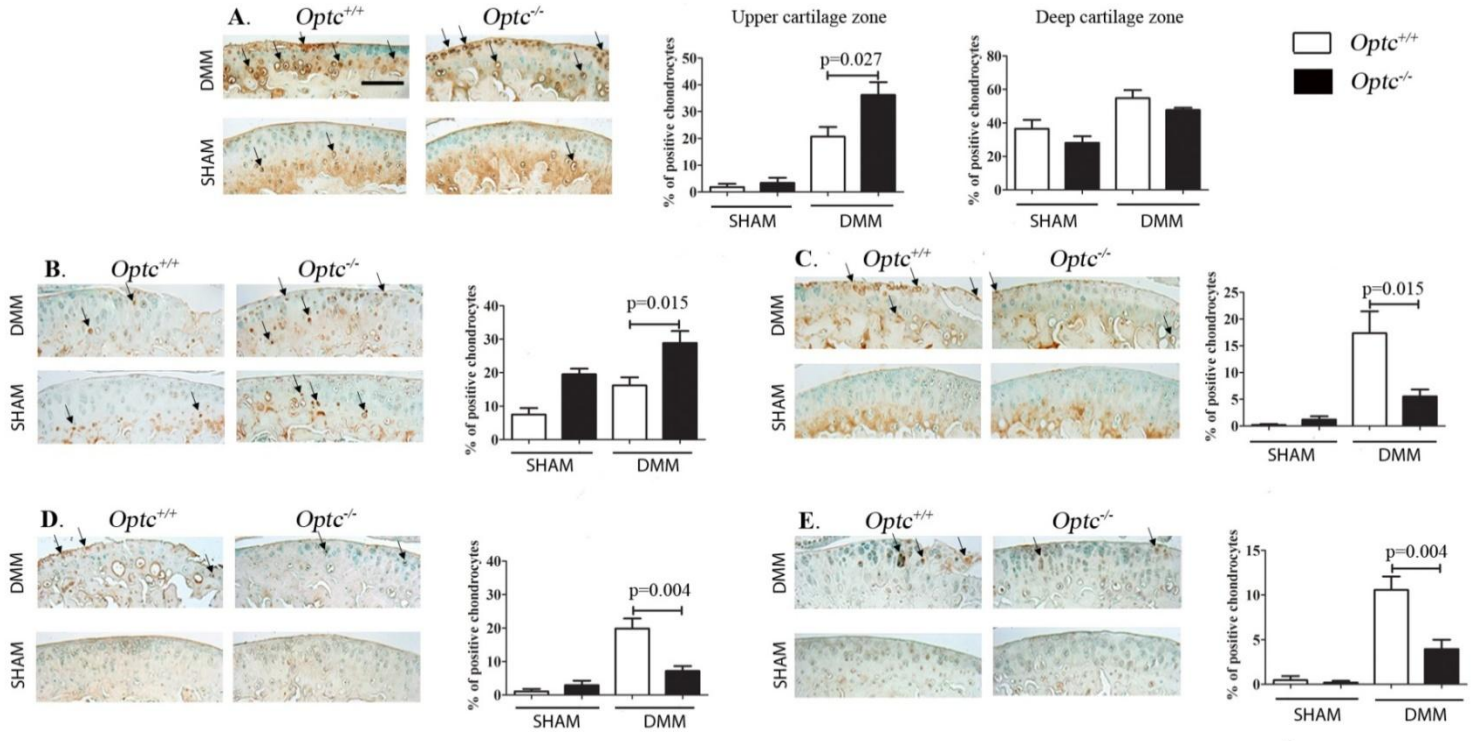

Figure 25. Immunohistochemistry of articular cartilage 10 weeks after DMM surgery. (A-E) Representative immunohistochemistry images and histograms of the percentage of positive chondrocytes of SLRP's from lumican **(A)** epiphycan **(B)** and fibromodulin **(C),** as well as complement factor C5b-9 **(D)** and CCL-2 **(E)** from *Optc*$^{+/+}$ and *Optc*$^{-/-}$ mice at 10 weeks after SHAM(Control) and DMM surgery, counterstained with methyl green. Black arrows in indicate positive-stained cells. Bar in **(A)** = 100 μm; original magnification X250. Values are the mean±SEM of

SHAM (n=6) and DMM (n=12). p values were determined by Mann-Whitney test, only significant p values are showed except for those between SHAM and DMM groups in that were < 0,01.

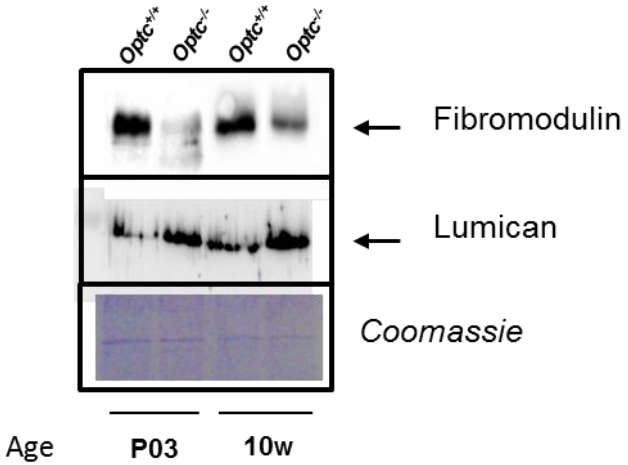

Figure 26. Articular cartilage small leucine-rich proteoglycans (SLRP's) production: Proteoglycan extraction from 3 days postnatal and 10-week-old *Optc*$^{+/+}$ and *Optc*$^{-/-}$ was analyzed by Western blot for fibromodulin and lumican production. Coomassie blue staining of the gel after proteins transference to the nitrocellulose membrane was performed to confirm equal protein loading between *Optc*$^{+/+}$ and *Optc*$^{-/-}$. Note that at 10-weeks-old the amount of cartilage is lower than at 3 days postnatal, thus less total proteins were loaded in the gel.

Results 2.4: Collagen fibers structure assessment of *Optc*$^{-/-}$ and *Optc*$^{+/+}$*.mice*

Since SLRPs are known to have a role in collagen fibrillogenesis, type II collagen fibril structure in articular cartilage (Figure 26, A-C) was examined by transmission electron microscopy (TEM) in 10-week-old *Optc*$^{+/+}$ (Figure 26, B) and *Optc*$^{-/-}$ mice (Figure 26, C). Furthermore the collagen organization 10 weeks after DMM surgery was also evaluated by picrosirius red staining (Figure 26, D). Fibril diameter distributions were analyzed in the superficial and deep zones of the cartilage. Data showed similar findings for both zones studied and only data of the deep zone are illustrated (Figure 26, B and C). Interestingly, *Optc*$^{-/-}$ mice collagen cartilage fibers were smaller in diameter than the fibers from *Optc*$^{+/+}$ mice, with a frequency peak at around 25 nm whereas the majority of *Optc*$^{+/+}$ fibers were around 35 nm. This was further substantiated by the use of the collagen birefringence methodology (Figure 26, D), which showed that collagen fibers in the *Optc*$^{+/+}$ DMM mice cartilage had a significantly lower birefringence intensity (p=0,038) indicating disorganization of the collagen fibers in the *Optc*$^{+/+}$ DMM mice.

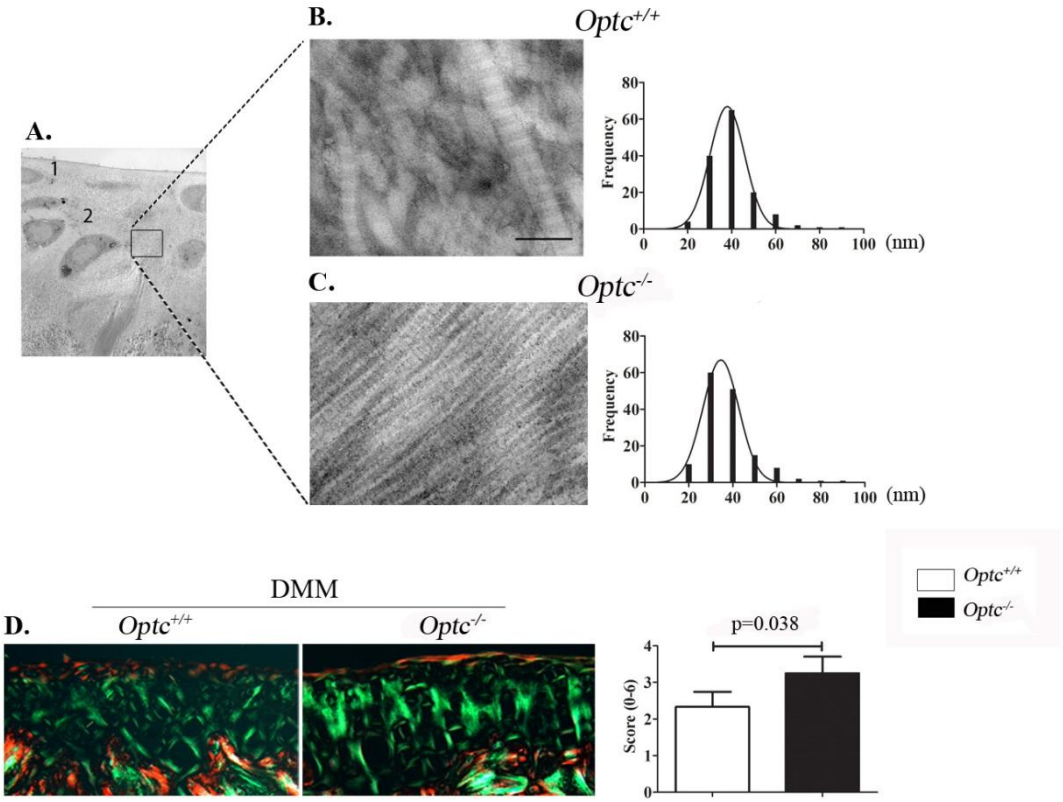

Figure 26. Ultrastructure of Type II collagen fibers. (A-C) Representative images obtained with transmission electron microscopy (TEM) of collagen fibers from the deep zone of articular cartilage from *Optc*$^{+/+}$ **(B)** and *Optc*$^{-/-}$ **(C)** mice at 10 weeks of age. Magnifications 1200X **(A)** and 30000X **(B, C).** Bar in **(B)** = 100nm. Histograms represent the frequency of each fiber diameter on *Optc*$^{+/+}$ **(B)** and *Optc*$^{-/-}$ **(C). (D)** Sirius red staining of mouse articular cartilage from *Optc*$^{+/+}$ and *Optc*$^{-/-}$ mice at 10 weeks after DMM surgery. Histogram on **(D)** represents the evaluation of birefringence on *Optc*$^{+/+}$ and *Optc*$^{-/-}$ cartilage mice**.**

RESULTS CHAPTER 3:

Summary chapter 3: Chondroitin sulfate effect on OA synovial fibroblasts under hypoxic and pro-inflammatory conditions.

Objective: Chondroitin sulfate (CS) is a Symptomatic Slow acting Drug against Osteoarthritis (SySADOA) with anti-inflammatory effects. In this study, we tried to unveil the mechanism of action on osteoarthritic synovial membrane.

Design: Osteoarthritic synoviocytes were pre-treated with or without CS (200µg/ml) for 24h and incubated with and without $CoCl_2$ (150mM) and IL-1β (0,1ng/ml) to mimic hypoxia and inflammatory environment, respectively. Pro-angiogenic factor VEGF-A expression (mRNA) and production (protein) were analyzed by qPCR and E.L.I.S.A/WB respectively. Anti-angiogenic factors TSP1 and VEGI production was analyzed by E.L.I.S.A. The mechanism of action by which CS regulates these factors was analyzed by WB.

Results: Data showed that pre-treatment with CS significantly counteracted VEGF-A gene overexpression produced by hypoxia and hypoxia plus inflammation environment, but no significant differences were observed in relation with the VEGF-A protein levels . Furthermore, synoviocytes under hypoxia and hypoxia plus inflammation environment pretreated with CS, present similar levels of HIF-1α translocation to the nucleus than controls. In addition, CS significantly increases TSP1 production under hypoxia ($CoCl_2$) and hypoxia plus inflammation.

Conclusions: In conclusion, data from this work suggests that CS could perform an anti-angiogenic effect on synovial membrane during osteoarthritis through the upregulation of the anti-angiogenic factor TSP1 and its apoptotic effect on endothelial cells. However, CS does not seem to have a direct effect on VEGF-A.

Result 3.1: Time-course of VEGF-A mRNA expression in human osteoarthritic synoviocytes under hypoxic and pro-inflammatory conditions.

VEGF-A is the most potent biologic angiogenic factor and it has been demonstrated its overexpression by synoviocytes from OA patients[192]. Therefore, the first objective was to demonstrate the overexpression of VEGF-A under hypoxic and both hypoxic and pro-inflammatory conditions. The time-course study of the VEGF-A expression at hypoxic conditions (Figure 27, A) showed that VEGF-A mRNA overexpression (2 fold over CTL) could be detected two hours after inducing hypoxia with $CoCl_2$ (150mM). The VEGF-A expression continued increasing until the end of the study (20 hours) reaching a 6.9 fold overexpression compare to control cells. However, under pro-inflammatory conditions, maximum overexpression of VEGF-A, corresponding to 5 fold over control, was reached only 1,5h after inducing proinflammatory condition with IL-1β (0,1ng/ml). After this initial overexpression, VEGF-A mRNA levels decreased progressively until reaching CTL levels (8h after induction).

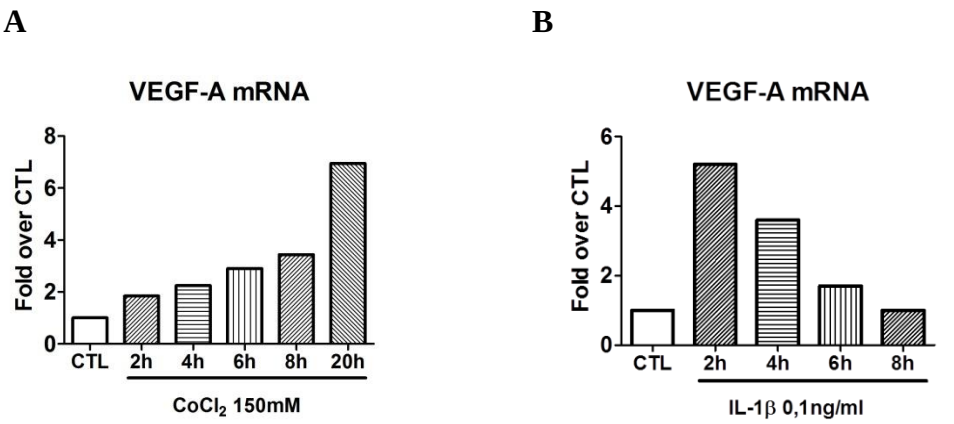

Figure 27: Time-course expression of VEGF-A mRNA. Synoviocytes from osteoarthritic human synovial membrane were incubated for increasing periods of time with **(A)** $CoCl_2$ (150mM) and **(B)** IL-1α 0,1ng/ml in order to analyze VEGF-A mRNA expression.

Results 3.2: Effect of CS on the pro-angiogenic factor VEGF-A *in vitro*:

In order to evaluate VEGF-A modulation by CS, human osteoarthritic synoviocytes were incubated for a period of time in which VEGF-A expression was activated by $CoCl_2$ (150mM) and IL-1β (0,1ng/ml) but the expression could be up- or down-regulated by the effect of CS. According to results 3.1, the ideal incubation time for this study was 4h. As expected, after 4h under hypoxic and hypoxic plus pro-inflammatory conditions, synoviocytes significantly overexpressed of VEGF-A gene (Figure 28, A). Interestingly, data showed that pre-treatment with CS (200µg/ml) for 24h significantly counteracted VEGF-A gene overexpression (Figure 28, A).

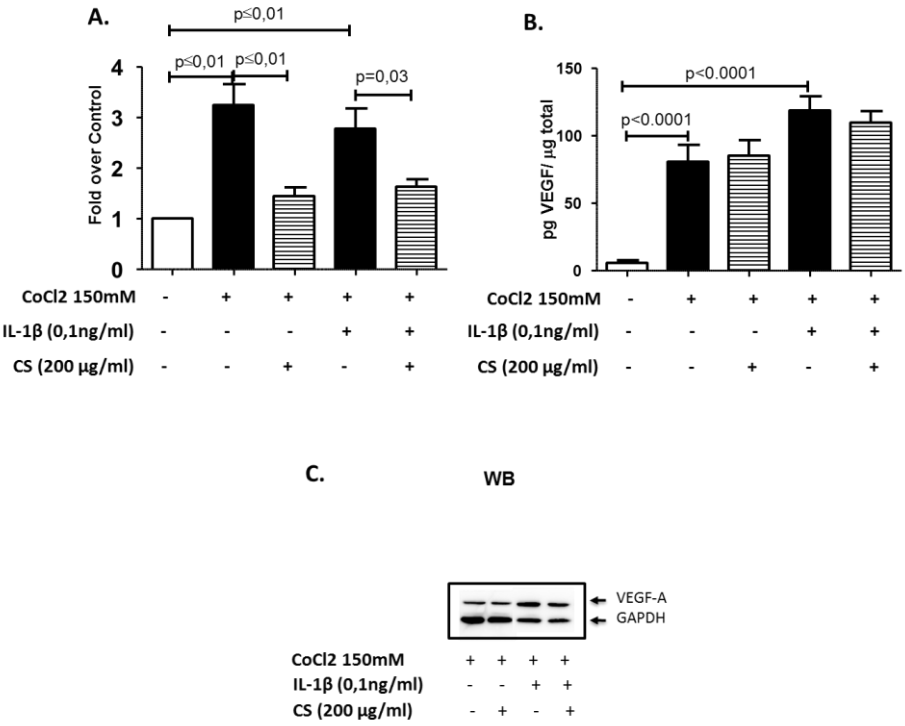

Figure 28: Effect of CS on human synoviocytes under hypoxic and hypoxic + pro-inflammatory conditions. (A), analysis of VEGF-A mRNA (n=5) expression by RT-qPCR. **(B and C),** analysis of VEGF-A protein levels by E.L.I.S.A (n=9) and WB (n=3), respectively.

However, no significant differences were observed when looking at VEGF-A protein levels by E.L.I.S.A and WB.

Results 3.3: CS anti-angiogenic effect on human synoviocytes.

Since we could not see any significant effect of CS in VEGF-A protein production we further studied if the effect of CS on synovial membrane angiogenesis is due to the modulation of HIF-1α mRNA expression or protein production on OA synoviocytes. As illustrated on figure 29(A), HIF-1α mRNA expression was significantly upregulated by the effect of CoCl2 and the combination of CoCl2 and IL-1b. Interestingly, HIF-1α mRNA expression showed a subtle downregulation by CS. At the protein level, a reduction of HIF-1α translocation to the nucleus was observed due to the action of CS pre-treatment on synoviocytes.

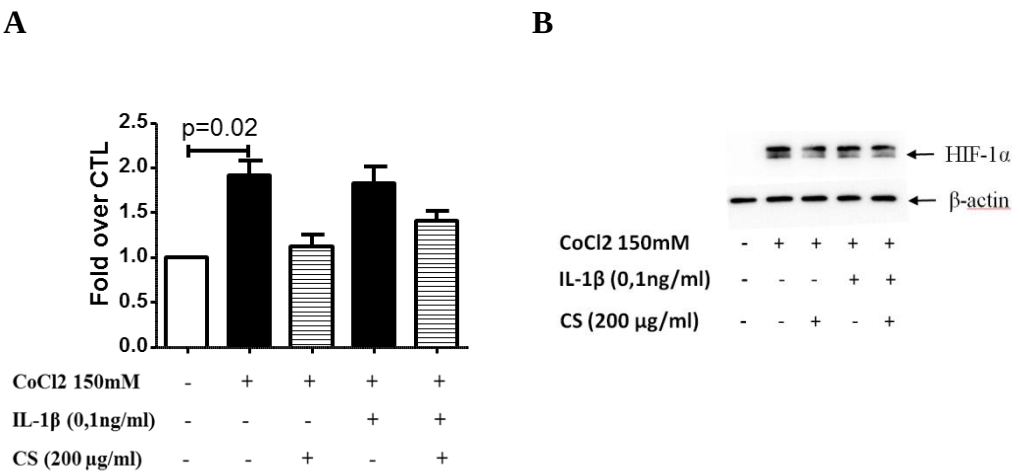

Figure 29: Effect of CS on human synoviocytes under hypoxic and hypoxic + pro-inflammatory conditions. (A), analysis of HIF-1α mRNA (n=3) expression by RT-qPCR. **(B)** Analysis of HIF-1α (n=3) nuclear translocation levels by WB.

Results 3.4: *In vitro* effect of CS on anti-angiogenic factors TSP1 and TL-1A (VEGI).

Since the effect of CS on pro-angiogenic factor VEGF-A showed no significant differences; the effect on anti-angiogenic factors TSP1 and VEGI was analyzed. First of all, data demonstrated that TSP1 protein levels were increased due to the effect of $CoCl_2$ and $CoCl_2$ + IL-1β suggesting that under these conditions, TSP1 is produced and secreted into the synovial fluid to regulate the angiogenic response. Results also showed that CS significantly increases TSP1 production under the same conditions (Figure 30, A). Although the levels were barely undetectable, a tendency towards an increase of VEGI by CS was observed (Figure 30, B).

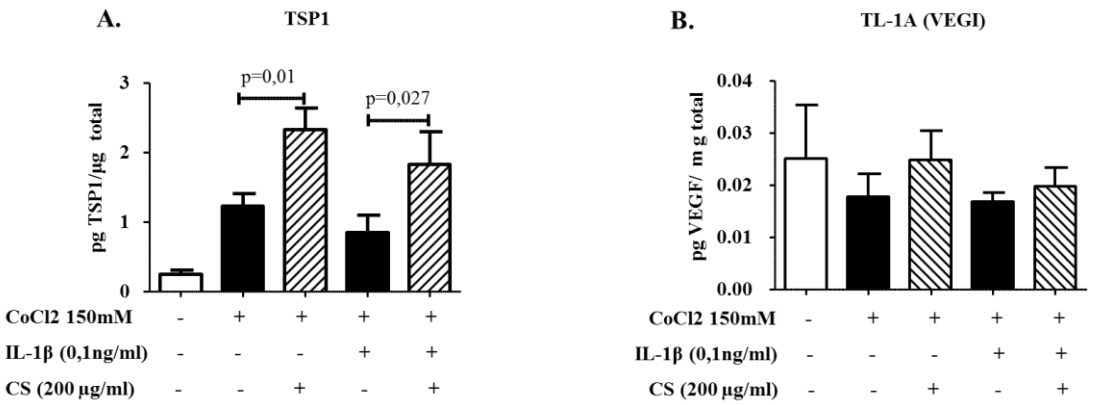

Figure 30: Effect of CS on human synoviocytes under hypoxic and hypoxic + pro-inflammatory conditions. (A) Analysis of TSP1 and **(B)** TL-1A (VEGI) protein production by E.L.I.S.A

.

Results 3.5: CS anti-angiogenic mechanism of action.

The anti-angiogenic effect of TSP1 has been described to be through the induction of apoptosis on endothelial cell. Therefore, the anti-angiogenic effect of CS in the synovial membrane was evaluated by incubating HUVEC cells with the conditioned medium of CS pre-treated synoviocytes under hypoxia conditions for 20min. Data showed that p.p38 was downregulated by the conditioned media of synoviocytes pre-treated with CS under normoxia (Figure 31, lane 2) and under hypoxia alone (Figure 31, lane 3) but, as expected, p.p38 was upregulated by the conditioned media from the synoviocytes pre-treated with CS under hypoxia (Figure 31, lane 4).

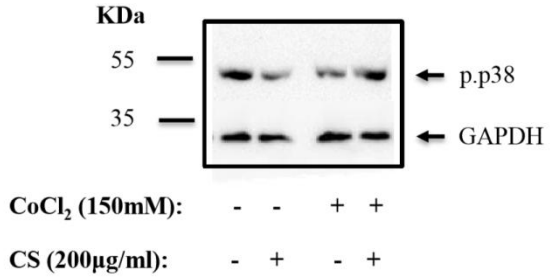

Figure 31: Indirect effect of CS on HUVEC cells. HUVEC cells were incubated for 20min with the conditioned media of synoviocytes pre-treated with or without CS for 24h and posteriorly incubated under normoxia or hypoxia conditions for 72h. Phosphorilated p38 levels were analyzed by WB. GAPDH levels were used as a loading control.

DISCUSSION

DISCUSSION CHAPTER 1

During OA progression, abnormal MMP upregulation takes place and degrades the articular cartilage ECM. In human pathologic cartilage, COL3 demonstrated a negative impact not only because of its high capacity for degrading type II collagen, but also for its ability to act on other extracellular proteins such as proteoglycans, which protect the collagen network. Although the knowledge of COL3 biochemistry and regulation has greatly increased over the years, data from the first chapter of this thesis is of significantly relevant clinical implication for pathologies related to this enzyme. Indeed, we demonstrated that COL3-DEL is produced in OA cartilage and has a faster rate of degrading two non-collagenous proteins, lumican and fibromodulin, than the canonical COL3. These data could have important implications; for example, this isoform could be used as a prognostic indicator of OA and could also open up a potential avenue in therapeutic strategies targeting this MMP.

In the present study, COL3-DEL isoform was detected in samples from human OA cartilage, corroborating that the COL3-DEL mRNA described by Tardif *et al.*[178] was translated *in vivo* and localized in the ECM. Tardif *et al*.[178] performed a transient transfection of different cell types with an expression plasmid containing the COL3-DEL transcript. They detected the isoform protein in the culture medium, showing the capacity of the COL3-DEL transcript to be translated *in vitro* into a secreted protein, although the protein level found was of low abundance. In contrast, in the present study, the isoform could be detected even without a previous immunoprecipitation of the protein. These differences could be explained by the low specificity of the antibody used in the previous study[178], problem that has been solved in the present work by the production of a specific antibody for the detection of the COL3-DEL isoform. Yamamoto *et*

al.[175] described that COL3 is constitutively produced in human chondrocytes and endocytosed by the receptor LRP1. They referred that the Hpx domain is necessary for the recognition and endocytosis of this MMP, so the partial lack of the Hpx domain found in the COL3-DEL isoform could have prevented its endocytosis by the chondrocytes through the LRP1 receptor, explaining the fact that COL3-DEL concentration in the ECM was higher than expected.

In this work, the observed size for COL3-DEL in human cartilage is 50 kDa compared to the expected 43 kDa due to the deletion of the Hpx domain[178]. Due to the similar size observed between the canonical COL3 and the high chain of the Ab used for the immunoprecipitation and the observed COL3-DEL isoform, different controls were performed to ensure the identity of the COL3-DEL isoform in our samples. Firstly, we showed that the antibody did not cross-react with the other COL3 isoforms or with a recombinant human COL3 and therefore the observed band could not correspond to canonical COL3. Secondly, protein A was used for immunoblotting detection. As protein A detects almost exclusively intact antibody molecules, the observed band could not correspond to the recognition of the heavy chain of the antibody used for the immunoprecipitation[193]. Hence, it could be speculated that the higher molecular weight of the COL3-DEL isoform found in the human cartilage is due to post-translational N-glycosylation, as previously demonstrated for the canonical enzyme and a truncated form generated *in vitro*[194].

Once the confirmation of production of at least one of the isoforms was performed, we compared the catalytic activity of COL3 isoforms. Other studies have previously examined canonical COL3 catalytic activities, but this is the first time to analyze COL3 isoforms activity. On one hand, Monfort *et al.*[186] studied the proteolytic activity of canonical COL3 against non-collagenous ECM

components. Human cartilage protein extraction was performed from non-fibrillated, slightly fibrillated, moderately and severely fibrillated cartilage and the time-course digestion of four SLRPs from these extracts by the canonical COL3 isoform was explored. Canonical COL3 presented the highest digestion efficiency for biglycan, followed by fibromodulin and lumican. Although the study was carried out with recombinant human MMP-13 produced in a mouse myeloma cell line, the results are in agreement with the irCOL3 data obtained in the present study. On the other hand, Knauper *et al.*[194] studied the proteolytic activity of the canonical COL3 and a truncated form lacking almost all the Hpx domain (amino acids from 249 to 451) on several collagenous and non-collagenous ECM components and demonstrated that the truncated form lacked collagenolytic activity while it maintained the gelatinolytic and peptidolytic activities. In the present study, the COL3-DEL isoform, that is also lacking most of the Hpx domain, appears to share such catalytic properties as it maintained gelatinolytic activity (demonstrated by the Azocoll assay) and its activity against the SLRPs tested.

Our data shows that lumican and fibromodulin were more efficiently digested by irCOL3-DEL than by irCOL3, while degradation of biglycan was more effective when incubated with irCOL3. Fibromodulin and biglycan share leucine rich region structures while biglycan presents a different structure. Futhermore, they also differ in the GAGs attached to the core protein (keratan sulfate in the case of fibromodulin and lumincan, and chondroitin and dermatan sulfate for biglycan). These distinctive characteristics generate patterns that present different recognition efficacy by the Hpx domain , and therefore are implicated in the protease affinity to each SLRP.

OA is the most prevalent rheumatologic disease and even so, it lacks a treatment that could modify the progression of the disease. This fact is probably related with its definition, which does not include its high heterogenic phenotype. In 2013, the FDA, in its report about personalized medicine, remarked that current definition of diseases, mainly based on their signs and symptoms, avoid the progress in personalized medicine. They encouraged investigators to define and describe diseases on the basis of their intrinsic biology. Data from the first chapter, aim to aid on this item, since it confirms the presence of a new COL3 isoform, COL3-DEL, that displays complementary and higher capabilities to degrade some non-collagenous proteins, SLRPs, present in the cartilage ECM and of importance in the OA pathological process. The presence of this isoform could be related with OA severity and prognosis, given its modified Hpx domain, which seems to be related with i) its increased proteolytic activity, compared to the canonical COL3, ii) its elevated presence in the ECM, due to a less endocytosis mediated by LRP1, and iii) the association rates with TIMPs[175].

Hence, the confirmation of the presence in OA cartilage of an isoform with a truncated domain and proteolytic activity could have implications in the understanding of OA pathophysiology. The presence of COL3-DEL could explain differences in disease progression observed in OA patients and therefore, its expression could be used as an indicator of the disease process as well as a target for new OA treatment avenues.

DISCUSSION CHAPTER 2:

OPTC is a class III member of the SLRP super-family that was firstly discovered in the vitreous humor of the eye. Bishop et al. demonstrated that OPTC binds to the collagen fibers and inhibits angiogenesis in the eye. Our group described for the first time OPTC expression and production in articular cartilage[121] and its degradation during human OA[122]. Because SLRPs contribute to the maintenance and integrity of articular cartilage, OPTC reduction/cleavage in OA was suggested to predispose cartilage to degeneration[121]. In the second chapter of this thesis, we further investigated the *in vivo* effect of the lack of OPTC during OA, using an *Optc*-null mouse model.

Mice with a deficiency of one or more SLRPs have been shown to develop premature OA[94, 114], however and in contrast to our initial hypothesis, the present study showed that OA *Optc*-null mice where OA was induced by DMM, exhibited a cartilage protective effect. The lack of OPTC in OA mouse cartilage resulted in significantly better histology features, markers of catabolic processes as well as a better preservation of collagen fibril organization. Findings of the OA *Optc*$^{-/-}$ cartilage protective effect also concur with those of the markers of the cartilage degradation, aggrecan, chondrocyte hypertrophy, MMP-3 and MMP-13, which were all significantly and markedly reduced in the DMM-*Optc*$^{-/-}$ mice compared to DMM-*Optc*$^{+/+}$ mice.

We then further explored the relevant *in vivo* mechanisms implicated in OA cartilage associated with the OPTC absence. Data revealed that the absence of OA come with an overexpression and an overproduction of two other members of the SRLP super-family, epiphycan and lumican, combined with a down-regulation of fibromodulin, The study of the

expression of SLRPs from each class on articular mouse cartilage at birth and in adults. revealed that in *Optc*$^{-/-}$ mice, lumican and epiphycan are overexpressed at birth (P03), and fibromodulin down-regulated in adult mice (10 weeks old).. This overexpression of some SLRPs to compensate the lack of other member of this superfamily has been already described by others[107, 108, 195, 196], and we hypothesized that is the main responsible of the better OA score showed by OPTC null mice. It has been described that epiphycan overexpression (SLRP of the same class as OPTC) concurs with a protection of the cartilage during OA, as this SLRP was shown to play an important role in maintaining joint integrity and its absence (knockout mice) resulted in OA development with aging[114]. In addition, interaction between SLRP members has also been documented, in which, for example, the epiphycan/biglycan double-deficient mice, exhibit a more severe OA phenotypethan with epiphycan absence alone[114].

Due to the SRLP content variance in ECM, and the already know participation of SLRPs in collagen fibrillogenesis, we analyzed the collagen ultrastructure and organization in cartilage by TEM and pricosirius red, respectively. We observed that cartilage form OPTC null mice presents collagen fibrils thinner but more organized that wild type mouse. Collagen fibrillogenesis during normal cartilage development is finely regulated and involves multiple steps. The stabilization of the mature collagen fibrils is mediated by interactions with fibril-associated molecules such as SLRPs[107], more specifically by lumican and fibromodulin, two SLRPs that we have demonstrated that present a modified regulation in the *Optc*$^{-/-}$ mice. Lumican and fibromodulin belong to the same SLRP subfamily (class II) and show a 47% sequence

identity. Additionally, these SLRPs are similar in their post-translational modifications. Both carry tyrosine sulfate residues in their N-terminal domains and are substituted with carbohydrates in a similar fashion[198]. They share the same binding site in type I collagen fibrils, although fibromodulin has a higher affinity than lumican[18]. Although not yet studied for type II collagen, one could speculate that these two SLRPs could also compete for binding tothis collagen type. Ezura et al have studied the tendon fibrillogenesis in wild type, lumican, fibromodulin and doble knock-out mice. They observed that fibromodulin and doble KO mice have an abnormally large number of small diameter fibrils present in the later stages of development while and lumican KO mice only present fibrils with irregular profiles, feature also observed in the other deficient condition mice. These data suggested that lumican and fibromodulin are implicated in early stages of fibrillogenesis while for the regulation of the later stages, fibromodulin seems to show a more prominent role. [107]. They hypostatized that during the collagen fibril growth phase, lumican and fibromodulin promote the lateral fibril growth by fusion of intermediate subunits.As fibrillogenesis progresses, the lumican level decreases to a barely detectable level, while the fibromodulin level increases modulating the diameter growth of the mature fiber at later stages[107] (Figure 32, B).

These data are in agreement with our findings on the SLRP expression/production and the cartilage collagen analysis. We observed that null and wild type mice at P03 present comparable cartilage fibromodulin content, while null OPTC mice 10 weeks old show significant fibromodulin reduction compared with wild type mice, together with thinner collagen fibrils. Taking these data together, they are suggestive of a model (Figure 32, B). Early lumican overpresence in cartilage did not alter initial fibrillogenesis, but it alter fibromodulin presence over time. As a result, the collagen fibers of the *Optc*$^{-/-}$ mice are over-coated by lumican and epiphycan molecules during the fibrillogenesis process, preventing fibromodulin role in the final steps of the fibril formation process. Therefore, fibers do not fusion laterally properly, remaining thinner and tightly packed, and consequently less susceptible to degradation. This scheme is strengthened by the picrosirius red data, which showed that OA *Optc*$^{-/-}$ mice maintained a better organization of the cartilage collagen network, while the OA *Optc*$^{+/+}$ cartilage showed a disorganization (less birefringence).

The mechanisms responsible of the compensatory SRLP expression observed in the present study have to be elucidated. SLRPs are encoded in 18 different genes clustered on 7 chromosomes, suggesting duplication to generate functional redundancy during evolution[91]. OPTC and fibromodulin share the same gene cluster, suggesting that OPTC could have a regulatory role in fibromodulin transcription[197]. This could explain, at least in part, the decrease in fibromodulin in the cartilage of *Optc*$^{-/-}$ mice. The fibromodulin downregulation could be also explain by a negative feedback to the overpresence of lumican and epiphycan. An any case, the decrease of the fibromodulin presence in the OPTC null mice

furthermore to affect the collagen fibrillogenesis, could be responsible for less catabolic activity in the cartilage. Indeed, fibromodulin, in addition to its structural role in the cartilage matrix, is known to activate the classical complement pathway[112]. Such a process occurs in OA cartilage[199] and unbalanced complement activation can play significant roles in chronic inflammatory conditions such as OA. The complement system consists of pathways that converge at the formation of the C3 and C5 convertases, enzymes that mediate activation, among others, of the formation of membrane attack complex (MAC), comprising the complement effector C5b-9[200]. The levels of C5b-9, as well as CCL2 (also referred to as monocyte chemoattractant protein 1 [MCP-1]), have been found elevated in OA synovial fluid when compared to healthy individuals[199, 201, 202]. Interestingly, MAC co-localized with MMP-13 around human OA chondrocytes and was shown to play a critical role in the pathophysiology of this disease, in which in addition to inducing cell lysis, it increases the chondrocytes' expression of multiple genes including MMPs, inflammatory cytokines and complement effectors[199]. We have observed that the lack of OPTC in surgically OA induced $OPTC^{-/-}$ mice, produce a significantly decreased in the levels of two complement canonical factors, (C5b-9 and CCL2), probably mediated by less fibromodulin presence, contributing to a reduction in the inflammatory/catabolic processes during the disease process.

In summary, this is the first report showing that the *in vivo* lack of OPTC destabilizes the natural balance of SLRP members in the cartilage, which is translated into a protective environment in OA cartilage. The effect is a result of different events comprising an overexpression of lumican and epiphycan expression/production at birth and over time and

therefore a protection of the collagen fibers by their surface deposition, enabling the fibrils to better resist catabolic factors. In addition, the decrease in fibromodulin content also reflects in a protective effect , which will result in a reduction of the classical complement pathway activation during the progression of the disease, favoring production of less catabolic factors and thus less degradation.

A

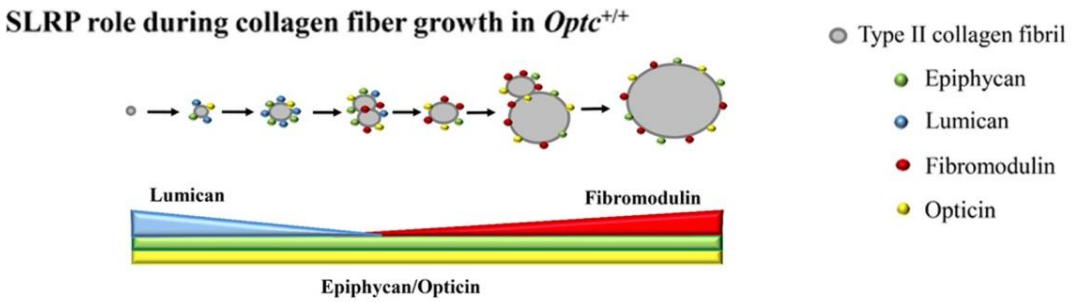

B

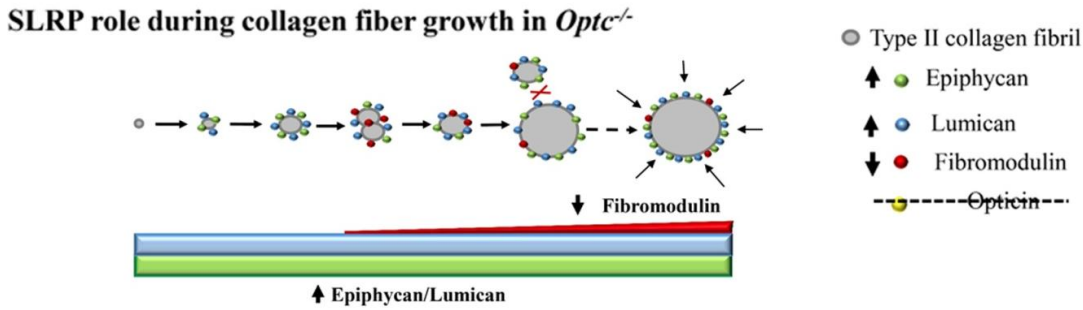

Figure 32: Involvement of SLRPs in the regulation of linear and lateral collagen fibril growth. SLRPs bind to the fibril surface, regulating the linear and lateral growth of collagen fibrils during the fibrillogenesis process. In *Optc*$^{+/+}$ mice, lumican and fibromodulin combine their actions during the process by differential temporal expression. Lumican is involved in the first steps of the fibril formation, and as the development progresses in time, lumican expression decreases and fibromodulin takes over to promote the final growth steps. However, in *Optc*$^{-/-}$ there is a downregulation of fibromodulin in adult mice leading to a compensating overexpression of lumican and therefore, a domination of this molecule during the later steps of the fibril growth process. The abnormal excess of lumican in adult *Optc*$^{-/-}$ mice together with the overexpression of epiphycan result in an over coating of the collagen fibril preventing the rapid access of collagenases during OA.

DISCUSSION CHAPTER 3:

Angiogenesis is a process mainly induced by hypoxic and inflammation conditions (derived from diseased or injured tissues) by the secretion of pro-angiogenic molecules. In OA, angiogenesis is mainly found from subchondral bone to cartilage, through the tidemark, and in the synovium where it has been described to be close related with OA chronicity. Specifically, in synovial membrane and during OA progression, infiltrated macrophages produce angiogenic factors such as vascular endothelial growth factor (VEGF) that induces the secretion of collagenases, as well as the proliferation and migration of endothelial cells, and increases vascular permeability, impairing homeostasis of the articular cartilage, and enhancing tissue inflammation. Hence, uncontrolled angiogenesis and inflammation of the synovial membrane are two interdependent processes that have a strong relation with the progression of OA. ,hypoxia inducible factor It has been reported that synovial angiogenesis in OA is hypoxia inducible factor (HIF-1α)-dependent[204] and, at the same time, this factor upregulated VEGF-A expression[205].

Calamia *et al*. recently described that CS could ameliorate angiogenesis in OA by the increase of an angiogenesic inhibitor, thrombospondin-1 (TSP-1). In the present study we aim to contribute to the better understanding of the mechanism leading CS to an antiangiogenic effect. The study was performed by incubating human osteoarthritic synoviocytes in simulated hypoxia and inflammation condition *in vitro*, with $CoCl_2$ (a chemical agent known to mimic hypoxia) and the pro-inflammatory cytokine IL-1β, respectively.

First of all we studied the effect of hypoxia and inflammation in the pro-angiogenic factor VEGF-A. It has been shown that synoviocytes from OA patients present VEGF-A overexpression. Our results showed that VEGF-A expression is also upregulated *in vitro* on synoviocytes in a time-dependent manner by the action of both $CoCl_2$ and IL-1β , suggesting that they induce similar behavior in cultured synoviocytes that the founded in synoviocytes from OA patients. When the synoviocytes were pre-treated with chondroitin sulphate (CS), this overexpression (mRNA) was significantly reverted suggesting an interaction of CS in the VEGF-A activating cascade. However, at the protein level, no significant differences were observed with or without CS pre-treatment. This discordance between CS effect in mRNA and protein levelscould be related with the several regulating ways present in the VEGF production. HIF-α is responsible not only of the overexpression of VEGF-A, but also to the stabilization of its mRNA, and the increases of its secretion. Therefore, it is possible that CS has the capacity to modulate the expression of VEGF, but not its secretion. In fact, CS did not produce significant changes in HIF-α expression and production although decreased levels were observed. This could be due to the effect of CoCl2, that acts stabilizing HIF-1α protein, probably by inhibiting its degradation[203].

Once the effect of CS over pro-angiogenic factors were studied, we focus on the effect on antiangiogenic factors. It has been described the modulation of expression and production not only of proinflammatory but also of antiinflamatory factors by CS in synoviocytes stimulated with IL-1b. Our purpose was to confirm this fact and observed if under

hypoxia conditions, CS showed the same effect. Furthermore, we also studied the behaviour of another antiangiogenic factor, Vascular endothelial growth inhibitor (VEGI). As an inhibitor of angiogenesis, TSP1 overexpression decreases inflammation and blood vessel density in synovial membrane. It also reduces cartilage lesions in rats where OA is induced by anterior cruciate ligament transection[210]. Thrombospondin-1 (TSP1) is one of the anti-angiogenic factors whose synthesis is driven by hypoxia[146]. TSP1 performed its antiantiogenic effect mainly by its capacity to interact with various ligands and receptors, including components of the extracellular matrix, growth factors, cell surface receptors and cytokines[206]. On the other hand, (VEGI), also known as tumor necrosis factor superfamily member 15 (TNFSF15) or TNF ligand related molecule 1 (TL1), is a cytokine with potent anti-angiogenic properties principally studied in cancer as an inhibitor of endothelial cell proliferation and tumor growth[147] that is upregulated in the synovial membrane of patients with rheumatoid arthritis[211]. Our results show that TSP1 protein levels are elevated after hypoxia and inflammation stimuli. This fact was described at mRNA levels by Lambert et al, at the time point performed in this study, but they described a significant reduction 24 hours induction. Even though, the increased of TSP1protein levels after CS pretreatment is significantly higher, analogously to what was observed for synoviocytes under inflammatory environment. However, No significant differences were observed in VEGI production, neither when comparing hypoxia and hypoxia plus inflammation conditions versus normoxia, nor comparing with or without CS pretreatment. Previous studies have shown that VEGI is less susceptible to CS concentration changes and its significant increase is observed at higher

concentrations than the ones needed for TSP1. Furthermore, the increases obtained are lower than the ones observed in TSP1. These experiments were performed after 24 hours of IL-1β stimulation, so our results could indicated that VEGI levels are not only CS concentration dependent, but also time dependent.

Once observed the significant increases of TSP1 induced by CS treatment, we aim to study how its effect in endothelial cells. One of the major pathways by which TSP1 inhibit angiogenesis is by its negatively regulation of the VEGF-VEGFR2 axis. It is reported that secreted TSP1 binds to its high affinity receptor CD47 and disrupts the association of VEGFR2 with CD47, thereby downregulating the pro-angiogenic signals downstream of VEGF (see Figure 33). Another reported TSP1 mechanism of action to reduce angiogenesis is by indirectly activating endothelial cell TSP1 receptors CD36. The scavenger receptor CD36 is required for TSP1 to inhibit endothelial migration *in vitro*. CD36 ligation induces p38 activity, leading to increased endothelial cell apoptosis[207].

We hypothesized that the mechanism of action of CS to inhibit angiogenesis on OA synovial membrane could be explained by the effect of TSP1 on endothelial cells. For this reason, we analyzed p38 phosphorylation levels on HUVEC cells previously incubated with the conditioned media of CS pre-treated synoviocytes. We observed that culture medium from synoviocytes preteated with CS reverted the increased levels of phosphorylated p38 observed when the HUVECs were incubated with the culture medium from synoviocytes grown in a hypoxic environment. Although previous results support the hypothesis that this reduction is mediated by the lower TSP-1 levels found in the

conditioned media, we could not ensure due to the high range of cellular stresses and inflammatory cytokines that can activate p38 and could be affected by CS treatment. In any case, it is the first time that CS effect over p.p38 levels are described. This effect could in part encompass the anti-inflammatory effect described for CS, as this MAP kinase is an important key in inflammatory disease, given that it's upstream of several processes related with inflammation, such as the regulation of the biosynthesis of the pro-inflammatory cytokines IL-1β and TNFα.

Synovial inflammation is an important source of hypoxic and pro-inflammatory mediators. VEGFA and IL-1β produced by synovial cells induce a degradative cascade leading to joint damage. In this work, we have studied the modulation of gene expression of pro-angiogenic (VEGF) and anti-angiogenic (TSP1 and VEGI), factors by CS under hypoxia ($CoCl_{2)}$ and inflammatory (IL-1β) conditions in synoviocytes. Data suggest that the anti-angiogenic effect of CS is due to an upregulation and release of the TSP1 factor by synoviocytes to the synovial fluid and thereafter, and activation of the apoptotic cascade of the abnormally activated endothelial cells through the interaction with CD47 and the phosphorylation of p38 (Figure 33).

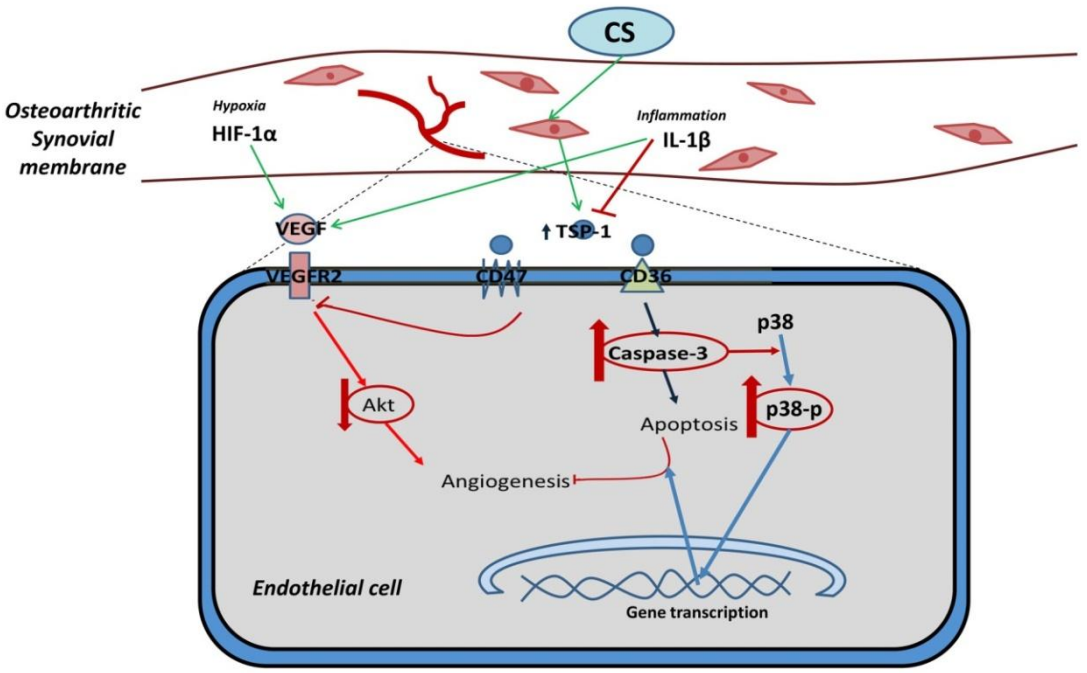

Figure 33: Representation of potential mechanism of action of CS. During OA, synovial membrane inflammation results in an increase of pro-inflammatory cytokines such as IL-1β and hypoxic factors such as HIF-1α that in turn, will increase the expression of the angiogenic factor VEGF-A. However, CS pre-treatment induces TSP1 expression and reduces synovial membrane angiogenesis by activating the apoptotic pathway of endothelial cells.

GLOBAL DISCUSSION SUMMARY

OA is a heterogeneous disease that encloses multiple phenotypes. In order to develop new diagnostic and prognostic tools and eventually advance in the discovery of successful treatments, clearly defining the different phenotypes of OA is of great importance. In this line, the findings comprised in this thesis reveal two different approaches to identify patient's subgroups. On one hand, and as described in chapter 1, the presence of a new discovered collagenase-3 (COL3) isoform (COL3-DEL) resulting from a mutation of the canonical COL3, could be used as an indicator of differential extracellular matrix degradation in human articular cartilage. On the other hand, results from chapter 2 suggest that the compositions of the members of SLRP super-family in the human extracellular matrix of the articular cartilage could be applied as a new tool for OA prognosis classification. Finally, the controversy regarding the efficacy of systemic treatment with nutraceuticals – including chondroitin sulfate - may arrive to an end if new tools are used to predict which patients are best suited for a given drug. Importantly, further work remains to be done to understand how to integrate these findings into a final and comprehensive concept that could explain the patient's heterogeneity and the differential prognosis of OA disease.

CONCLUSIONS

1. **Collagenase-3 is expressed and produced in human OA cartilage as, at least, two different isoform, the canonical COL3 and a deleted form, COL3-DEL.**

   1.1. The polyclonal antibody created against COL3-DEL isoform can be used for its specific detection in human samples without cross reacting with other COL3 isoforms.

   1.2. irCOL3-DEL isoform digests *in vitro* lumican and fibromodulin more efficiently than COL3, although the digestion of biglycan is more efficient by the canonical COL3.

   1.3. The value of the new discovered collagenase isoform as an indicator of the disease progress or as a new therapeutic target warrants further studies.

2. **OPTC knock-out mice present a protection against articular cartilage degeneration during OA.**

   2.1. The lack of OPTC encompass an increased level of lumican and epiphycan and a diminish level of fibromodulin.

   2.2. The different composition of the ECM seems to be related to the modified collagen fibers observed as they appear smaller in diameter and more organized.

   2.3. The reduction of fibromodulin level leads to a reduction of the activation of the inflammatory complement system during OA.

2.4. The new collagen irganization, together with the redution of complement system activation may be related with the protection of the collagen fibril from degradation in the cartilage from OPTC null-mice.

2.5. This work suggests that the evaluation of the composition of the different SLRPs in human OA cartilage could be applied as a new tool for OA prognosis classification.

3. Chondroitin sulfate may have anti-angiogenic effect on OA synovial membrane.

3.1. CS significantly downregulates VEGF-A mRNA expression in osteoarthritic synoviocytes under hypoxic and hypoxic-inflammatory conditions, probably due to a decrease of HIF-1*a* nuclear translocation that activates its expression.

3.2. At the protein level, CS significantly increases anti-angiogenic factor TSP1 but does not modify angiogenic factor VEGF-A and anti-angiogenic factor VEGI under hypoxic and hypoxic-inflammatory conditions.

3.3. The activation of pP38 on HUVEC cells is upregulated by the conditioned media of synoviocytes pre-treated with CS, suggesting that CS through the overexpression of TSP1 by synoviocytes, induces apoptosis on endothelial cells while decreases inflammatory activating pathway.

REFERENCES

1. Martel-Pelletier, J. *et al.* Osteoarthritis. *Nat Rev Dis Primers* **2**, 72 (2016).
2. Arden, N. & Nevitt, M.C. Osteoarthritis: epidemiology. *Best Pract Res Clin Rheumatol* **20**, 3-25 (2006).
3. Kellgren, J.H. & Lawrence, J.S. Radiological assessment of osteo-arthrosis. *Ann Rheum Dis* **16**, 494-502 (1957).
4. Schiphof, D., Boers, M. & Bierma-Zeinstra, S.M. Differences in descriptions of Kellgren and Lawrence grades of knee osteoarthritis. *Ann Rheum Dis* **67**, 1034-1036 (2008).
5. Garstang, S.V. & Stitik, T.P. Osteoarthritis: epidemiology, risk factors, and pathophysiology. *American Journal of Physical Medicine and Rehabilitation* **85**, S12-14 (2006).
6. Nevitt, M.C. *et al.* Very low prevalence of hip osteoarthritis among Chinese elderly in Beijing, China, compared with whites in the United States: the Beijing osteoarthritis study. *Arthritis and rheumatism* **46**, 1773-1779 (2002).
7. Zhang, Y. *et al.* Comparison of the prevalence of knee osteoarthritis between the elderly Chinese population in Beijing and whites in the United States: The Beijing Osteoarthritis Study. *Arthritis and rheumatism* **44**, 2065-2071 (2001).
8. Dudda, M. *et al.* Morphologic differences between the hips of Chinese women and white women: could they account for the ethnic difference in the prevalence of hip osteoarthritis? *Arthritis and rheumatism* **63**, 2992-2999 (2011).
9. Zhang, Y. *et al.* Association of squatting with increased prevalence of radiographic tibiofemoral knee osteoarthritis: the Beijing Osteoarthritis Study. *Arthritis and rheumatism* **50**, 1187-1192 (2004).
10. Helmick, C.G. *et al.* Estimates of the prevalence of arthritis and other rheumatic conditions in the United States. Part I. *Arthritis and rheumatism* **58**, 15-25 (2008).
11. van Saase, J.L., van Romunde, L.K., Cats, A., Vandenbroucke, J.P. & Valkenburg, H.A. Epidemiology of osteoarthritis: Zoetermeer survey. Comparison of radiological osteoarthritis in a Dutch population with that in 10 other populations. *Annals of the Rheumatic Diseases* **48**, 271-280 (1989).
12. Martin, J.A., Brown, T.D., Heiner, A.D. & Buckwalter, J.A. Chondrocyte senescence, joint loading and osteoarthritis. *Clin Orthop Relat Res* **427**, S96-103 (2004).
13. Li, Y.S., Xiao, W.F. & Luo, W. Cellular aging towards osteoarthritis. *Mechanisms of Ageing and Development* **31**, 30281-30280 (2016).
14. Srikanth, V.K. *et al.* A meta-analysis of sex differences prevalence, incidence and severity of osteoarthritis. *Osteoarthritis and Cartilage* **13**, 769-781 (2005).

15. Prieto-Alhambra, D. *et al.* Incidence and risk factors for clinically diagnosed knee, hip and hand osteoarthritis: influences of age, gender and osteoarthritis affecting other joints. *Annals of the Rheumatic Diseases* (2013).
16. van Meurs, J.B. Osteoarthritis year in review 2016: genetics, genomics and epigenetics. *Osteoarthritis Cartilage* **25**, 181-189 (2017).
17. Storm, E.E. & Kingsley, D.M. GDF5 coordinates bone and joint formation during digit development. *Dev Biol* **209**, 11-27 (1999).
18. Rodriguez-Fontenla, C. & Gonzalez, A. Genetics of osteoarthritis. *Reumatol Clin* **11**, 33-40 (2015).
19. Zhang, Y. *et al.* Bone mineral density and risk of incident and progressive radiographic knee osteoarthritis in women: the Framingham Study. *J Rheumatol* **27**, 1032-1037 (2000).
20. Bergink, A.P. *et al.* Bone mineral density and vertebral fracture history are associated with incident and progressive radiographic knee osteoarthritis in elderly men and women: the Rotterdam Study. *Bone* **37**, 446-456 (2005).
21. Hart, D.J. *et al.* The relationship of bone density and fracture to incident and progressive radiographic osteoarthritis of the knee: the Chingford Study. *Arthritis and rheumatism* **46**, 92-99 (2002).
22. Lee, J.Y. *et al.* Relationship of bone mineral density to progression of knee osteoarthritis. *Arthritis and rheumatism* **65**, 1541-1546 (2013).
23. Johnston, J.D., McLennan, C.E., Hunter, D.J. & Wilson, D.R. In vivo precision of a depth-specific topographic mapping technique in the CT analysis of osteoarthritic and normal proximal tibial subchondral bone density. *Skeletal Radiology* **40**, 1057-1064 (2011).
24. Burnett, W. *et al.* Patella bone density is lower in knee osteoarthritis patients experiencing moderate-to-severe pain at rest. *J Musculoskelet Neuronal Interact* **16**, 33-39 (2016).
25. Burnett, W.D. *et al.* Knee osteoarthritis patients with severe nocturnal pain have altered proximal tibial subchondral bone mineral density. *Osteoarthritis and Cartilage* **23**, 1483-1490 (2015).
26. Wright, D.A., Meguid, M., Lubovsky, O. & Whyne, C.M. Subchondral bone density distribution in the human femoral head. *Skeletal Radiology* **41**, 677-683 (2012).
27. Sturmer, T. *et al.* Serum cholesterol and osteoarthritis. The baseline examination of the Ulm Osteoarthritis Study. *J Rheumatol* **25**, 1827-1832 (1998).
28. Berenbaum, F. Diabetes-induced osteoarthritis: from a new paradigm to a new phenotype. *Postgrad Med J* **88**, 240-242 (2012).
29. Chen, Y.J. *et al.* PPARgamma is involved in the hyperglycemia-induced inflammatory responses and collagen degradation in human chondrocytes and diabetic mouse cartilages. *J Orthop Res* **33**, 373-381 (2015).

30. Heidari, B., Heidari, P. & Hajian-Tilaki, K. Association between serum vitamin D deficiency and knee osteoarthritis. *Int Orthop* **35**, 1627-1631 (2011).
31. Buckwalter, J.A., Anderson, D.D., Brown, T.D., Tochigi, Y. & Martin, J.A. The Roles of Mechanical Stresses in the Pathogenesis of Osteoarthritis: Implications for Treatment of Joint Injuries. *Cartilage* **4**, 286-294 (2013).
32. McKinley, T.O., Rudert, M.J., Koos, D.C. & Brown, T.D. Incongruity versus instability in the etiology of posttraumatic arthritis. *Clin Orthop Relat Res* **423**, 44-51 (2004).
33. Murrell, G.A., Maddali, S., Horovitz, L., Oakley, S.P. & Warren, R.F. The effects of time course after anterior cruciate ligament injury in correlation with meniscal and cartilage loss. *American Journal of Sports Medicine* **29**, 9-14 (2001).
34. Christensen, R. *et al.* Effect of weight maintenance on symptoms of knee osteoarthritis in obese patients: a twelve-month randomized controlled trial. *Arthritis Care and Research* **67**, 640-650 (2015).
35. Reijman, M. *et al.* Body mass index associated with onset and progression of osteoarthritis of the knee but not of the hip: the Rotterdam Study. *Ann Rheum Dis* **66**, 158-162 (2007).
36. Messier, S.P. Obesity and osteoarthritis: disease genesis and nonpharmacologic weight management. *Medical Clinics of North America* **93**, 145-159 (2009).
37. Carman, W.J., Sowers, M., Hawthorne, V.M. & Weissfeld, L.A. Obesity as a risk factor for osteoarthritis of the hand and wrist: a prospective study. *American Journal of Epidemiology* **139**, 119-129 (1994).
38. Wetterholm, M., Turkiewicz, A., Stigmar, K., Hubertsson, J. & Englund, M. The rate of joint replacement in osteoarthritis depends on the patient's socioeconomic status. *Acta Orthop* **87**, 245-251 (2016).
39. Buckwalter, J.A. & Martin, J.A. Sports and osteoarthritis. *Current Opinion in Rheumatology* **16**, 634-639 (2004).
40. Kujala, U.M. *et al.* Knee osteoarthritis in former runners, soccer players, weight lifters, and shooters. *Arthritis and rheumatism* **38**, 539-546 (1995).
41. Agricola, R. *et al.* Cam impingement: defining the presence of a cam deformity by the alpha angle: data from the CHECK cohort and Chingford cohort. *Osteoarthritis and Cartilage* **22**, 218-225 (2014).
42. Agricola, R. *et al.* Cam impingement of the hip: a risk factor for hip osteoarthritis. *Nat Rev Rheumatol* **9**, 630-634 (2013).
43. Neogi, T. *et al.* Magnetic resonance imaging-based three-dimensional bone shape of the knee predicts onset of knee osteoarthritis: data from the osteoarthritis initiative. *Arthritis and rheumatism* **65**, 2048-2058 (2013).
44. Lawrence, R.C. *et al.* Estimates of the prevalence of arthritis and other rheumatic conditions in the United States. Part II. *Arthritis Rheum* **58**, 26-35 (2008).

45. Litwic, A., Edwards, M.H., Dennison, E.M. & Cooper, C. Epidemiology and burden of osteoarthritis. *British Medical Bulletin* **105**, 185-199 (2013).
46. Fernandez-Lopez, J.C., Laffon, A., Blanco, F.J. & Carmona, L. Prevalence, risk factors, and impact of knee pain suggesting osteoarthritis in Spain. *Clin Exp Rheumatol* **26**, 324-332 (2008).
47. Parkinson, L. *et al.* Incident osteoarthritis associated with increased allied health services use in 'baby boomer' Australian women. *Australian and New Zealand journal of public health* **40**, 356-361 (2016).
48. Oliveria, S.A., Felson, D.T., Reed, J.I., Cirillo, P.A. & Walker, A.M. Incidence of symptomatic hand, hip, and knee osteoarthritis among patients in a health maintenance organization. *Arthritis and rheumatism* **38**, 1134-1141 (1995).
49. Maetzel, A., Li, L.C., Pencharz, J., Tomlinson, G. & Bombardier, C. The economic burden associated with osteoarthritis, rheumatoid arthritis, and hypertension: a comparative study. *Ann Rheum Dis* **63**, 395-401 (2004).
50. Penninx, B.W. *et al.* Psychological status among elderly people with chronic diseases: does type of disease play a part? *Journal of Psychosomatic Research* **40**, 521-534 (1996).
51. Hopman, W.M. *et al.* Associations between chronic disease, age and physical and mental health status. *Chronic Diseases in Canada* **29**, 108-116 (2009).
52. Koster, I.M. *et al.* Predictive factors for new onset or progression of knee osteoarthritis one year after trauma: MRI follow-up in general practice. *Eur Radiol* **21**, 1509-1516 (2011).
53. Oei, E.H., van Tiel, J., Robinson, W.H. & Gold, G.E. Quantitative radiologic imaging techniques for articular cartilage composition: toward early diagnosis and development of disease-modifying therapeutics for osteoarthritis. *Arthritis Care Res* **66**, 1129-1141 (2014).
54. Guermazi, A. *et al.* Prevalence of abnormalities in knees detected by MRI in adults without knee osteoarthritis: population based observational study (Framingham Osteoarthritis Study). *Bmj* **29** (2012).
55. Blanco, F.J. Osteoarthritis year in review 2014: we need more biochemical biomarkers in qualification phase. *Osteoarthritis and Cartilage* **22**, 2025-2032 (2014).
56. Hosnijeh, F.S., Runhaar, J., van Meurs, J.B. & Bierma-Zeinstra, S.M. Biomarkers for osteoarthritis: Can they be used for risk assessment? A systematic review. *Maturitas* **82**, 36-49 (2015).
57. van Spil, W.E., DeGroot, J., Lems, W.F., Oostveen, J.C. & Lafeber, F.P. Serum and urinary biochemical markers for knee and hip-osteoarthritis: a systematic review applying the consensus BIPED criteria. *Osteoarthritis and Cartilage* **18**, 605-612 (2010).
58. Lotz, M. *et al.* Value of biomarkers in osteoarthritis: current status and perspectives. *Annals of the Rheumatic Diseases* **72**, 1756-1763 (2013).

59. Kumm, J., Tamm, A., Lintrop, M. & Tamm, A. Diagnostic and prognostic value of bone biomarkers in progressive knee osteoarthritis: a 6-year follow-up study in middle-aged subjects. *Osteoarthritis and Cartilage* **21**, 815-822 (2013).
60. Charni-Ben Tabassi, N. *et al.* The type II collagen fragments Helix-II and CTX-II reveal different enzymatic pathways of human cartilage collagen degradation. *Osteoarthritis and Cartilage* **16**, 1183-1191 (2008).
61. Verma, P. & Dalal, K. Serum cartilage oligomeric matrix protein (COMP) in knee osteoarthritis: a novel diagnostic and prognostic biomarker. *Journal of Orthopaedic Research* **31**, 999-1006 (2013).
62. Hochberg, M.C. Osteoarthritis: The Rheumatologist's Perspective. *Hss J* **8**, 35-36 (2012).
63. Gudbergsen, H. *et al.* Correlations between radiographic assessments and MRI features of knee osteoarthritis--a cross-sectional study. *Osteoarthritis and Cartilage* **21**, 535-543 (2013).
64. Uthman, O.A. *et al.* Exercise for lower limb osteoarthritis: systematic review incorporating trial sequential analysis and network meta-analysis. *BMJ* **20** (2013).
65. Hartig-Andreasen, C., Troelsen, A., Thillemann, T.M. & Soballe, K. What factors predict failure 4 to 12 years after periacetabular osteotomy? *Clin Orthop Relat Res* **470**, 2978-2987 (2012).
66. Clohisy, J.C., Nepple, J.J., Ross, J.R., Pashos, G. & Schoenecker, P.L. Does surgical hip dislocation and periacetabular osteotomy improve pain in patients with Perthes-like deformities and acetabular dysplasia? *Clin Orthop Relat Res* **473**, 1370-1377 (2015).
67. Pelletier, J.P., Martel-Pelletier, J., Rannou, F. & Cooper, C. Efficacy and safety of oral NSAIDs and analgesics in the management of osteoarthritis: Evidence from real-life setting trials and surveys. *Semin Arthritis Rheum* **45**, 2 (2016).
68. du Souich, P. Absorption, distribution and mechanism of action of SYSADOAS. *Pharmacol Ther* **142**, 362-374 (2014).
69. Rutjes, A.W. *et al.* Viscosupplementation for osteoarthritis of the knee: a systematic review and meta-analysis. *Annals of Internal Medicine* **157**, 180-191 (2012).
70. Bannuru, R.R. *et al.* Comparative effectiveness of pharmacologic interventions for knee osteoarthritis: a systematic review and network meta-analysis. *Ann Intern Med* **162**, 46-54 (2015).
71. Chan, P.S., Caron, J.P., Rosa, G.J. & Orth, M.W. Glucosamine and chondroitin sulfate regulate gene expression and synthesis of nitric oxide and prostaglandin E(2) in articular cartilage explants. *Osteoarthritis Cartilage* **13**, 387-394 (2005).
72. McAlindon, T.E. *et al.* OARSI guidelines for the non-surgical management of knee osteoarthritis. *Osteoarthritis and Cartilage* **22**, 363-388 (2014).

73. Jevsevar, D.S. *et al.* The American Academy of Orthopaedic Surgeons evidence-based guideline on: treatment of osteoarthritis of the knee, 2nd edition. *Journal of Bone and Joint Surgery* **95**, 1885-1886 (2013).
74. Tat, S.K., Pelletier, J.P., Mineau, F., Duval, N. & Martel-Pelletier, J. Variable effects of 3 different chondroitin sulfate compounds on human osteoarthritic cartilage/chondrocytes: relevance of purity and production process. *J Rheumatol* **37**, 656-664 (2010).
75. Murphy, L. *et al.* Lifetime risk of symptomatic knee osteoarthritis. *Arthritis and rheumatism* **59**, 1207-1213 (2008).
76. Martel-Pelletier, J., Farran, A., Montell, E., Verges, J. & Pelletier, J.P. Discrepancies in composition and biological effects of different formulations of chondroitin sulfate. *Molecules* **20**, 4277-4289 (2015).
77. Schipani, E. *et al.* Hypoxia in cartilage: HIF-1alpha is essential for chondrocyte growth arrest and survival. *Genes Dev* **15**, 2865-2876 (2001).
78. Poole, C.A. Articular cartilage chondrons: form, function and failure. *J Anat* **191**, 1-13 (1997).
79. Wilusz, R.E., Sanchez-Adams, J. & Guilak, F. The structure and function of the pericellular matrix of articular cartilage. *Matrix Biol* **39**, 25-32 (2014).
80. Askary, A. *et al.* Ancient origin of lubricated joints in bony vertebrates. *Elife* **19**, 16415 (2016).
81. Rhee, D.K. *et al.* The secreted glycoprotein lubricin protects cartilage surfaces and inhibits synovial cell overgrowth. *J Clin Invest* **115**, 622-631 (2005).
82. Bhosale, A.M. & Richardson, J.B. Articular cartilage: structure, injuries and review of management. *Br Med Bull* **87**, 77-95 (2008).
83. Ricard-Blum, S. The collagen family. *Cold Spring Harb Perspect Biol* **3** (2011).
84. Gordon, M.K. & Hahn, R.A. Collagens. *Cell Tissue Res* **339**, 247-257 (2010).
85. Persikov, A.V., Ramshaw, J.A. & Brodsky, B. Prediction of collagen stability from amino acid sequence. *J Biol Chem* **280**, 19343-19349 (2005).
86. Fallas, J.A., Gauba, V. & Hartgerink, J.D. Solution structure of an ABC collagen heterotrimer reveals a single-register helix stabilized by electrostatic interactions. *J Biol Chem* **284**, 26851-26859 (2009).
87. Chen, S. & Birk, D.E. The regulatory roles of small leucine-rich proteoglycans in extracellular matrix assembly. *Febs J* **280**, 2120-2137 (2013).
88. Wight, T.N. Provisional matrix: A role for versican and hyaluronan. *Matrix Biol* **6**, 30309-30302 (2016).
89. Wang, P. *et al.* The NCAN gene: schizophrenia susceptibility and cognitive dysfunction. *Neuropsychiatr Dis Treat* **12**, 2875-2883 (2016).
90. Knudson, W. & Loeser, R.F. CD44 and integrin matrix receptors participate in cartilage homeostasis. *Cell Mol Life Sci* **59**, 36-44 (2002).
91. Schaefer, L. & Iozzo, R.V. Biological functions of the small leucine-rich proteoglycans: from genetics to signal transduction. *Journal of Biological Chemistry* **283**, 21305-21309 (2008).

92. Ni, G.X., Li, Z. & Zhou, Y.Z. The role of small leucine-rich proteoglycans in osteoarthritis pathogenesis. *Osteoarthritis Cartilage* **22**, 896-903 (2014).
93. Raspanti, M., Congiu, T., Alessandrini, A., Gobbi, P. & Ruggeri, A. Different patterns of collagen-proteoglycan interaction: a scanning electron microscopy and atomic force microscopy study. *Eur J Histochem* **44**, 335-343 (2000).
94. Ameye, L. & Young, M.F. Mice deficient in small leucine-rich proteoglycans: novel in vivo models for osteoporosis, osteoarthritis, Ehlers-Danlos syndrome, muscular dystrophy, and corneal diseases. *Glycobiology* **12**, 107R-116R (2002).
95. Gill, M.R., Oldberg, A. & Reinholt, F.P. Fibromodulin-null murine knee joints display increased incidences of osteoarthritis and alterations in tissue biochemistry. *Osteoarthritis and Cartilage* **10**, 751-757 (2002).
96. Geng, Y., McQuillan, D. & Roughley, P.J. SLRP interaction can protect collagen fibrils from cleavage by collagenases. *Matrix Biology* **25**, 484-491 (2006).
97. Sjoberg, A.P. *et al.* Short leucine-rich glycoproteins of the extracellular matrix display diverse patterns of complement interaction and activation. *Molecular Immunology* **46**, 830-839 (2009).
98. Nuka, S. *et al.* Phenotypic characterization of epiphycan-deficient and epiphycan/biglycan double-deficient mice. *Osteoarthritis Cartilage* **18**, 88-96 (2010).
99. Wadhwa, S., Embree, M.C., Kilts, T., Young, M.F. & Ameye, L.G. Accelerated osteoarthritis in the temporomandibular joint of biglycan/fibromodulin double-deficient mice. *Osteoarthritis and Cartilage* **13**, 817-827 (2005).
100. Svensson, L. *et al.* Fibromodulin-null mice have abnormal collagen fibrils, tissue organization, and altered lumican deposition in tendon. *Journal of Biological Chemistry* **274**, 9636-9647 (1999).
101. Schaefer, L. & Iozzo, R.V. Biological functions of the small leucine-rich proteoglycans: from genetics to signal transduction. *J Biol Chem* **283**, 21305-21309 (2008).
102. Fisher, L.W., Termine, J.D. & Young, M.F. Deduced protein sequence of bone small proteoglycan I (biglycan) shows homology with proteoglycan II (decorin) and several nonconnective tissue proteins in a variety of species. *J Biol Chem* **264**, 4571-4576 (1989).
103. Casar, J.C., McKechnie, B.A., Fallon, J.R., Young, M.F. & Brandan, E. Transient up-regulation of biglycan during skeletal muscle regeneration: delayed fiber growth along with decorin increase in biglycan-deficient mice. *Developmental biology* **268**, 358-371 (2004).
104. Mochida, Y. *et al.* Decorin modulates collagen matrix assembly and mineralization. *Matrix Biology* **28**, 44-52 (2009).
105. Ruhland, C. *et al.* The glycosaminoglycan chain of decorin plays an important role in collagen fibril formation at the early stages of fibrillogenesis. *Febs J* **274**, 4246-4255 (2007).

106. Mohan, R.R., Tovey, J.C., Gupta, R., Sharma, A. & Tandon, A. Decorin biology, expression, function and therapy in the cornea. *Curr Mol Med* **11**, 110-128 (2011).
107. Ezura, Y., Chakravarti, S., Oldberg, A., Chervoneva, I. & Birk, D.E. Differential expression of lumican and fibromodulin regulate collagen fibrillogenesis in developing mouse tendons. *J Cell Biol* **151**, 779-788 (2000).
108. Jepsen, K.J. *et al.* A syndrome of joint laxity and impaired tendon integrity in lumican- and fibromodulin-deficient mice. *Journal of Biological Chemistry* **277**, 35532-35540 (2002).
109. Sjoberg, A., Onnerfjord, P., Morgelin, M., Heinegard, D. & Blom, A.M. The extracellular matrix and inflammation: fibromodulin activates the classical pathway of complement by directly binding C1q. *J Biol Chem* **280**, 32301-32308 (2005).
110. Naito, Z. Role of the small leucine-rich proteoglycan (SLRP) family in pathological lesions and cancer cell growth. *J Nippon Med Sch* **72**, 137-145 (2005).
111. Bengtsson, E., Neame, P.J., Heinegard, D. & Sommarin, Y. The primary structure of a basic leucine-rich repeat protein, PRELP, found in connective tissues. *J Biol Chem* **270**, 25639-25644 (1995).
112. Happonen, K.E., Heinegard, D., Saxne, T. & Blom, A.M. Interactions of the complement system with molecules of extracellular matrix: relevance for joint diseases. *Immunobiology* **217**, 1088-1096 (2012).
113. Malmsten, M., Davoudi, M. & Schmidtchen, A. Bacterial killing by heparin-binding peptides from PRELP and thrombospondin. *Matrix Biol* **25**, 294-300 (2006).
114. Nuka, S. *et al.* Phenotypic characterization of epiphycan-deficient and epiphycan/biglycan double-deficient mice. *Osteoarthritis and Cartilage* **18**, 88-96 (2010).
115. Bentz, H. *et al.* Purification and characterization of a unique osteoinductive factor from bovine bone. *J Biol Chem* **264**, 20805-20810 (1989).
116. Osawa, A. *et al.* Activation of genes for growth factor and cytokine pathways late in chondrogenic differentiation of ATDC5 cells. *Genomics* **88**, 52-64 (2006).
117. Kampmann, A. *et al.* The proteoglycan osteoglycin/mimecan is correlated with arteriogenesis. *Mol Cell Biochem* **322**, 15-23 (2009).
118. Reardon, A.J. *et al.* Identification in vitreous and molecular cloning of opticin, a novel member of the family of leucine-rich repeat proteins of the extracellular matrix. *Journal of Biological Chemistry* **275**, 2123-2129 (2000).
119. Le Goff, M.M. *et al.* The vitreous glycoprotein opticin inhibits preretinal neovascularization. *Invest Ophthalmol Vis Sci* **53**, 228-234 (2012).
120. Pellegrini, B., Acland, G.M. & Ray, J. Cloning and characterization of opticin cDNA: evaluation as a candidate for canine oculo-skeletal dysplasia. *Gene* **282**, 121-131 (2002).

121. Monfort, J. *et al.* Identification of opticin, a member of the small leucine-rich repeat proteoglycan family, in human articular tissues: a novel target for MMP-13 in osteoarthritis. *Osteoarthritis and Cartilage* **16**, 749-755 (2008).
122. Tio, L. *et al.* Characterization of opticin digestion by proteases involved in osteoarthritis development. *Joint Bone Spine* **81**, 137-141 (2014).
123. Ohta, K. *et al.* Tsukushi functions as an organizer inducer by inhibition of BMP activity in cooperation with chordin. *Dev Cell* **7**, 347-358 (2004).
124. Bech-Hansen, N.T. *et al.* Mutations in NYX, encoding the leucine-rich proteoglycan nyctalopin, cause X-linked complete congenital stationary night blindness. *Nat Genet* **26**, 319-323 (2000).
125. Mansson, B., Wenglen, C., Morgelin, M., Saxne, T. & Heinegard, D. Association of chondroadherin with collagen type II. *J Biol Chem* **276**, 32883-32888 (2001).
126. Camper, L., Heinegard, D. & Lundgren-Akerlund, E. Integrin alpha2beta1 is a receptor for the cartilage matrix protein chondroadherin. *J Cell Biol* **138**, 1159-1167 (1997).
127. O'Connor, E. *et al.* Species specific membrane anchoring of nyctalopin, a small leucine-rich repeat protein. *Hum Mol Genet* **14**, 1877-1887 (2005).
128. Shimizu-Hirota, R., Sasamura, H., Kuroda, M., Kobayashi, E. & Saruta, T. Functional characterization of podocan, a member of a new class in the small leucine-rich repeat protein family. *FEBS Lett* **563**, 69-74 (2004).
129. Mochida, Y. *et al.* Podocan-like protein: a novel small leucine-rich repeat matrix protein in bone. *Biochem Biophys Res Commun* **410**, 333-338 (2011).
130. Sellam, J. & Berenbaum, F. The role of synovitis in pathophysiology and clinical symptoms of osteoarthritis. *Nat Rev Rheumatol* **6**, 625-635 (2010).
131. Burr, D.B. Anatomy and physiology of the mineralized tissues: role in the pathogenesis of osteoarthrosis. *Osteoarthritis Cartilage* **12**, S20-30 (2004).
132. Findlay, D.M. & Kuliwaba, J.S. Bone-cartilage crosstalk: a conversation for understanding osteoarthritis. *Bone research* **4**, 16028 (2016).
133. Sanchez, C. *et al.* Osteoblasts from the sclerotic subchondral bone downregulate aggrecan but upregulate metalloproteinases expression by chondrocytes. This effect is mimicked by interleukin-6, -1beta and oncostatin M pre-treated non-sclerotic osteoblasts. *Osteoarthritis Cartilage* **13**, 979-987 (2005).
134. Sanchez, C. *et al.* Carnosol Inhibits Pro-Inflammatory and Catabolic Mediators of Cartilage Breakdown in Human Osteoarthritic Chondrocytes and Mediates Cross-Talk between Subchondral Bone Osteoblasts and Chondrocytes. *PloS one* **10**, e0136118 (2015).
135. Burr, D.B. & Gallant, M.A. Bone remodelling in osteoarthritis. *Nat Rev Rheumatol* **8**, 665-673 (2012).
136. Goldring, M.B. & Otero, M. Inflammation in osteoarthritis. *Curr Opin Rheumatol* **23**, 471-478 (2011).

137. Henrotin, Y., Pesesse, L. & Lambert, C. Targeting the synovial angiogenesis as a novel treatment approach to osteoarthritis. *Ther Adv Musculoskelet Dis* **6**, 20-34 (2014).
138. Lund-Olesen, K. Oxygen tension in synovial fluids. *Arthritis and rheumatism* **13**, 769-776 (1970).
139. Schneider, U., Miltner, O., Thomsen, M., Graf, J. & Niethard, F.U. [Intra-articular oxygen partial pressure measurements under functional conditions]. *Z Orthop Ihre Grenzgeb* **134**, 422-425 (1996).
140. Forsythe, J.A. *et al.* Activation of vascular endothelial growth factor gene transcription by hypoxia-inducible factor 1. *Mol Cell Biol* **16**, 4604-4613 (1996).
141. Salceda, S. & Caro, J. Hypoxia-inducible factor 1alpha (HIF-1alpha) protein is rapidly degraded by the ubiquitin-proteasome system under normoxic conditions. Its stabilization by hypoxia depends on redox-induced changes. *J Biol Chem* **272**, 22642-22647 (1997).
142. Movafagh, S., Crook, S. & Vo, K. Regulation of hypoxia-inducible factor-1a by reactive oxygen species: new developments in an old debate. *Journal of cellular biochemistry* **116**, 696-703 (2015).
143. Sartori-Cintra, A.R., Mara, C.S., Argolo, D.L. & Coimbra, I.B. Regulation of hypoxia-inducible factor-1alpha (HIF-1alpha) expression by interleukin-1beta (IL-1 beta), insulin-like growth factors I (IGF-I) and II (IGF-II) in human osteoarthritic chondrocytes. *Clinics (Sao Paulo, Brazil)* **67**, 35-40 (2012).
144. Lee, J.W., Bae, S.H., Jeong, J.W., Kim, S.H. & Kim, K.W. Hypoxia-inducible factor (HIF-1)alpha: its protein stability and biological functions. *Experimental & molecular medicine* **36**, 1-12 (2004).
145. Lambert, C. *et al.* Characterization of synovial angiogenesis in osteoarthritis patients and its modulation by chondroitin sulfate. *Arthritis Res Ther* **14** (2012).
146. Bornstein, P. Thrombospondins function as regulators of angiogenesis. *J Cell Commun Signal* **3**, 189-200 (2009).
147. Yu, J. *et al.* Modulation of endothelial cell growth arrest and apoptosis by vascular endothelial growth inhibitor. *Circ Res* **89**, 1161-1167 (2001).
148. Qi, J.W. *et al.* TNFSF15 inhibits vasculogenesis by regulating relative levels of membrane-bound and soluble isoforms of VEGF receptor 1. *Proceedings of the National Academy of Sciences of the United States of America* **110**, 13863-13868 (2013).
149. Lawler, J. Thrombospondin-1 as an endogenous inhibitor of angiogenesis and tumor growth. *Journal of cellular and molecular medicine* **6**, 1-12 (2002).
150. Pfander, D., Cramer, T., Deuerling, D., Weseloh, G. & Swoboda, B. Expression of thrombospondin-1 and its receptor CD36 in human osteoarthritic cartilage. *Ann Rheum Dis* **59**, 448-454 (2000).
151. Pearle, A.D. *et al.* Elevated high-sensitivity C-reactive protein levels are associated with local inflammatory findings in patients with osteoarthritis. *Osteoarthritis Cartilage* **15**, 516-523 (2007).

152. Scanzello, C.R. *et al.* Local cytokine profiles in knee osteoarthritis: elevated synovial fluid interleukin-15 differentiates early from end-stage disease. *Osteoarthritis Cartilage* **17**, 1040-1048 (2009).
153. Chadjichristos, C. *et al.* Sp1 and Sp3 transcription factors mediate interleukin-1 beta down-regulation of human type II collagen gene expression in articular chondrocytes. *J Biol Chem* **278**, 39762-39772 (2003).
154. Stove, J., Huch, K., Gunther, K.P. & Scharf, H.P. Interleukin-1beta induces different gene expression of stromelysin, aggrecan and tumor-necrosis-factor-stimulated gene 6 in human osteoarthritic chondrocytes in vitro. *Pathobiology* **68**, 144-149 (2000).
155. Kapoor, M., Martel-Pelletier, J., Lajeunesse, D., Pelletier, J.P. & Fahmi, H. Role of proinflammatory cytokines in the pathophysiology of osteoarthritis. *Nat Rev Rheumatol* **7**, 33-42 (2011).
156. Bowles, R.D. *et al.* In vivo luminescence imaging of NF-kappaB activity and serum cytokine levels predict pain sensitivities in a rodent model of osteoarthritis. *Arthritis Rheumatol* **66**, 637-646 (2014).
157. Pratta, M.A. *et al.* Aggrecan protects cartilage collagen from proteolytic cleavage. *Journal of Biological Chemistry* **278**, 45539-45545 (2003).
158. Melrose, J. *et al.* Fragmentation of decorin, biglycan, lumican and keratocan is elevated in degenerate human meniscus, knee and hip articular cartilages compared with age-matched macroscopically normal and control tissues. *Arthritis Res Ther* **10**, 14 (2008).
159. Hollander, A.P. *et al.* Damage to type II collagen in aging and osteoarthritis starts at the articular surface, originates around chondrocytes, and extends into the cartilage with progressive degeneration. *J Clin Invest* **96**, 2859-2869 (1995).
160. Grenier, S., Bhargava, M.M. & Torzilli, P.A. An in vitro model for the pathological degradation of articular cartilage in osteoarthritis. *J Biomech* **47**, 645-652 (2014).
161. Tang, B.L. ADAMTS: a novel family of extracellular matrix proteases. *The international journal of biochemistry & cell biology* **33**, 33-44 (2001).
162. Karsdal, M.A. *et al.* Cartilage degradation is fully reversible in the presence of aggrecanase but not matrix metalloproteinase activity. *Arthritis Res Ther* **10**, 30 (2008).
163. Majumdar, M.K. *et al.* Double-knockout of ADAMTS-4 and ADAMTS-5 in mice results in physiologically normal animals and prevents the progression of osteoarthritis. *Arthritis and rheumatism* **56**, 3670-3674 (2007).
164. Freije, J.M. *et al.* Molecular cloning and expression of collagenase-3, a novel human matrix metalloproteinase produced by breast carcinomas. *Journal of Biological Chemistry* **269**, 16766-16773 (1994).

165. Visse, R. & Nagase, H. Matrix metalloproteinases and tissue inhibitors of metalloproteinases: structure, function, and biochemistry. *Circulation Research* **92**, 827-839 (2003).
166. Knauper, V., Lopez-Otin, C., Smith, B., Knight, G. & Murphy, G. Biochemical characterization of human collagenase-3. *Journal of Biological Chemistry* **271**, 1544-1550 (1996).
167. Fanjul-Fernandez, M., Folgueras, A.R., Cabrera, S. & Lopez-Otin, C. Matrix metalloproteinases: evolution, gene regulation and functional analysis in mouse models. *Biochimica et Biophysica Acta* **1**, 3-19 (2010).
168. Cao, J., Rehemtulla, A., Bahou, W. & Zucker, S. Membrane type matrix metalloproteinase 1 activates pro-gelatinase A without furin cleavage of the N-terminal domain. *Journal of Biological Chemistry* **271**, 30174-30180 (1996).
169. Pardo, A. & Selman, M. MMP-1: the elder of the family. *Int J Biochem Cell Biol* **37**, 283-288 (2005).
170. Nwomeh, B.C., Liang, H.X., Cohen, I.K. & Yager, D.R. MMP-8 is the predominant collagenase in healing wounds and nonhealing ulcers. *J Surg Res* **81**, 189-195 (1999).
171. Reboul, P., Pelletier, J.P., Tardif, G., Cloutier, J.M. & Martel-Pelletier, J. The new collagenase, collagenase-3, is expressed and synthesized by human chondrocytes but not by synoviocytes. A role in osteoarthritis. *J Clin Invest* **97**, 2011-2019 (1996).
172. Chung, L. *et al.* Collagenase unwinds triple-helical collagen prior to peptide bond hydrolysis. *The EMBO journal* **23**, 3020-3030 (2004).
173. Danielsen, P.L. *et al.* Matrix metalloproteinase-8 overexpression prevents proper tissue repair. *Surgery* **150**, 897-906 (2011).
174. Mitchell, P.G. *et al.* Cloning, expression, and type II collagenolytic activity of matrix metalloproteinase-13 from human osteoarthritic cartilage. *Journal of Clinical Investigation* **97**, 761-768 (1996).
175. Yamamoto, K. *et al.* MMP-13 is constitutively produced in human chondrocytes and co-endocytosed with ADAMTS-5 and TIMP-3 by the endocytic receptor LRP1. *Matrix Biology* **56**, 57-73 (2016).
176. Tetlow, L.C., Adlam, D.J. & Woolley, D.E. Matrix metalloproteinase and proinflammatory cytokine production by chondrocytes of human osteoarthritic cartilage: associations with degenerative changes. *Arthritis and rheumatism* **44**, 585-594 (2001).
177. Fields, G.B. New strategies for targeting matrix metalloproteinases. *Matrix Biology* **46**, 239-246 (2015).
178. Tardif, G. *et al.* Identification and differential expression of human collagenase-3 mRNA species derived from internal deletion, alternative splicing, and different polyadenylation and transcription initiation sites. *Osteoarthritis and Cartilage* **11**, 524-537 (2003).

179. McCoy, A.M. Animal Models of Osteoarthritis: Comparisons and Key Considerations. *Vet Pathol* **52**, 803-818 (2015).
180. Glasson, S.S., Blanchet, T.J. & Morris, E.A. The surgical destabilization of the medial meniscus (DMM) model of osteoarthritis in the 129/SvEv mouse. *Osteoarthritis and Cartilage* **15**, 1061-1069 (2007).
181. Rousset, F. *et al.* IL-1beta mediates MMP secretion and IL-1beta neosynthesis via upregulation of p22(phox) and NOX4 activity in human articular chondrocytes. *Osteoarthritis Cartilage* **23**, 1972-1980 (2015).
182. Yuan, Y., Hilliard, G., Ferguson, T. & Millhorn, D.E. Cobalt inhibits the interaction between hypoxia-inducible factor-alpha and von Hippel-Lindau protein by direct binding to hypoxia-inducible factor-alpha. *J Biol Chem* **278**, 15911-15916 (2003).
183. Vanecko, S. & Laskowski, M., Sr. Studies of the specificity of deoxyribonuclease I. II. Hydrolysis of oligonucleotides carrying a monoesterified phosphate on carbon 3'. *J Biol Chem* **236**, 1135-1140 (1961).
184. Ruiz-Romero, C. *et al.* Strategies to optimize two-dimensional gel electrophoresis analysis of the human joint proteome. *Talanta* **80**, 1552-1560 (2010).
185. Chavira, R., Jr., Burnett, T.J. & Hageman, J.H. Assaying proteinases with azocoll. *Analytical Biochemistry* **136**, 446-450 (1984).
186. Monfort, J. *et al.* Degradation of small leucine-rich repeat proteoglycans by matrix metalloprotease-13: identification of a new biglycan cleavage site. *Arthritis Res Ther* **8**, 3 (2006).
187. Le Goff, M.M. *et al.* The vitreous glycoprotein opticin inhibits preretinal neovascularization. *Investigative Ophthalmology and Visual Science* **53**, 228-234 (2012).
188. Valverde-Franco, G. *et al.* In vivo bone-specific EphB4 overexpression in mice protects both subchondral bone and cartilage during osteoarthritis. *Arthritis and rheumatism* **64**, 3614-3625 (2012).
189. Amiable, N. *et al.* Proteinase-activated receptor-2 gene disruption limits the effect of osteoarthritis on cartilage in mice: a novel target in joint degradation. *J Rheumatol* **38**, 911-920 (2011).
190. Glasson, S.S., Chambers, M.G., Van Den Berg, W.B. & Little, C.B. The OARSI histopathology initiative - recommendations for histological assessments of osteoarthritis in the mouse. *Osteoarthritis and Cartilage* **18**, 025 (2010).
191. Drexler, W. *et al.* Correlation of collagen organization with polarization sensitive imaging of in vitro cartilage: implications for osteoarthritis. *J Rheumatol* **28**, 1311-1318 (2001).
192. Haywood, L. *et al.* Inflammation and angiogenesis in osteoarthritis. *Arthritis Rheum* **48**, 2173-2177 (2003).

193. Lal, A., Haynes, S.R. & Gorospe, M. Clean Western blot signals from immunoprecipitated samples. *Molecular and Cellular Probes* **19**, 385-388 (2005).
194. Knauper, V. *et al.* The role of the C-terminal domain of human collagenase-3 (MMP-13) in the activation of procollagenase-3, substrate specificity, and tissue inhibitor of metalloproteinase interaction. *Journal of Biological Chemistry* **272**, 7608-7616 (1997).
195. Zhang, G. *et al.* Genetic evidence for the coordinated regulation of collagen fibrillogenesis in the cornea by decorin and biglycan. *Journal of Biological Chemistry* **284**, 8888-8897 (2009).
196. Tasheva, E.S. *et al.* Mimecan/osteoglycin-deficient mice have collagen fibril abnormalities. *Molecular Vision* **8**, 407-415 (2002).
197. Takanosu, M. *et al.* Structure, chromosomal location, and tissue-specific expression of the mouse opticin gene. *Investigative Ophthalmology and Visual Science* **42**, 2202-2210 (2001).
198. Grover, J., Chen, X.N., Korenberg, J.R. & Roughley, P.J. The human lumican gene. Organization, chromosomal location, and expression in articular cartilage. *J Biol Chem* **270**, 21942-21949 (1995).
199. Wang, Q. *et al.* Identification of a central role for complement in osteoarthritis. *Nature Medicine* **17**, 1674-1679 (2011).
200. Kemper, C. & Atkinson, J.P. T-cell regulation: with complements from innate immunity. *Nat Rev Immunol* **7**, 9-18 (2007).
201. Gobezie, R. *et al.* High abundance synovial fluid proteome: distinct profiles in health and osteoarthritis. *Arthritis Res Ther* **9** (2007).
202. Sohn, D.H. *et al.* Plasma proteins present in osteoarthritic synovial fluid can stimulate cytokine production via Toll-like receptor 4. *Arthritis Res Ther* **14** (2012).
203. Triantafyllou, A. *et al.* Cobalt induces hypoxia-inducible factor-1alpha (HIF-1alpha) in HeLa cells by an iron-independent, but ROS-, PI-3K- and MAPK-dependent mechanism. *Free Radic Res* **40**, 847-856 (2006).
204. Giatromanolaki, A. *et al.* Upregulated hypoxia inducible factor-1alpha and -2alpha pathway in rheumatoid arthritis and osteoarthritis. *Arthritis Res Ther* **5**, 29 (2003).
205. Terashima, J. *et al.* VEGF expression is regulated by HIF-1alpha and ARNT in 3D KYSE-70, esophageal cancer cell spheroids. *Cell Biol Int* **40**, 1187-1194 (2016).
206. Resovi, A., Pinessi, D., Chiorino, G. & Taraboletti, G. Current understanding of the thrombospondin-1 interactome. *Matrix Biol* **37**, 83-91 (2014).
207. Jimenez, B. *et al.* Signals leading to apoptosis-dependent inhibition of neovascularization by thrombospondin-1. *Nat Med* **6**, 41-48 (2000).
208. Tsuchida, R. *et al.* BMP4/Thrombospondin-1 loop paracrinically inhibits tumor angiogenesis and suppresses the growth of solid tumors. *Oncogene* **33**, 3803-3811 (2014).

209. Lindner, D.J. *et al.* Thrombospondin-1 expression in melanoma is blocked by methylation and targeted reversal by 5-Aza-deoxycytidine suppresses angiogenesis. *Matrix Biol* **32**, 123-132 (2013).
210. Hsieh, J.L. *et al.* Intraarticular gene transfer of thrombospondin-1 suppresses the disease progression of experimental osteoarthritis. *J Orthop Res* **28**, 1300-1306 (2010).
211. Cassatella, M.A. *et al.* Soluble TNF-like cytokine (TL1A) production by immune complexes stimulated monocytes in rheumatoid arthritis. *J Immunol* **178**, 7325-7333 (2007).

ANNEX

BUFFERS, REACTIVES AND MEDIA

- CELL CULTURE MEDIA

OA synoviocytes (human)	
DMEM (Gibco BRL)	
FBS (Biological Industries)	10%
Penicillin (Gibco BRL)	100 U/ml
Streptomycin (Gibco BRL)	0,1 mg/ml

Human umbilical vascular endothelial cells (HUVEC)	
M200 (Invitrogen)	
low serum growth supplement LSGS	(Gibco; Cascades Biologics; Invitrogen)
FBS (Biological Industries)	2%
Hydrocortisone	1 µg/ml
Human epidermal growth factor	10 ng/ml
Basic fibroblast growth factor	3 ng/ml
Gentamycin (Wisent)	50 µg/ml

- PCR MIX

Master Mix for RT	
PCR buffer	10X
MgCl2	25mM
dNTP mix	10mM
Random hexamers	50 µM
RNase inhibitor	20 U ul
Reverse Transcriptase	200 U µl
H2O	Up to 25 µl
TOTAL	**25 µl**

Dilute cDNA at 1/4 for RT-PCR		
Template (cDNA, 5 ng/µl)		**5 µl**
Qiagen SYBRGreen mix		**6,25 µl**
UNG		**0,13 µl**
Primer 1 (20µM)		**0,13 µl**
Primer 2 (20µM)		**0,13 µl**
H_2O		**0,88 µl**
	mix	**7,5 µl**
	Total	**12,5 µl**

- CELLULAR PROTEIN EXTRACTION BUFFERS

RIPA buffer	
Tris-HCl (pH7,4)	50mM
NP-40	1%
NA-deoxycholate	0,25%
NaCl	150mM
EDTA	0.5M
Na-orthovanadate	1mM

Nuclear extraction buffer A	
HEPES (ph7,9)	10 mM
$MgCl_2$	1,5 mM
KCl	10 mM
NP-40	1%

Nuclear extraction buffer B	
HEPES (ph7,9)	20 mM
$MgCl_2$	1,5 mM
NaCl	420 mM
Glycerol	25%
EDTA	0.2mM

**Buffers were aliquoted and kept at -20C. Protease inhibitors were added before using.*

- CARTILAGE PROTEOGLYCAN EXTRACTION BUFFERS

4M GuHCl buffer	
NaOAc (pH6)	0,1M
GuHCl	4M

Dialysis buffer	
Tris pH7.5	500mM
NaCl	1,5M
Brij 35	0,5%

- CARTILAGE PROTEOGLYCAN QUANTIFICATION BUFFERS

DMMB solution 1 (for PG quantification)	
1,9-dimethylemethylene blue	16mg
Ethanol	5ml

DMMB solution 2	
Formic acid	2ml
Sodium format	2g
H2O	900ml

- PROTEIN ELECTROPHORETIC SEPARATION BUFFERS AND ACRYLAMIDE GELS

Stacking gel 4%, 0.125M Tris, pH6.8	
ddH20	6.1 ml
Tris-HCl 0.5M, pH6.8	2.5 ml
10% (w/v) SDS	100 µl
Acrylamide Bis (30%)	1.3 ml
10% Ammonium persulfate (APS)	50 µl
TEMED	10 µl
TOTAL	**10 ml**

Separating gel 0.375M Tris, pH8.8

Acrylamide	**15%**	**12%**	**10%**	**9%**	**7.5%**
Distilled water	2.35ml	3.35ml	4ml	4.35ml	4.85ml
1.5M Tris-HCl, pH8.8	2.5ml	2.5ml	2.5ml	2.5ml	2.5ml
10% (w/v) SDS	100µl	100µl	100µl	100µl	100µl
Acrylamide Bis (30%)	5ml	4ml	3.33ml	3ml	2.5ml
10% (APS)	50µl	50µl	50µl	50µl	50µl
TEMED	5µl	5µl	5µl	5µl	5µl
TOTAL	**10ml**	**10ml**	**10ml**	**10ml**	**10ml**

- 2 DIMENSIONAL GEL ELECTROPHORESYS

Sample Rehydration Buffer*:	
7M Urea	4.20 g
2M Thiourea	1.52 g
4% CHAPS	400 mg

Re-equilibration Buffer:**		
Tris HCl (1.5M stock pH 8.8 w/HCI)	13.4ml	50mM
Urea	144.14g	6M
Glycerol (87% stock)	138mL	30%
SDS	8.0g	2%

*Make up to 10ml in milli-Q water, store in 1ml aliquots at -20ºC.

**Make up to 400ml in ddH2O, store in 40ml aliquots at –20ºC.

IPG Strip Length:	**Rehydration Buffer Needed:**
7cm IPG Strip	125ul*
11cm IPG Strip	200ul*
18cm IPG Strip	350ul*

*1mL Stock Rehydration Buffer needs the following added before use:

DTT	5 mg (=30mM)
Ampholytes	5ul (=0.5%)
Bromophenol blue	Trace (add with pipette tip)

- COOMASSIE GEL STAINING

Coomassie concentrated stain solution	
Bromophenol Blue	1.2 g
Methanol	30ml
Acetic acid	6ml
Coomassie working stain solution	
Coomassie concentrated stain solution	3 ml
Methanol	50ml
Acetic acid	10ml
H_2O	40ml
Fixative solution	
Methanol	50%
Acetic acid	10%
H_2O	40%
Destaining solution	
Methanol	270%
Acetic acid	30%
H_2O	270%

- MMP ACTIVATION SOLUTIONS

APMA (pH7.3)	
APMA	0,5mM
TNCB (pH7.5)*	

TNCB (pH7.5)*	
Tris–HCl (pH 7.5)	50mM
$CaCl_2$	100mM
NaCl	150mM
Brij-35	0.05%

* add cocktail of protease inhibitors that do not inhibit metallo- and aspartic proteases (Complete^{TM} EDTA-free, Roche)

- FIXATIVE SOLUTION FOR MICE TISSUE HISTOLOGY

4% Paraformaldehyde (PFA) fixative pH 7.4	
PFA (4%)	4g
boiling ddH2O	86ml
NaOH (10M)	"a drop"
PBS 10X	10ml